HELSINKI UNIVERSITY OF TECHNOLOGY
Department of Automation and Systems Technology
Automation Technology Laboratory

Tomi Ylikorpi

A Biologically inspired rolling robot for planetary surface exploration

Thesis submitted 21.11.2005 in partial fulfillment of the requirements for the degree of Licentiate of Technology

Supervisor: Professor Aarne Halme

Lisensiaattityön tiivistelmä

TEKNILLINEN KORKEAKOULU (abstract in Finnish)

Tekijä:	Tomi Ylikorpi
Työn nimi:	Luontoa jäljittelevän pallorobotin kehittäminen planeettatutkimukseen
Päivämäärä:	21.11.2005 **Sivumäärä:** 112
Osasto:	Automaatio- ja systeemitekniikan osasto
Professuuri:	Automaatiotekniikka (Aut-84)
Työn valvoja:	Professori Aarne Halme

Planeetoille suuntautuvat tutkimusmatkat tähtäävät usein maaperänäytteiden keräämiseen ja tutkimiseen, usein myös näytteiden palauttamiseen Maahan tarkempia tutkimuksia varten. Äskettäiset Marsiin suuntautuneet robottimissiot ovat osoittaneet liikkuvien robottien kyvyn suorittaa tutkimustehtäviä. Vieraalla planeetalla robotin liikkumiskyky on tarpeen tutkittavan alueen laajentamiseksi ja tutkimusten kohdentamiseksi haluttuihin tieteellisesti kiinnostavimpiin kohteisiin. Luonnon kehittämiä ratkaisuja jäljittelevä liikkumistapa saattaa tarjota liikkuvalle robotille nykyisiä parempaa mukautumis- ja viansietokykyä. Tämä tutkimustyö etsii luonnosta uusia innovaatioita ja tähtää uudenlaisten joustavien ja tehokkaiden liikkumistapojen kehittämiseen liikkuville roboteille. Erityisesti työ keskittyy pallomaisen, aro-ohdakkeen mukaan englanniksi ’Thistle’:ksi nimetyn, robotin määrittelyyn ja alustavaan kehitystyöhön. Tutkimus käsittelee myös keinoja hyödyntää liikkumisessa Marsin paikallisia energialähteitä, kuten tuuli- ja lämpöenergiaa. Useita erilaisia energiankeruutapoja esitellään ja arvioidaan. Vaikka kaikki tutkitut konseptit eivät heti vaikuta toteuttamiskelpoisilta, on ne kuitenkin esitelty mitään pois jättämättä, jotta ne voisivat olla innoittajina tuleville uusille asiaan liittyville tutkimuksille.

Avainsanat: Mars-tutkimus, bioniikka, liikkuvat robotit, pallorobotti, aro-ohdake, salsola tragus

HELSINKI UNIVERSITY OF TECHNOLOGY

Abstract of the Licentiate Thesis

Author: Tomi Ylikorpi

Name of the thesis: A Biologically inspired rolling robot for planetary surface exploration

Date: 21.11.2005 **Number of pages:** 112

Faculty: Automation and System Technology

Professorship: Automation Technology (Aut-84)

Supervisor: Professor Aarne Halme

Planetary exploration missions often aim to carry out in-situ analysis and possibly return samples to Earth for more thorough examination. Recent robotic missions to Mars have demonstrated effectiveness of robotic exploration of planetary surface. Purpose of a mobile robot on planet surface is to enlarge the area to be investigated, and to concentrate investigations on subjects with most scientific interest. The application of biomimetic locomotion to the Martian surface offers the possibility of increased robustness and failure tolerance of a mobile robot. This study searches for new innovations from nature and aims to develop a novel system to provide robust and efficient locomotion system to be used for exploring surface of foreign planets. Especially this work describes definition and conceptual development of a rolling robot –later called 'The Thistle' mimicking a Russian Thistle –plant. The study considers locomotion and power generation methods that would utilize local power generation resources like wind or heat. This study involves the identification and conceptual development of innovative concepts for planetary surface locomotion and energy collection. Several concepts are presented and evaluated. Considering nature of the study, although evaluation reveals some concepts probably not adequate, these are not removed from the thesis, but are left here for the interest and further inspiration of the reader.

Keywords: Planetary exploration, mobile robots, tumbleweed, salsola tragus, biomimetics, wind propulsion, ball-shaped robots

Acknowledgments

The research for this Licentiate Thesis was done at the Helsinki University of Technology's Automation Technology Laboratory during the years 2004-2005. The Thesis is partly based on work performed under ESA-Contract in Ariadna program 'Biologically inspired solutions for robotic surface mobility', Call AO4532-03/6201. I wish to thank ESTEC personnel for their support, especially Mr. Mark Ayre and Mr. Andres Galvez, as well as our whole project team at the lab. Laboratory engineer Mr. C-G Rosenblad made an excellent work in manufacturing the fancy sails that in addition to being completely functional also give the inspiring outlook for the Thistle prototype. Our technician Mr. Tapio Leppänen manufactured the mechanical details that made the ball to roll.

I wish to express my gratitude to Professor Dr. Aarne Halme who supported this space-related research and encouraged me to prepare the Thesis. Many thanks to my colleague Dr. Matti Anttila for our shared interest, dedication and co-operation in space research, as well as for helping in finalizing the literary work. Credits for assistance in Thesis lay-out belong also to Mr. Ilkka Leppänen. Finally great thanks to my wife Eija for being supportive and interested in such a peculiar branch of science.

Otaniemi, 21.11. 2005

Tomi Ylikorpi

Table of Contents

List of Tables

List of Figures

1 Foreword

This thesis rests on and continues author's work performed in context of European Space Agency's (ESA) project 'Biologically inspired solutions for robotic surface mobility', Call AO4532-03/6201 under ARIADNA-program of ESA's Advanced Concepts Team (ACT). The work was performed at Automation Technology Laboratory of Helsinki University of Technology and the results were reported in the final report delivered to ESA Aug. 18th 2004. [1]

This work describes definition and conceptual development of a rolling robot –later called 'The Thistle' mimicking a Russian Thistle –plant. Although an extensive search on similar studies concerning ball-shaped robots on Earth and for Martian exploration was carried out during the ARIADNA-project, the continuing study and search for references revealed some additional information also after the ARIADNA-project was concluded. In this thesis these new sources of information are included and discussed, -among new developments and testing of the prototype robot. Contents of this thesis concentrate more on the on-surface rolling motion and passes discussion on alternative locomotion methods that was included in ARIADNA-report.

2 Introduction

The planetary objects to be explored in future have surfaces of varying properties. Some planets are covered with fluid; some moons or asteroids have icy or snowy cover. When considering scientific results that would be gained through moving around and exploring planet surface, objects with sandy or rocky surface seem the most interesting at the moment, although swimming and diving -or even flying- robots might be very interesting subjects on planets covered by fluid or a gaseous atmosphere. Even these rocky planetary objects have a much varying nature; some are hot, some are cold, some have atmosphere, some do not, some have volcanic activity and some do not, some have magnetosphere and some do not, etc. etc.

Purpose of a mobile robot on (or even below or above) planet surface is to enlarge the area to be investigated, and to concentrate investigations on subjects with most scientific interest. To fulfill this objective the robot can carry out necessary investigations while it is moving around, or it can transfer the instruments to the places of interest –or soil/rock samples back to the lander for more accurate investigations.

Requirements on mobility are directly derived from the scientific requirements. The required distance between measurement points drives the design of the locomotion system and, in particular, its speed. This latter, in turn, together with the minimum number of measurements, drives the minimum time of presence on the surface needed to accomplish the scientific goal. According to ESA ExoMars09 CDF Study Report [2] minimum distance specified is 0.5 km, and maximum is 2 km, and number of samples to be collected is 10, which makes minimum travel distance 5 km, in case the system does not return to the lander at all, but acquires and sends the data autonomously.

Basic problematic is shared among all the rocky/sandy planets: we do not exactly know what the terrain would be like. We can assume that there is some sand and some boulders, but we cannot tell what would be the bearing capacity of the sand and what would be the size and distribution of the boulders. The largest amount of information on planetary surface composition considers nowadays the Moon and the Mars. From these two the Mars is currently more interesting regarding the missions and landers being planned at the moment.

Having already visited on surface of Mars (with the aid of robotic landers), one can already make some assumptions on size and distribution of the rocks on Mars surface, and one already knows, that sand appears to have a good bearing capacity there. Therefore moving around on Mars surface is merely a question of generating the necessary propulsion force and avoiding to get stuck on any obstacle that could be a boulder, a sandy dyne, a slope or even a canyon. Fig. 1 presents an anticipated model of Martian terrain as presented in ESA ExoMars09 CDF Study Report. [2]

In order to avoid obstacles there are basically two options: a) navigate among obstacles and avoid them, and b) build a robust platform that can overcome the obstacles. Obviously the optimal solution uses both approaches; one cannot build such a big robot that would never fall or get stuck in any size of a slope, crack or canyon. It is also obvious that for a small vehicle a small object can become an obstacle, while a large vehicle usually can overcome larger obstacles. It is also clear, that on a planet surface there usually exist numerically much more small obstacles than large ones. Therefore, navigation needs for a moving robot increase rapidly as robot size decreases, unless robot mobility is increased significantly to overcome the obstacles.

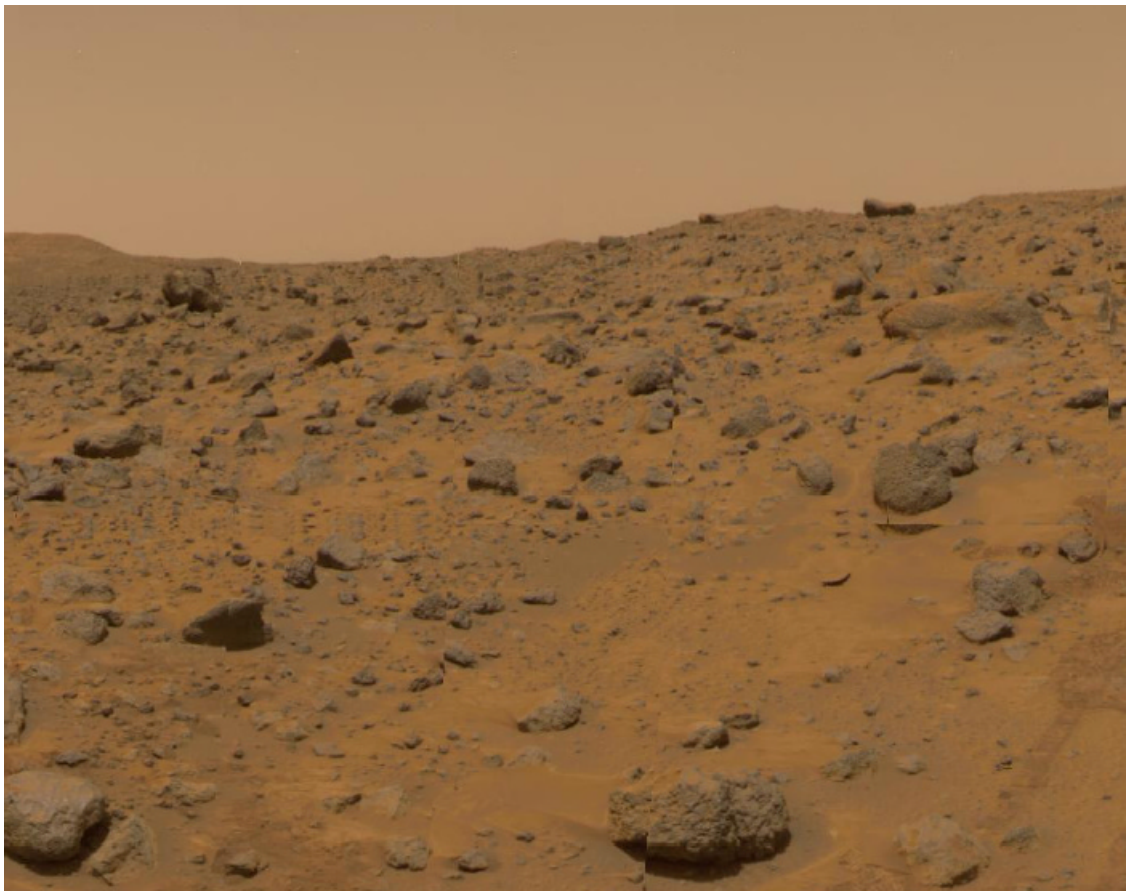

	Maximum	Minimum	Units
Terrain assumptions			
Percentage of rocks with size bigger than 0.5 m in the landing site	1.00		%
Percentage of rock coverage (rocks from 10 to 20 cm high)	20.00		%
Max slope	15.00		deg
Percentage of gaps with depth bigger than 0.25 m and width less than 0.25 m	1.00		%
Max altitude landing site	1.00		Km

Fig. 1. Anticipated model of Martian terrain. [2]

This leads us to one possible conclusion (among several possible conclusions): to build a robust and reliable moving robot it must either: a) be small in size and navigate with high performance -like a snake or a mouse etc., b) be small in size and have exceptional locomotion capability to overcome any obstacles (i.e. climbing, flying, jumping) -like a grasshopper or c) be large enough to overcome most of the expected obstacles (and have some navigation to avoid the larger rocks or cracks) -like an elephant.

Intelligent mechanical models of snakes, mice, cockroaches etc. have already been developed. However, although the corresponding biological animals living in Martian-like environment in deserts have amazing mobility, so far the robots have not demonstrated such a locomotion capability, speed or payload capacity, which would

justify their design as a surveying rover platform. Either they are too small to carry any payload, or they become far too heavy and clumsy. Never they have been fast. Wheeled vehicles do have capability for fast motion and payload capacity too, but their performance decreases rapidly when terrain becomes soft or uneven.

It is desirable to develop new locomotion methods that would exceed performance of currently familiar systems. In question then become the small vehicles with exceptional locomotion capability, or more large vehicles with novel techniques that would solve problematic with mass and power generation.

3 Locomotion on Mars and other planets

3.1 Objective

Purpose of a mobile robot on planet surface is to enlarge the area to be investigated, and to concentrate investigations on subjects with most scientific interest. Area covered by the robot depends on its speed and available travelling time, as well as on possible tether and communication methods that bind it on the lander. The travelling time may be limited by power sources and mechanical durability. Locomotion speed depends on rover cross-country capabilities, power, navigation and autonomy.

The strongest limitations for mobility are the available power and challenges caused by the terrain, which deserve close investigation when developing new efficient locomotion methods. If challenges caused by complex geography can be reduced (i.e. cross-country capability can be increased), needed locomotion power can be expected to be reduced and locomotion speed increased.

3.2 History

A quick glimpse on past planetary rovers and vehicles reveals majority of wheeled vehicles, while also a couple of novel designs has been presented.

3.2.1 Phobos hopper

For the Martian moon Phobos hopping was found to be a suitable way of mobility because of its low gravity (1/500 of that of Earth). The Russian PROP-F hopper presented in Fig. 2 was designed to travel on Phobos' surface. This robot was mounted on the Phobos 2 spacecraft. Contact to the spacecraft was lost in 1989 before deployment of the hopper. [3] Hopping mechanism relies on release of spring stored energy, and the 'aerials' that are used to re-position the hopper after landing in correct position. The spring could be re-loaded with the aid of an electric motor.

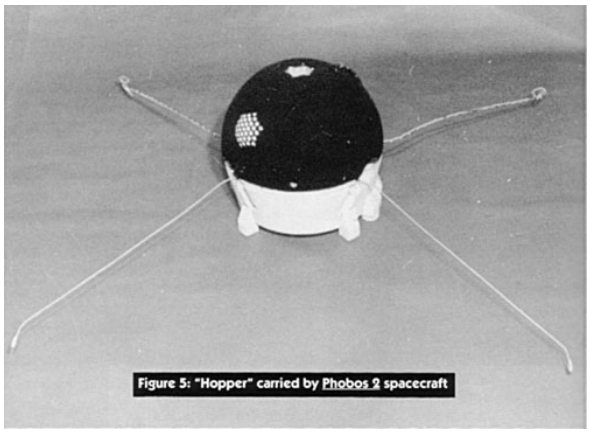

Fig. 2. The Phobos Hopper.

3.2.2 Soviet Mars-rovers

In 1971 the Soviet Mars 2 and 3 missions carried two small robotic rovers (one shown in Fig. 3) onto Mars. Another mission crashed onto Mars, while contact to the other was lost before deployment of the rover. The rovers were connected to the lander with a 15 m long tether. Mobility was provided by two skis that were used to walk along the surface. Between the steps the rover would lay down on its belly. Opposite direction of ski-motion would make the rover to turn. With an external mechanical sensor the rover would detect any obstacles and then would autonomously back-off a few steps and change direction before continuing its travel. [3]

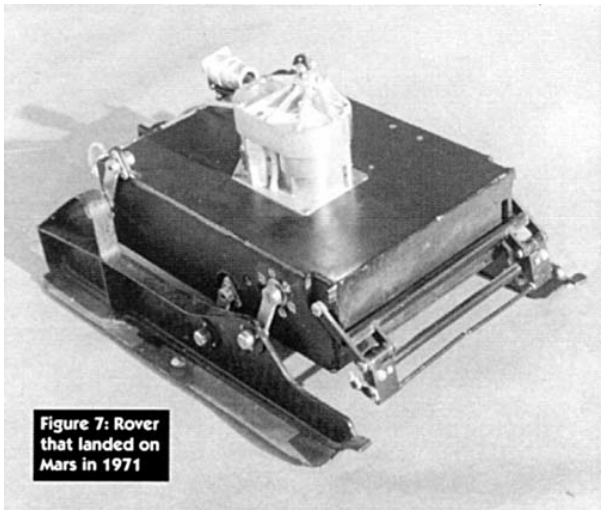

Fig. 3. The Mars Rover.

3.2.3 Lunokhod

The Soviet Lunokhod-vehicles explored the surface of the Moon. The Lunokhod's mass was 750 kilograms, and its speed was 0.8 to 2 kilometres per hour. The robot was tele-operated from Earth. The Lunokhod, illustrated in Fig. 4, carried an airtight compartment with a temperature-control system, an isotope heat source, a radio and television transmitter, a command receiver, a power plant, a remote control, a small-frame television, panoramic tele-photometers and scientific instruments. [3]

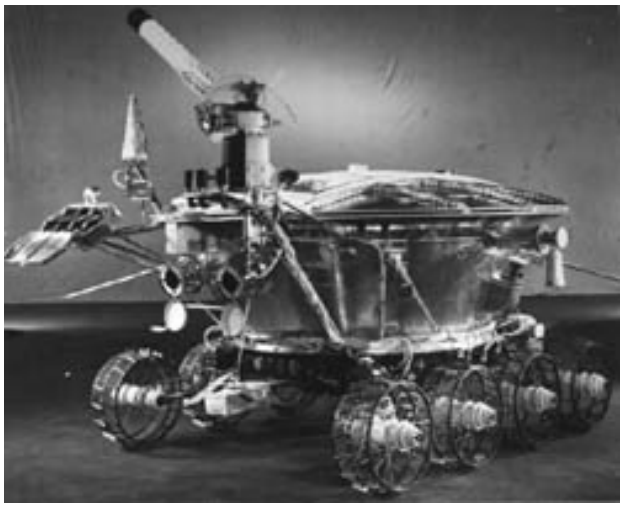

Fig. 4. The Lunokhod.

3.2.4 Apollo Moon vehicle

The Lunar Roving Vehicle (LRV) was an electric vehicle designed to operate in the low-gravity vacuum of the Moon. Three LRVs were driven on the Moon, as seen in Fig. 5. In practice the LRV was an electric car used by the astronauts. The LRV had a mass of 210 kg and it was designed to hold a payload of an additional 490 kg on the lunar surface. The frame was 3.1 meters long with a wheelbase of 2.3 meters. Two 36-volt silver-zinc potassium hydroxide non-rechargeable batteries provided power with a capacity of 121 amp hr. [4]

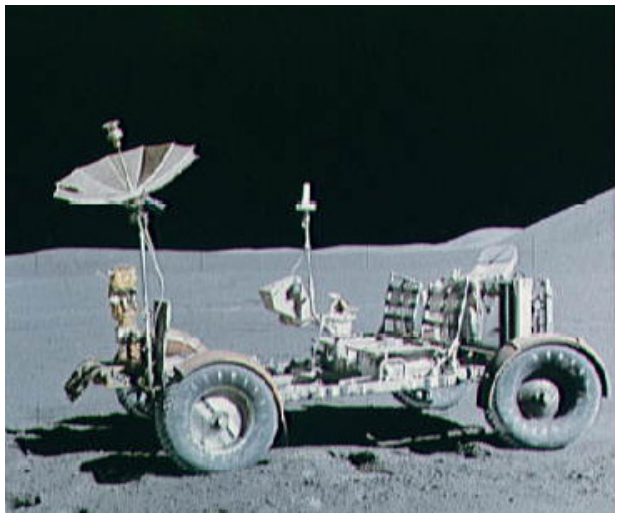

Fig. 5. The Apollo Lunar Rover.

3.2.5 Sojourner, Opportunity, Spirit

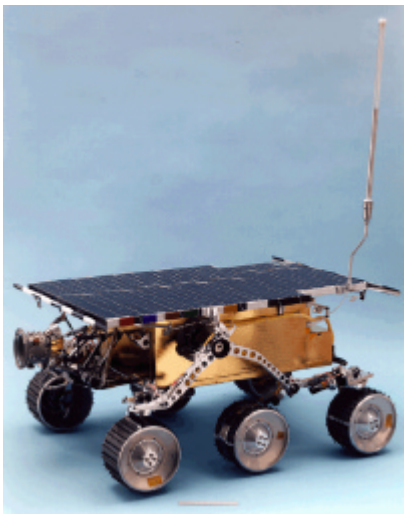

Fig. 6. The Sojourner.

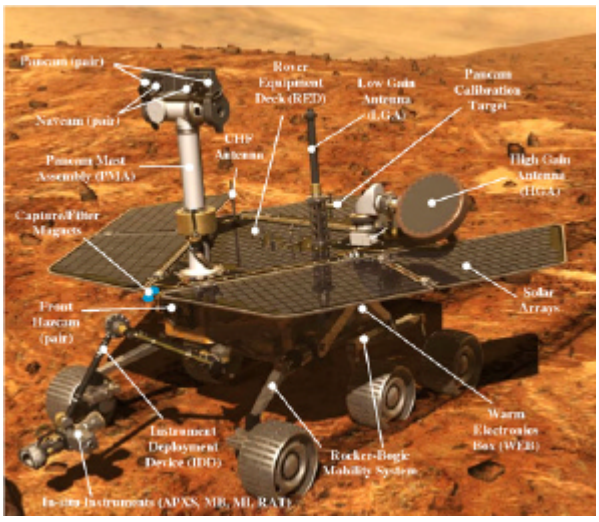

Fig. 7. The Opportunity.

The NASA rovers ‘Sojourner’ (Fig. 6), and ‘Opportunity’ and ‘Spirit’ (Fig. 7) present the latest roving technology on surface of Mars. The Sojourner being of a smaller size (11 kg) and the two other of a larger scale (185 kg) present all a similar basic structure with a rocker-bogie type chassis equipped with 6 wheels. The Sojourner could travel 40 cm/min while the bigger ones have a speed of 3 m/min. (Images [5] [6].)

3.2.6 Pluto

Pluto (planetary under surface tool) as the mole is called, has the ability to crawl across the surface at the rate of 1cm every 5 seconds. The device is shown in Fig. 8. Pluto’s locomotion is based on internal hammering mechanism and shocks, like in terrestrial penetrometers. Pluto can collect samples in a cavity in the tip, which opens when the mole reaches a sampling location. The mole could crawl up to three metres away from the lander, including the burrowing phase; it is recovered by rewinding the cable with a winch. The device has a total weight of 950g and power consumption only a couple of watts. [7]

Fig. 8. The Pluto.

3.3 Future

Plans for coming planetary vehicles seem to rely largely on wheeled rovers. However, also a large magnitude of research is being carried out to develop alternative solutions. Main drivers for the new innovations are in general smaller mass, smaller power, longer life time, increased area coverage and higher robustness.

3.3.1 Mars Science Laboratory

Mars Science Laboratory, illustrated in Fig. 9, would be a rover similar to previous ones, but significantly larger. A long duration rover equipped to perform many scientific studies of Mars is planned for a late 2009 launch. The mission is planned to last at least one Martian year (687 days). The rover would be four- to five-times larger than the current Mars rovers, i.e. it would have a size of a mini-van. [8]

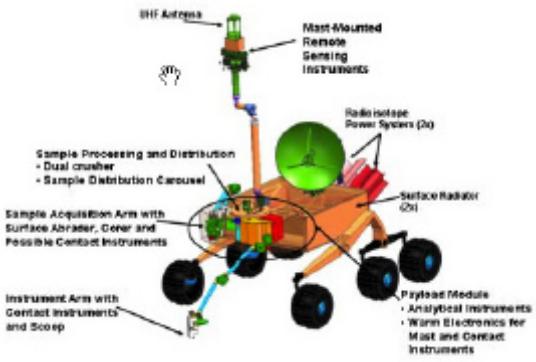

Fig. 9. The Mars Science Laboratory.

3.3.2 Marsokhod

Marsokhod, shown in Fig. 10, is a Russian 6-wheeled rover with articulated body. It possesses remarkable locomotion capability and multiple locomotion techniques. Marsokhod has been studied widely in Europe, USA and Asia for future Mars and Moon missions. (Image [3])

Fig. 10. The Marsokhod.

4 Biomimicry

Biomimetics is essentially the practice of taking ideas and concepts from nature and implementing them in a field of technology. Already Leonardo DaVinci studied plants and animals and designed mechanical solutions to provide similar structures and operations. Biomimetic engineering is, like any organism or function that it is imitating, highly multidisciplinary, and includes aspects related to materials, structures, mechanical

properties, computing and control, design integration, optimization, functionality and cost effectiveness.

As robotic exploration of the Solar System continues, the requirements for autonomy and robustness will increase; the long communication times involved between the Earth and Mars for example mean that the next generation of surface rovers will be required to act autonomously. Abundance, survivability and performance of terrestrial plants and animals demonstrate the potential that biomimetic engineering could provide. The application of biomimetic locomotion to the Martian surface offers the possibility of increased robustness and failure tolerance. [9]

5 Rolling locomotion in nature

To begin with one should first check, what has been already invented in nature. The possible advantages of biomimetic locomotion are a robust negotiation of obstacles and rapid motion on complex and unpredictable terrain. The preferred mode of locomotion is obviously environment-dependent, and the suitability of proposed techniques must be justified in the context of the environment in which they will operate. The existing environmental features to aid the locomotion can reveal interesting solutions: like rolling down the slopes (totally free energy), or flying around carried by the wind (like a dandelion seed). The ‘rolling bush’ or ‘tumbleweed’ does the both: rolls around driven by the wind.

Water flow or snow avalanche express exceptional traveling capacity: although without any propulsion of their own, they travel driven by the gravity and pass by or over any obstacles placed in the way. Here the traveling object has enough flexibility to naturally go around or over the obstacle. Similar action takes place in car tire: small stones and bumps enter inside the tire, while center of gravity of the tire/car travels straight forward above the ‘obstacle’. In a similar manner a large ‘almost flat’ tire or a flexible ball would overcome any smaller obstacles on Martian surface.

Considering the efficiency and speed of the wheeled vehicles, it seems a bit surprising that nature does not seem to utilize a wheel-design at all, despite of a few curiosities among insects and sea-animals.

Some bacteria have a flagellum-like swimming device, which has no counterpart in more complex cells. These bacteria swim by rotating their flagella and the flagellum acts as a rotary propeller. The flagellum is a long, hair-like filament embedded in the cell membrane, as may be seen in Fig. 11. The flagellum filament is the paddle surface that contacts the liquid during swimming. The ‘motor’ that rotates the filament-propeller is located at the base of the flagellum, where several ring-shaped structures are made visible by electron microscopy. Obviously these bacteria do utilize a sort of rotary mechanism, but not as directly as a wheel for locomotion. [10]

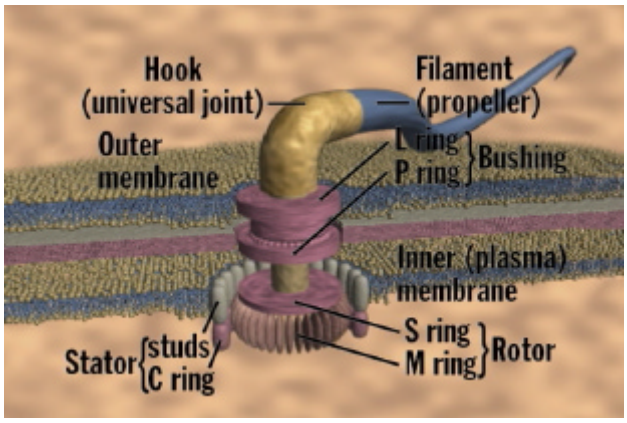

Fig. 11. A bacteria utilizing a rotary mechanism. [10]

Several smaller and bigger animals can also adopt a form of a wheel and rotate in a more or less controlled manner. However, even these creatures do not have any wheels, but they roll themselves, as unity.

Stomatopods, living mainly in shallow waters, are elongated organisms with only short and modest legs. Occasional storm may sometimes drop them on the beach where the creature's swimmerets and legs are of almost useless. Some stomatopods have developed an ingenious solution to get back to the sea. The small stomatopod Nannosquilla decemspinosa (Fig. 12) lives along the Pacific coast of Panama, and is frequently washed on shore by waves. This mantis shrimp has legs completely insufficient to get the animal safely back to ocean. Instead the animal moves across the sand by backwards somersaulting, moving as far as 2 meters at a time, rolling 20-40 times with speeds of up to 72 revolutions per minute, or 1.5 body lengths per second (3.5 cm/s). The stomatopod functions as a true wheel around 40% of the time making a series of rolls. In between it has to restart a roll by using its whole body to thrust itself upwards and forwards. This little creature shows clearly an active method of locomotion by rolling. The rolling energy seems to be adopted from kinetic energy of body motions. [11]

Fig. 12, Image showing movement of N. decemspinosa as it rolls along a beach. [11]

The salamander Hydromantes platycephalus has adopted a novel antipredator mechanism that consists of body and tail coiling and limb tucking followed by passive rolling escape. Although coiling is widespread among salamanders, H. platycephalus performs it in the novel context of the steep slopes of the northern Sierra Nevada of California. This results in the peculiar anti-predator mechanism of rolling escape. Obviously the defense mechanism is active; i.e. the salamander adopts a spherical posture actively, but the following rolling phase is passive; the animal will roll downwards if it happens to be located on a slope steep enough. [12]

Possibly inspired by above mentioned salamanders the Dutch artist Escher imagined and illustrated a 6-legged animal that also had an ability to cover large distances by rolling. The animal would give and maintain speed by pushing forward with its legs. Escher also describes procedures how to enter into rolling mode and two options how to return into walking mode. Entering is a straight-forward curling of animal body –as shown in Fig. 13. Return to walking mode can happen in two ways; the animal can straighten abruptly which finally sets the animal laying on its back, or the animal can un-curl slowly in a controlled manner starting from the tail and so return to original walking mode. Locomotion is clearly active, and while rolling itself is continuous, the power implementation (by kicking speed from ground) is sequential. [13]

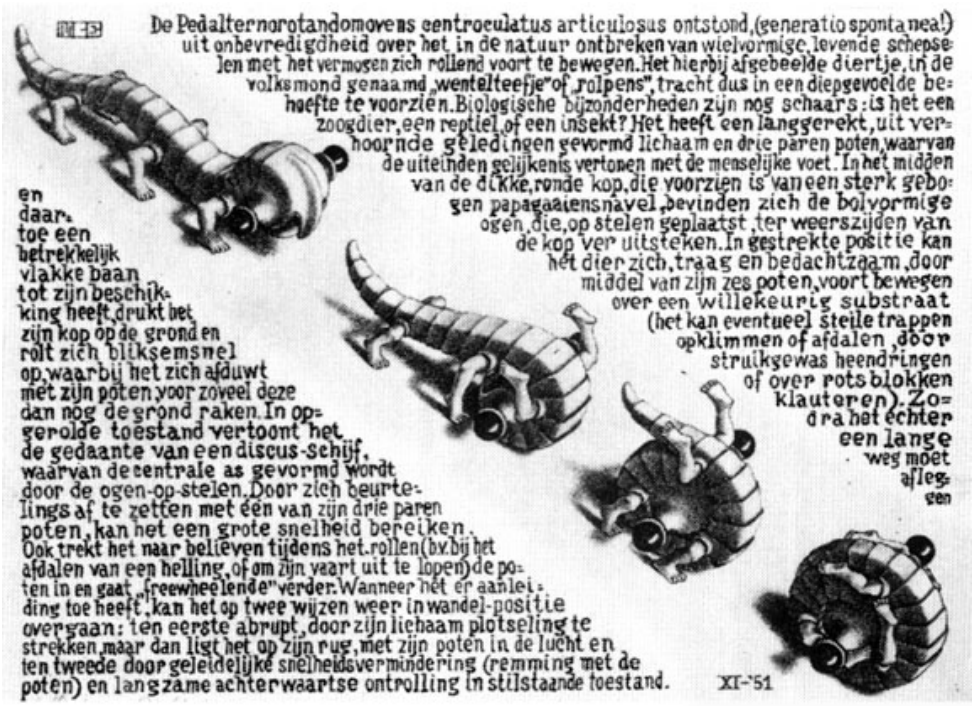

Fig. 13. M.C. Escher's Curl-up
Cordon Art B.V. - Baarn - Holland. [13]

Some existing animals; at least bears, chimpanzees and humans are able to curl-up in a similar way and do somersaults. Human athletes can also cartwheel. Possibly due to our nervous system, vision, and balance, and also due to our physical structure these methods of locomotion can not be utilized as a mean for covering long distances, but are only used for fun and to present physical skills. However, these stunts indicate methods to transfer energy to rotational motion. Obviously these stunts use legs and hands to push speed from ground, and rotation is assisted with unbalancing body weight.

The Russian thistle looks like the skeleton of a normal shrub. Plants may be as small as a soccer ball or as large as a small car. By autumn the plant has reached maximum size, it has flowered and it starts to dry out. A specialized structure in the stem facilitates the

easy break between plant and root, and the plant can be carried away by the wind. As it rolls away blown by the wind a Russian thistle disperses seeds, which typically number 250,000 per plant. Each seed is a small, embryonic plant. To survive winter the plant does not germinate until warm weather arrives. When moisture falls, the plant is ready to germinate. All that is needed is temperature between 28 and 110 degrees Fahrenheit (-2-43°C). [14]

Fig. 14. A Tumbleweed [14]

Considering the limited existence of a wheel in nature, a conclusion can be made that the nature has not invented it all, and not all man-made inventions are bad. An ultimate solution might well be a hybrid construction of natural and man-made inventions. Or the construction may even rely on solutions that are not based on nature nor technology, but on human imagination.

6 Some existing ball-robot designs

Sphere is “the set of all points in three-dimensional space lying the same distance (the radius) from a given point (the centre).” (Encyclopedia Britannica Online).

Spherical shape provides a complete symmetry and a soft, safe and friendly outlook without any sharp corners or protrusions which is of advantage when a robotic device is dealing with people. In view of robotics a spherical structure can freely rotate in any direction and all positions are stable, it can not fall down. While propulsion system is located inside the ball it can be made hermetically sealed to provide the best possible shield for the interior parts. Spherical shape maximizes the internal volume with respect to surface area and provides an optimal strength against internal overpressure or underpressure which is an important feature for underwater and space applications. The greatest technical challenges related to the spherical shape are limited off-road capability and challenging controllability. Step climbing capability is defined by the radius of the ball and the ratio of the masses of the cover and the unbalanced mass. Typically the static step climbing capability is less than 0.25 x R.

6.1 Terrestrial applications

History of ball-shaped autonomously moving vehicles is long while also recent studies have presented a variety of applications in different environments including marine, indoors, outdoors, zero-gravity and planetary exploration. Engineers are often advised not to invent a wheel again. However, a quick search on U.S. Patent office database reveals immediately more than 50 patents related to autonomous mobility of a ball-shaped object. These patents date from 1897 to 2003 and all comprise a motorized counterweight that is used to generate ball motion. Obviously number of related patents in USA and worldwide is much larger than the result of this quick search. Number of similar one-wheeled and two-wheeled counterweight-based vehicles is even larger.

6.1.1 History of self-propelled movable balls in relation to some U.S. patents

The first vehicles were small spring-powered toys with one fixed axis of rotation. The patents concentrate on methods to store and convert spring energy with different mechanical solutions. In 1906 B. Shorthouse patented a design that had a possibility to manually adjust position of the internal counterweight in order to make the ball to roll along a desired curved trajectory instead of a straight path (U.S. Patent 819,609). Ever since several different mechanisms has been patented to produce more or less irregular rolling paths for self-propelled balls. Fig. 15. dating 1909 presents one innovative way to produce a wobbly rolling motion for an amusement toy.

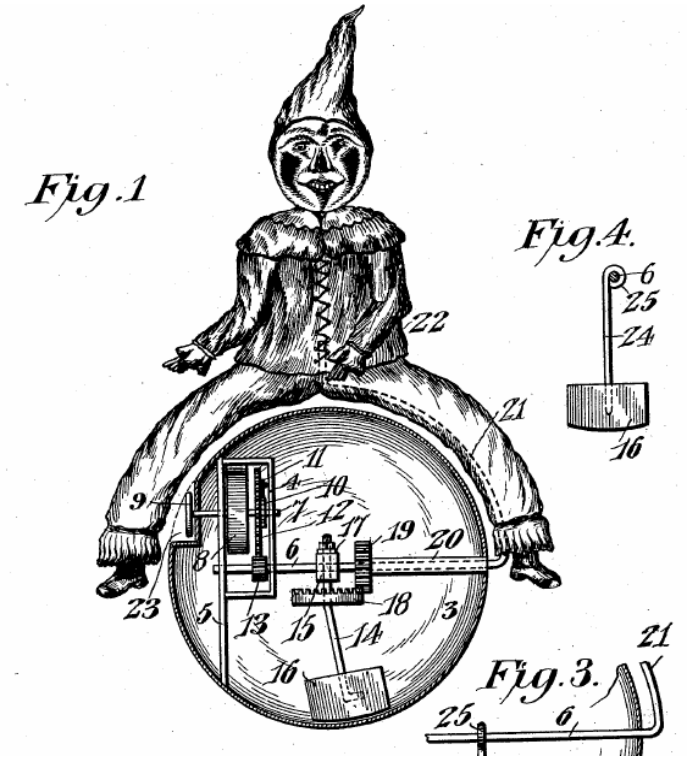

Fig. 15. Mechanical Toy by E.E. Cecil, (U.S. Patent 933,623)

The counterweight was usually constructed with a lever rotating around the ball axis. Mobility was provided by generating a torque directly to the lever. Amount of torque needed from the power system was directly proportional to the mass of the counterweight and length of the lever arm. In 1918 A.D. McFaul patented a ‘hamster-ball’-design (a derivative of hamster running wheel) where the counterweight was moved by friction between ball inner surface and traction wheels mounted on the counterweight (Fig. 16.) In this construction the length of lever arm does not any more affect on needed power system torque, and similar mobility can be achieved with smaller internal torque. Obviously this is a great benefit for spring-driven toys, at least if they would have a large diameter.

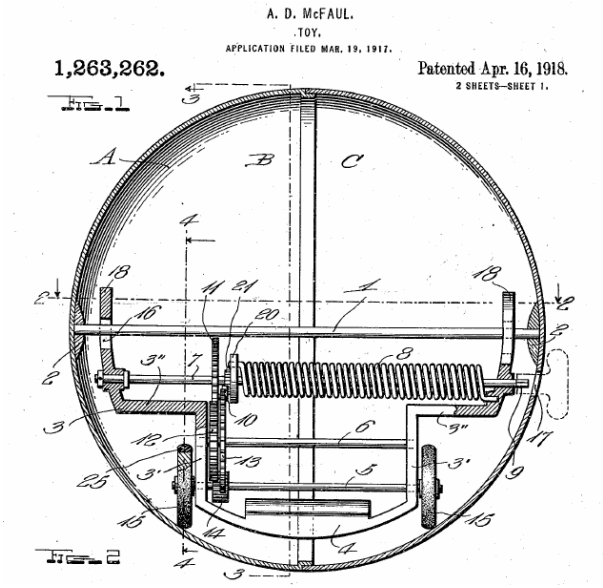

Fig. 16. Early ‘hamster-ball’ by A.D. McFaul, (U.S. Patent 1,263,262)

A mechanical spring as a power source was displaced by a battery and an electric motor in a patented design made by J.M. Easterling in 1957 (U.S. patent 2,949,696). Consequently electric motors were introduced with several different mechanical solutions that were at least partly familiar already from earlier spring-driven inventions. Further development introduced shock and attitude sensing with mercury switches that would control motor operation and rolling direction, as well as added light and sound effects.

“Squiggle ball” is a small one-dof. toy that, not so different from Easterling’s patent in 1957 or the ‘Toy ball’ by E.A. Glos II in 1958 (U.S. Patent 2,939,246), wanderers around floor and with an amazing capability gets around almost any obstacle. A similar design is presented also in U.S. patent 5,934,968 in 1999. This patent has become familiar from furry toy-creatures attached onto a small ball bouncing endlessly inside a box. Squiggle balls were studied when developing the Rollo-robots at HUT in 1996.

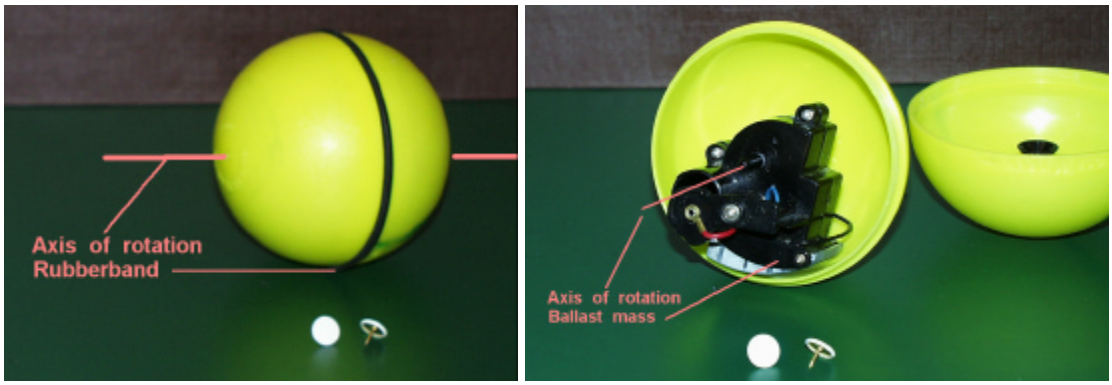

Fig. 17. A ballast driven "Squiggle ball". (Image: TKK)

The Squiggleball motion is based on ballast drive, see Fig. 17. One important feature of the ball is the rubber band running around the ball and sharing the axis of rotation. First of all the rubber band gives friction so that upon contact on an obstacle the ball does not start slipping, but the ballast mass starts to rise around the axis of rotation. As the ballast reaches the top dead centre the ball suddenly rotates ½ revolutions backwards. The rubber band also extends a bit outside the sphere surface. This causes the axis of rotation to be slightly tilted from horizontal plane. Because of this, as the ballast mass elevates above the axis, it also generates a torque on sideways. So, as the ball autonomously reverses its rotation for ½ rotations, it at the same time tends to fall aside and in this way it automatically changes its direction of motion. Acting in this manner with very simple mechanical solutions this small ball can get around almost any obstacle and it exits also dead-ends of a labyrinth. The tilted axis of rotation makes the ball to arc instead of running straight forward. This way the ball follows any walls in vicinity and finds slots or doors without any intelligence or guidance.

An active second freedom for a motorized ball was introduced by McKeehan in 1974, as shown in Fig. 18. In addition to reversible rolling motion, upon impact on obstacle the ball would also change its axis of rotation with the aid of additional motors. This opens the way towards radio-controlled (introduced in 1985 in U.S. Patent 4,541,814) and finally computer controlled ball-robots. As (radio-controlled) toy-cars became more common they were since 1984 (U.S. Patent 4,438,588) frequently inserted inside the ball to provide a fully steerable 2-dof. rolling toy.

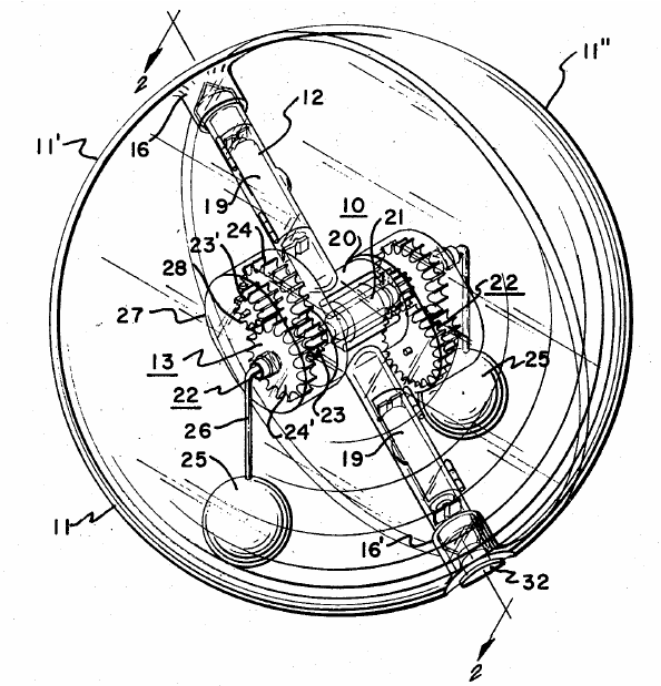

Fig. 18. A 2-dof. ball by R.W. McKeehan, (U.S. Patent 3,798,835)

The ball robot ‘Rollo’, developed at Helsinki University of Technology, Automation Technology Laboratory in 1996, is probably the first modern model of a ball shaped mobile device. It is a mobile robot based on a ball structure. The robot has two degrees of freedom which it can use for selecting the rolling direction and then for rolling back- and forward. Mobility is based on internal off-balance, i.e. the mass inside the robot ball is moved away from the center which makes the ball to rotate.

Fig. 19. Mobile Ball-Shaped Robot ‘Rollo’.

The construction of the 2-dof. mechanism is completely different from any other of the spherical robots introduced so far. It has a horizontal rolling axis similar to most of the above mentioned examples. An unique feature is that the rolling axis is mounted on a circumferential rail, that may be seen in Fig. 19, so that direction of the axis can be rotated with respect to spherical shell. Quite challenging kinematics and control requirements develop as the circumferential rail rotates along with the shell during ball locomotion. However, locomotion is possible using either of the rotating freedoms.

The robot is designed to act as a small platform to carry sensing devices or actuators in an environment where stability of the platform is critical, like in surveying unstructured hostile industrial environment or exploring other planets, or simply being a part of a human place, like office or home, which has not been designed for mobile machines. The robot is easily made liquid and gas proof, it recovers easily from collisions, the cover can be made mechanically durable and the robot cannot turn over or fall down. All the robot systems are fully constrained inside the ball cover. Dynamical properties, motion control and mechanics have been studied with the prototype robots and simulator. The spherical construction offers extraordinary motion properties in cases where turning over or falling down are risks for the robot to continue its motion. Also it has full capability to recover from collisions with obstacles or another robots traveling in the environment. Prior to current design two earlier versions for the robot IDU (Inside Drive Unit), both shown in the Fig. 20 below, were built. The first version (on the right) was quickly replaced with the second version on the left. The second generation had two completely de-coupled freedoms which made it easy to control and drive. However, requirements set for the spherical shell were most stringent and the cover was difficult and expensive to manufacture. The current third generation allows a transparent and inexpensive cover. [20]

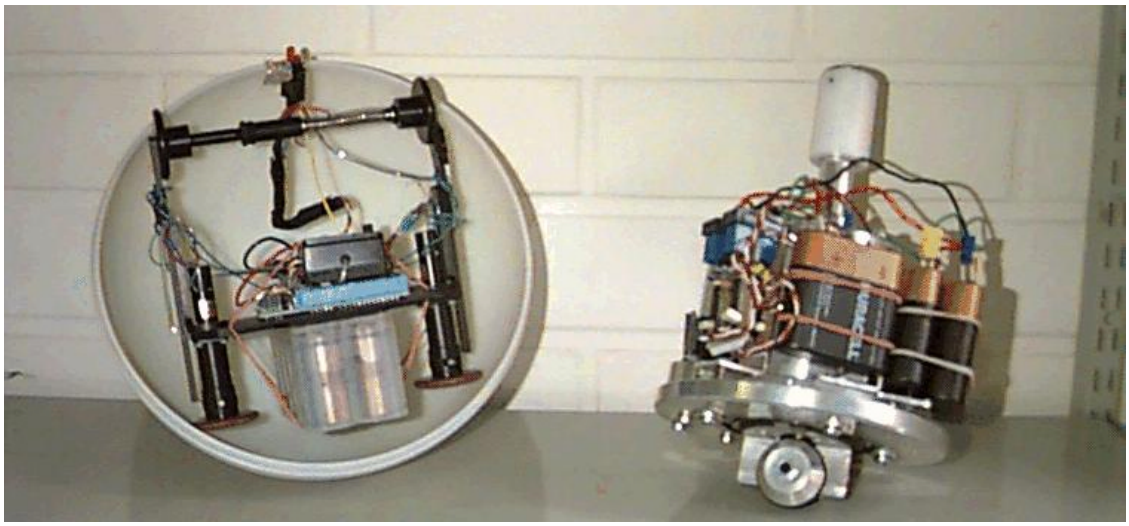

Fig. 20. Earlier prototypes of the TKK ball robot.
'Hamster ball'-inspired type on the left and an 'unicycle' on the right.

The Sphricle is an Italian ball robot based on unicycle-design (similar to hamster-ball but with a single wheel inside the sphere as may be seen in Fig. 21). It was developed in

1997 and is used for education and investigation of kinematics, dynamics and control of this nonholonomic system. [19]

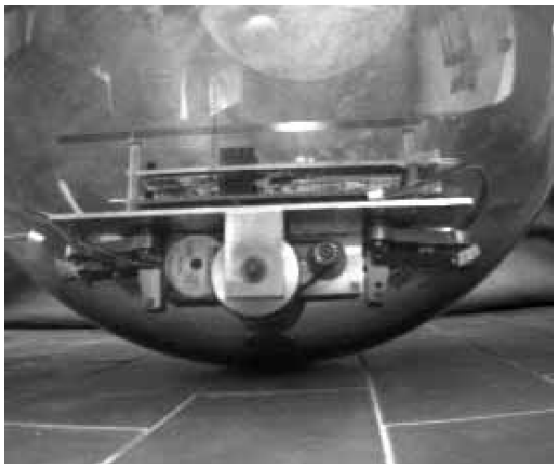

Fig. 21. The Sphericle. [19]

Cyclops (developed in 1998), shown in Fig. 22, was funded by U.S. Defence Advanced Research Project Agency (DARPA) and is a teleoperated 5.5 inches (14 cm) diameter and 4.5 pounds (2 kg) Miniature Robotic Reconnaissance System developed either for a reconnaissance to gather information in unknown environment, or to patrol in an already secured area in indoor space. It has 2-dof. mobility provided by forward/reverse roll mechanism based on off-balanced mass and novel inertial steering that has not been presented in any of the other ball robots described in this thesis. [16]

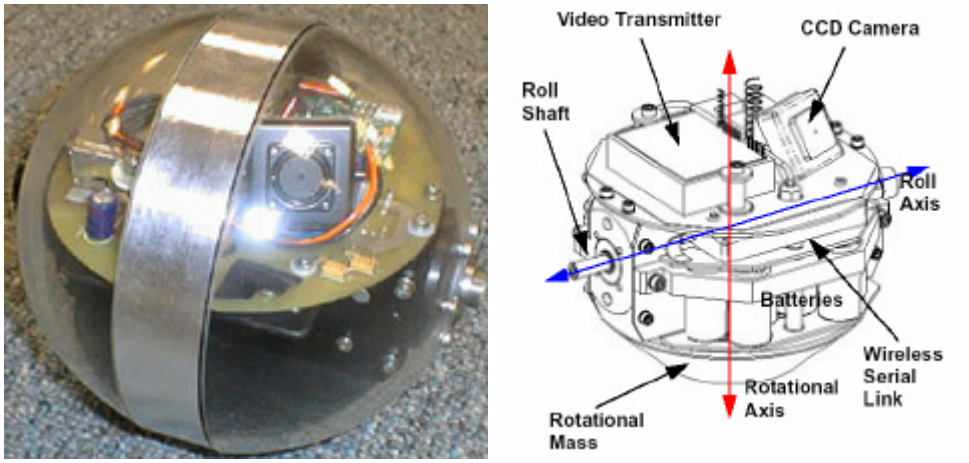

Fig. 22. The Cyclops. [16]

The Canadian Roball (developed in 1998, U.S. patent 6,227,933) has basically similar driving system as the Rotondus (see Fig. 23 and Fig. 24). It is 6 inches (15 cm) in diameter and weights 4 pounds (1.8 kg). The Roball has been developed to act as an interactive toy for children, and an extensive study has been performed explore

interaction between people and this robot. The findings are used to develop lay-out and behavior of the robot further to generate a genuinely interactive robot. [18]

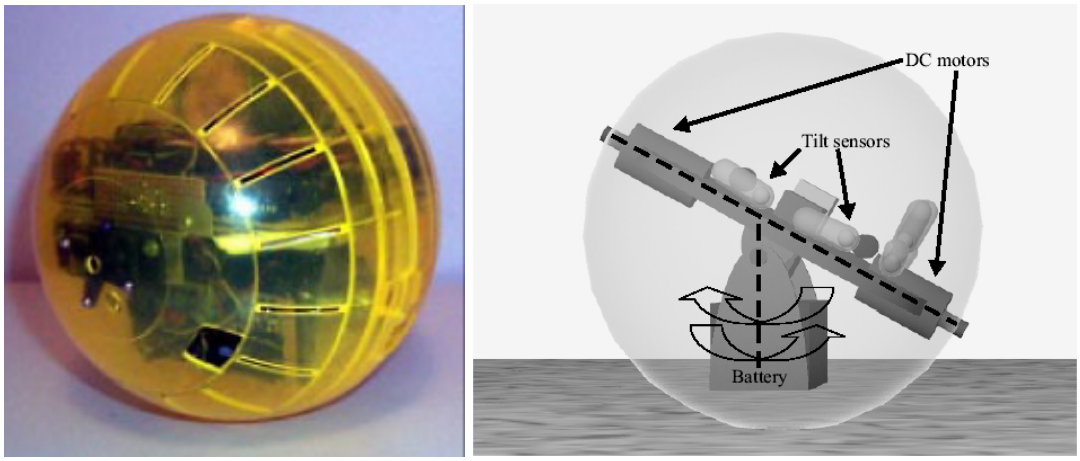

Fig. 23. The Roball. [18]

The most recent inventions introduce new novel solutions to alter position of the ball center-of-gravity. One example is the Spherical Mobile Robot by R. Mukherjee patented in 2001 that uses several separate weights that are moved with the aid of linear feed systems (U.S. Patent 6,289,263). [15]

Rotundus, developed around 2004 and pictured in Fig. 24, is a Swedish pendulum driven (equals to movable off-balanced mass) and steered rolling robot for surveillance, reconnaissance and inspection applications. It has a diameter approx. 0.5 m, it weights few kilograms and it can reach 30 km/h speed. Principle of pendulum steering was introduced also in U.S. Patent 819,609 by B. Shorthouse in 1906 (manual pre-set) and U.S. Patent 4,501,569 by Clark et.al. in 1985 (electric steering). [17]

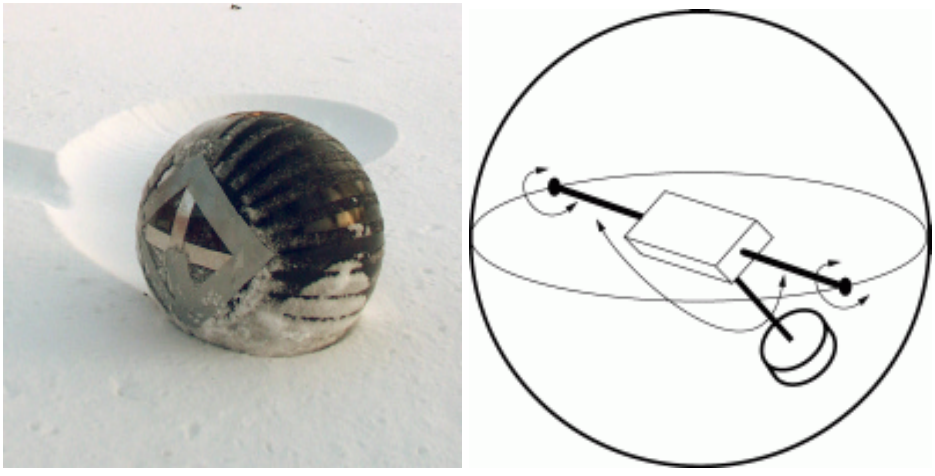

Fig. 24. Rotundus. [17]

6.1.2 Spherical vehicles to carry people

Spherical vehicles to carry people were first developed for marine applications, like the one by W. Henry in 1889 (Fig. 18.) This vehicle with its passenger floats in the water, balanced by ballast mass and weight of the passenger. The vehicle would move in a very similar manner as the toys described above with balanced mass inside and outer surface rolling. Steering would happen by tilting the axis of rotation by moving the passenger mass inside the vehicle. In 1941 J.E. Reilley patented a ball-shaped car (Fig. 26.) and later different types of chairs have been inserted inside a spherical vehicle. In some cases a person would enter a ball and operate it directly without any additional means, like a hamster inside his running wheel.

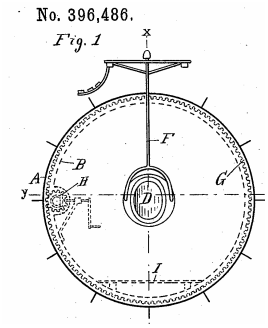

Fig. 25. A marine vessel by W. Henry (U.S. Patent 396,486)

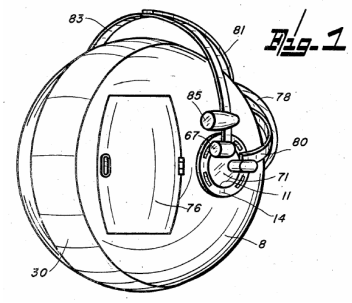

Fig. 26. A Spherical vehicle by J.E. Reilley (U.S. Patent 2,267,254)

6.2 Applications for planetary exploration

Most of the above mentioned developments of the rolling robots have been shortly presented also in references [21] and [23]. However, these articles concentrate more to give an overview on large wind-driven spherical devices intended for exploration of Mars surface. It has been shown that development of wind-driven rovers for Mars has been under investigation in several places already since late 1970's. Here follows a short conclusion of work done so far.

6.2.1 The First Tumbleweed

Jacques Blamont in France developed the first idea of a wind-driven rover for Mars exploration already in 1977. The concept constituted of a 3-10 m inflatable ball that also had an inner drive mechanism for powered locomotion. [21]

6.2.2 Mars ball

In 1987 Blamont's idea was developed further in Arizona University where a 500-kg Mars Ball was prototyped. The Mars Ball was not actually a ball, but a cylindrical rover with two wheels composed of several inflatable sections, as seen in Fig. 27. The rover would move driven by sequential deflation and inflation of wheel sections. [21]

Fig. 27. The Arizona University Mars Ball. [21]

6.2.3 JPL Tumbleweed

In 1995 JPL produced large wind-driven ball that also had a steering and driving capability with a movable mass mounted on the central axis. The motorized concept was rejected because of its modest capability to cross obstacles and development was re-directed towards large three-wheeled rovers with inflatable tires. [21] Fig. 28 presents some such concepts in [22].

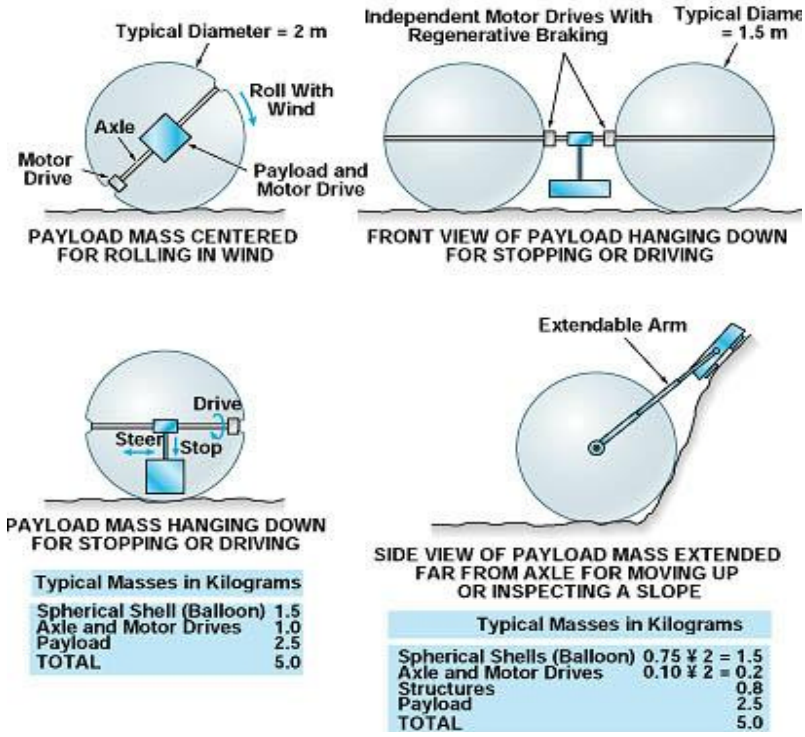

Fig. 28. Early JPL Tumbleweed. [22]

In 2000 during testing of the three-wheeler the idea of a wind-propelled ball was re-born and development to produce a new wind-driven exploration rover was initiated again. The Tumbleweed robot shown in Fig. 29 and developed at NASA JPL has been demonstrated and tested successfully in small 1.5 m diameter scale on deserts and Antarctica. The Tumbleweed rover derives its name from the dead sagebrush balls that blow across the deserts of the American southwest. Likewise, the rover's only means of locomotion is the ambient wind. A 6-meter diameter Tumbleweed is envisaged for deployment on the surface of Mars. Such a ball could potentially serve as its own descent and landing system, replacing parachutes and airbags. While its mobility is dependant on the wind, the Tumbleweed rover will have some ability to control its speed by regulating its level of internal pressure. The Martian Tumbleweed would be comprised of a 20 kg ball and a 20 kg payload suspended from the center. Traveling at speeds up to 10 m/s in the 20 m/s wind of a typical Martian afternoon, the ball is expected to climb 20° slopes with ease. [30]

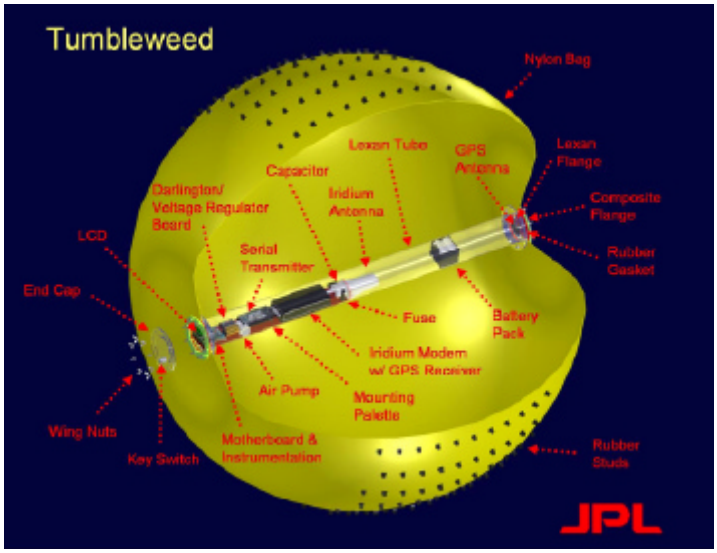

Fig. 29. The Tumbleweed developed in JPL. [30]

6.2.4 LaRC

NASA Langley Research Center (LaRC) development on Tumbleweed concept was inspired by the Pathfinder landing on Mars in 1997. The above mentioned JPL-driven development relies on an inflatable structure, but LaRC approach has adopted deployable rigid structures as seen in Fig. 30. A lot of research has been paid on aerodynamic properties and foldability of the system. [23]

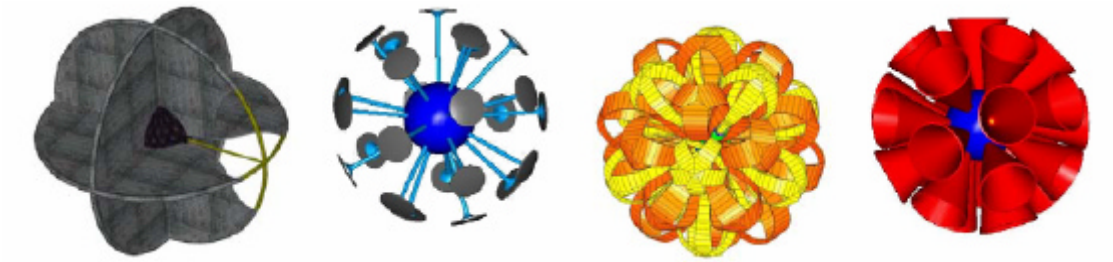

Fig. 30. LaRC Deployable Tumbleweed Concepts: Box Kite, Dandelion, Eggbeater Dandelion, and Tumble-cup. [23]

6.2.5 Texas Tech University

In Texas Tech University (TTU) a senior Mechanical Engineering design class project has developed additional Tumbleweed concepts in 2001, as shown in Fig. 31. [24]

Fig. 31. TTU Tumbleweed concepts. [24]

6.2.6 NCSU and Fred J. Carnage Middle School

The Mars Tumbleweed Design Project was also attended in collaboration between the NASA Langley Research Center and the North Carolina State University (NCSU) Aerospace Engineering Space Senior Design Class. In addition Tumbleweed was introduced to sixth grade science students at Fred J. Carnage Magnet Middle School in August 2002. [21], [25]. Some of the designs may be seen in Fig. 32.

Fig. 32. NCSU and Fred J. Carnage Magnet Middle School Tumbleweed designs. [25]

6.2.7 Windball

Windball is a Swiss study on a wind-propelled exploration rover for Mars. Also here an extensive research effort has been paid for aerodynamic properties and cross-country performance. Two versions of wind-ball were developed: a shape memory alloy (SMA) actuated Hardball (Fig. 33 left) and an inflatable Softball (right). [26]

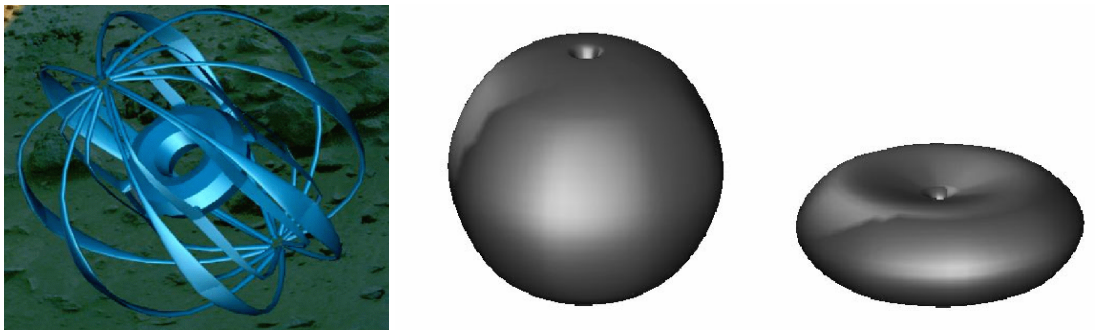

Fig. 33. The Swiss Hardball and Softball. [26]

6.2.8 Wormsphere Rover

An Iranian proposal for a Wormsphere Rover introduces a design quite similar to that of Arizona University. Although of a spherical design, also this concept would move actively driven by sequential shape change of spherical shells located in the outer wall of the ball (Fig. 34). [27]

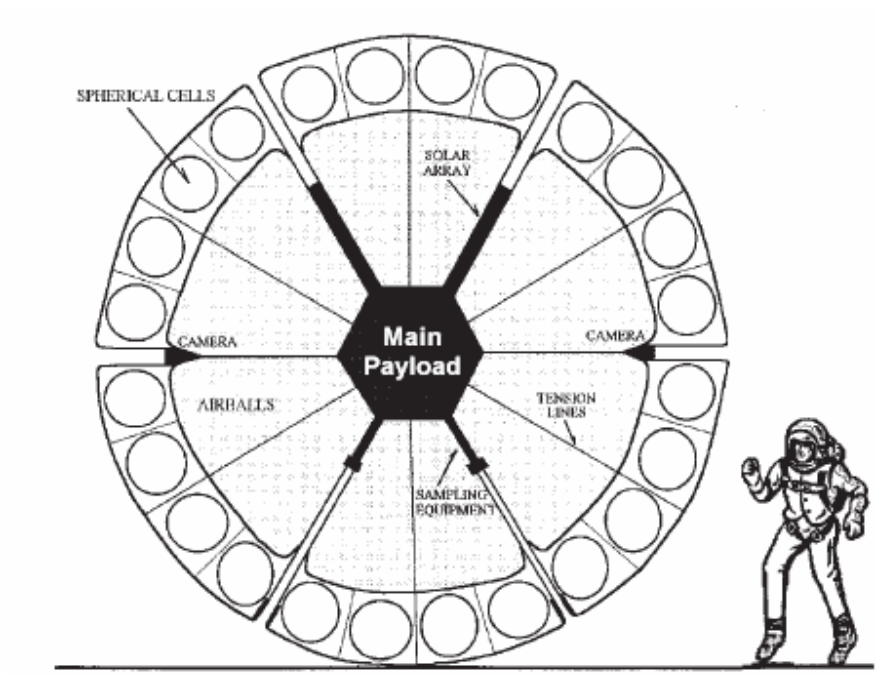

Fig. 34. The Wormsphere Rover. [27]

7 Mars environment

7.1 Gravity

Gravitational acceleration on Mars surface is 0.38 times of that of Earth. According to NASA National Space Science Data Centre (NSSDC) Mars Fact Sheet [33] Gravitational acceleration on Mars surface is 3.727 m/sec^2.

7.2 Terrain and rock distribution

Discussion here on the Martian terrain is limited to aspects concerning mainly surface mobility. Important factors then are slope angles and size and distribution of rocks.

On basis of existing experience load carrying capacity of Martian sand can be expected to be sufficient. Rolling resistance and slippage on loose sand may become a challenge on areas with smaller number of rocks and on sandy dynes.

The Fig. 35 and table below present terrain properties assumed for European Mars rover and the following picture illustrates analytical results on the size and distribution of rocks over several Martian landing sites.

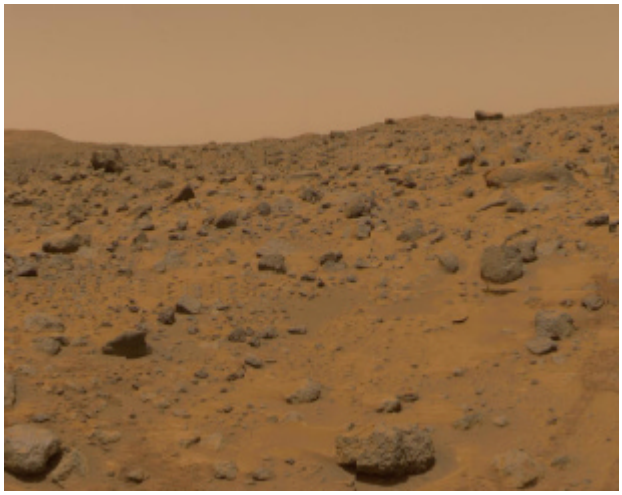

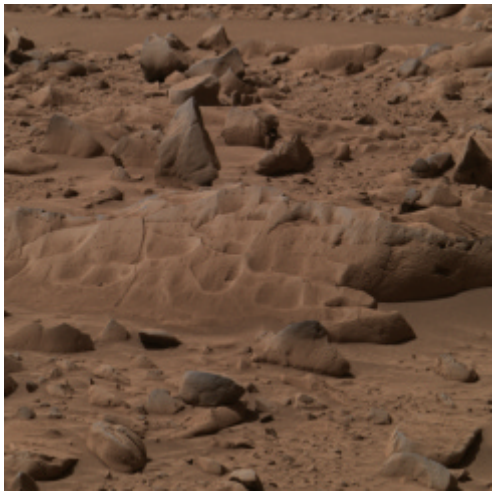

	Maximum	Minimum	Units
Terrain assumptions			
Percentage of rocks with size bigger than 0.5 m in the landing site	1.00		%
Percentage of rock coverage (rocks from 10 to 20 cm high)	20.00		%
Max slope	15.00		deg
Percentage of gaps with depth bigger than 0.25 m and width less than 0.25 m	1.00		%
Max altitude landing site	1.00		Km

Fig. 35. Images (Courtesy NASA/JPL-Caltech) and anticipated model of Martian terrain. [2][6]

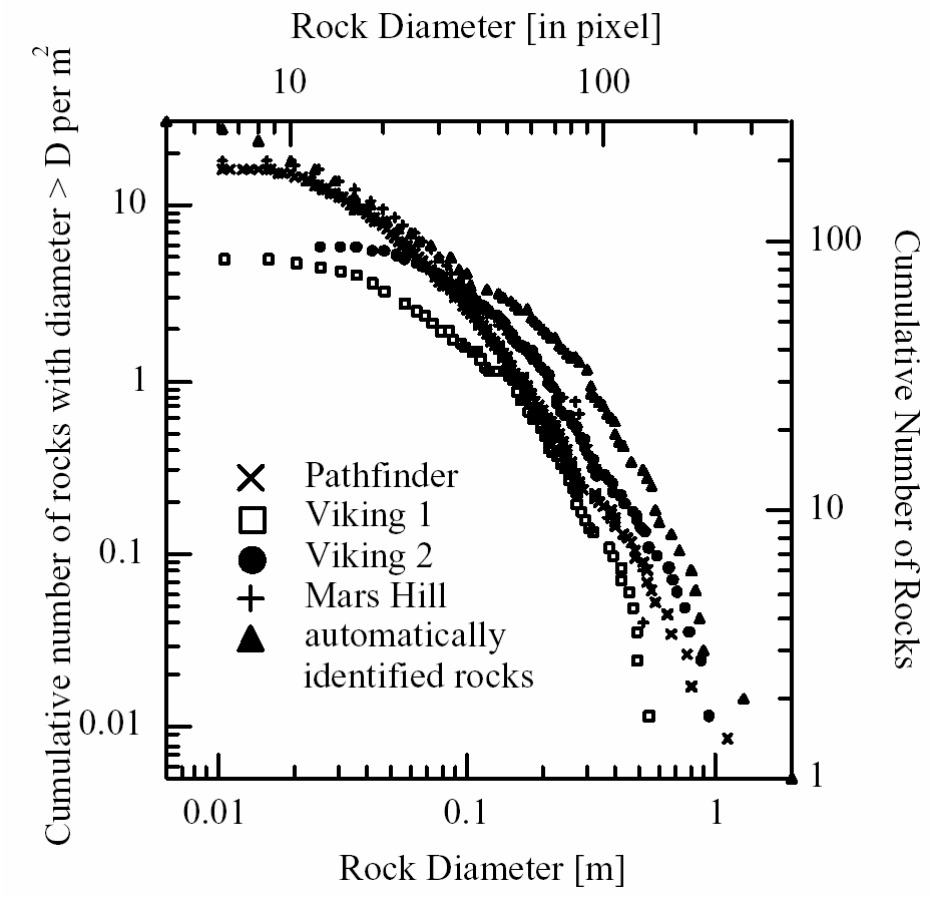

Fig. 36. Rock Diameter vs. Cumulative Number of Rocks [35]

Quick study of the Fig. 36 presenting cumulative number of rocks with different diameter reveals that abundance of rocks 1 m in diameter or larger is roughly 2 per 100 m^2, number of rocks 0.5 m or bigger would be 3-30 per 100 m^2. Number of rocks 10 cm or bigger would be 1-8 per m^2, (or 100-800 per 100 m^2). Rocks smaller than 10 cm are not considered since the project expects to develop a system that would overcome those rocks regardless of their abundance.

The rock distribution is mostly fully randomized, i.e. the rocks do not lie within constant distance from each other. Therefore it is practically impossible to calculate any real mean distance between the rocks. In some locations they may be visible and close to each other in high numbers, while only a short distance away may reveal a smooth and rock-free terrain. Variation in rock distribution is large between different landing locations. In the following discussion we consider the worst-case scenario and assume even distribution of rocks.

If we assume that 1 m rock height is the limit for the rover climbing capability, we attempt to calculate mean distance of travel after which the rover probably needs to carry out an obstacle avoidance procedure (go around or jump over). If we assume that we

have 2 large rocks per 100 m^2, and we have a 50 m^2 circle around each, radius of circle would be ~ 4 m, and distance between the rocks would be ~8 m.

In a similar manner we can calculate the mean distance between rocks of any particular size. The results have been collected into Table 1 below.

The table shows that in the worst case during a 100 meter journey we have to go around 22 rocks bigger than 90 cm, or overcome total of 87 stones bigger than 50 cm but smaller than 90 cm. Every 80 cm travel we have to overcome a stone that is larger than 10 cm but smaller than 20 cm.

The calculation assumes, that the robot would accidentally travel straight from stone to stone, but in reality distance between 90 cm stones would be 11 meters, so even a probabilistic chance would be high to pass by the stones already by coincidence, not to mention possible use of camera and navigation system. Perhaps only one rock out of three happens to lie on the robot's path of travel. Between rocks smaller than 90 cm the mean distance starts to approach dimensions of the robot and probability to meet the stone increases.

It should be noted that this is a worst-case approximation. Variation of rock-distribution may reveal a 10 times smaller number of rocks and more than three times (square root of 10) longer mean distance between.

Table 1. Calculated mean distance between rocks on Mars surface.

Rock size	Abundance	Limited size envelope	Abundance	Mean distance between	Number per 100 m travel
cm	per 100 m2	cm	per 100 m2	m	
>100	2	>100	2	8.0	13
>90	3	90-100	1	11.3	9
>80	6	80-90	3	6.5	15
>70	10	70-80	4	5.6	18
>60	15	60-70	5	5.0	20
>50	30	50-60	15	2.9	34
>40	60	40-50	30	2.1	49
>30	100	30-40	40	1.8	56
>20	200	20-30	100	1.1	89
>10	400	10-20	200	0.8	125

In this analysis an attempt was made to picture how often (in terms of meters traveled) a rover would encounter a rock of a specific size. A rather discouraging result was obtained: distance between rocks 1 m in diameter or larger appears to be only rough 8 meters. In some photographs from Mars landers this appears to be true, however.

A different approach was adopted in [29] where a mathematical expression was developed to describe rock size distribution and likelihood to encounter a rock of

specified size was calculated. A statement is made that number of rocks encountered is approximately 4 per square meter, which agrees on with calculations presented above. The probability distribution function is expressed as:

$$F(D) = 1 - e^{-sD}$$
$$where:$$
$$s = 3.38 \quad (1)$$

A F(D) is defined as a likelihood that the rock encountered has a diameter less than or equal to D. If we set D=0.9 m we can calculate F(D) to be 0.952. So, likelihood that the rock encountered is larger than 0.9 m is 1-0.952 or 0.0477. So, for 400 rocks encountered 19 (0.0477 x 400 = 19) of those would be larger than 90 cm. This mathematical model indicates somewhat higher number of large rocks than the table above. This is well understood as the mathematical model is based on Viking data which is more towards large rocks than the Pathfinder data, as shown in Fig. 36.

Also [26] presents a table with rock size distribution data. When compared to table above [26] indicates a smaller number of small rocks (166 pieces in dia. >10 cm per 100 m^2) and a similar number of large rocks (5 pieces in dia. >90 cm per 100 m^2). This is even though the source data is mentioned to be the same as for the calculations in [29].

7.3 Atmosphere and winds

Discussion handles atmospheric properties that can be of importance for surface mobility and power generation. Such properties are air pressure, air density, wind speed, and air temperature.

NASA National Space Science Data Center (NSSDC) Mars Fact Sheet [33], The DLR HRSC-Experiment web page [31] and [32] present the following data on Martian atmosphere:

"Atmospheric pressure is 7 mbar with quite high variation (25-30%). (Atmospheric pressure on Earth sea-level is 1013 mbar.) Atmospheric density on Martian surface is ~0.020 kg/m^3, while on Earth at sea-level it is for standard temperature of 15°C 1.225 kg/m^3."

"Mean molecular weight of Martian air is 43.34 g/mole. The Mars atmosphere constitutes of the following gases: CO_2 (95.32%), N_2 (2.7%), ^{40}Ar (1.6%), O_2 (0.13%), CO (0.07%), H_2O (0.03%)." [31]

NSSDC Mars Fact Sheet [33] reports Martian wind speeds 2-7 m/s (N summer), 5-10 m/s (N fall), and 17-30 m/s (dust storm).

Nasa QUEST discussion [36] on the Pathfinder wind measurements indicates that the wind direction rotated throughout the day: from the south at night, westerly in the mornings, northerly in late afternoon, and from the east in the evening. Naturally

fluctuation of wind direction would have an effect on any mobile device driven by the wind. In general, winds were strongest in the early morning hours and were relatively strong around noon. The lightest winds were seen in late afternoon and early evening.

Mars Pathfinder Historical Weather Data [37] reports measurements performed by the Pathfinder over more than 30 sols starting July 4 1997. The landing site in the Ares Vallis region is at 19.33°N, 33.55°W. The prevailing winds were light (less than 10 meters per second, or 36 kilometers per hour) and variable. The Fig. 37 below shows how the wind direction and speed changes during one sol and repeats sol after sol. (The wind-speed chart lacks quantitative information on real wind velocity.)

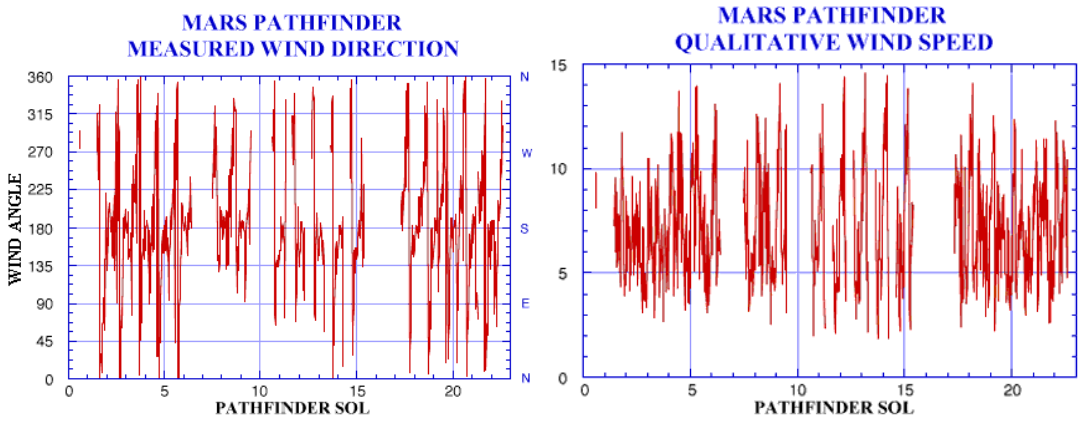

Fig. 37. Wind measurements made by the Pathfinder. [37]

7.4 Solar flux

Solar flux is of interest in terms of energy production by direct conversion to electricity with solar cells or by utilization of collected thermal energy with novel techniques.

Length of a Martian day is 24h and 39.6 min, and a Martian year lasts 669.60 Martian days (roughly 1.88 Earth years). Solar irradiance at the Martian distance from Sun is 595 W/m^2. [31]

However, because of the harsh atmospheric conditions on Mars, the solar irradiance may be significantly decreased at the surface. [38]

7.5 Temperature

As well as solar flux also temperature is of interest in terms of energy production. However, heat as itself is usually difficult to use as an energy source. In general a temperature difference is needed to produce any activity. This thermal gradient may realize in terms of geometry (cold and hot parts of the system) or in time (repeated heating and cooling).

On Mars surface average temperature is ~210 K-220 K (-63 - -53°C) , while Viking Lander-1 measured diurnal temperature range 184 K-242 K (-89 - -31°C) [33].

The Fig. 38 below shows air temperatures measured by the Pathfinder at Ares Vallis region (19.5 deg. N, 32.8 deg. W) [37]. In July, 1997, the sun was directly over the 15 degrees north latitude region of the planet. The temperature reached its maximum of 263 Kelvins (–10 degrees Celsius) every day at 2 p.m. local solar time, and its minimum of 197 Kelvins (–76 degrees Celsius) just before sunrise.

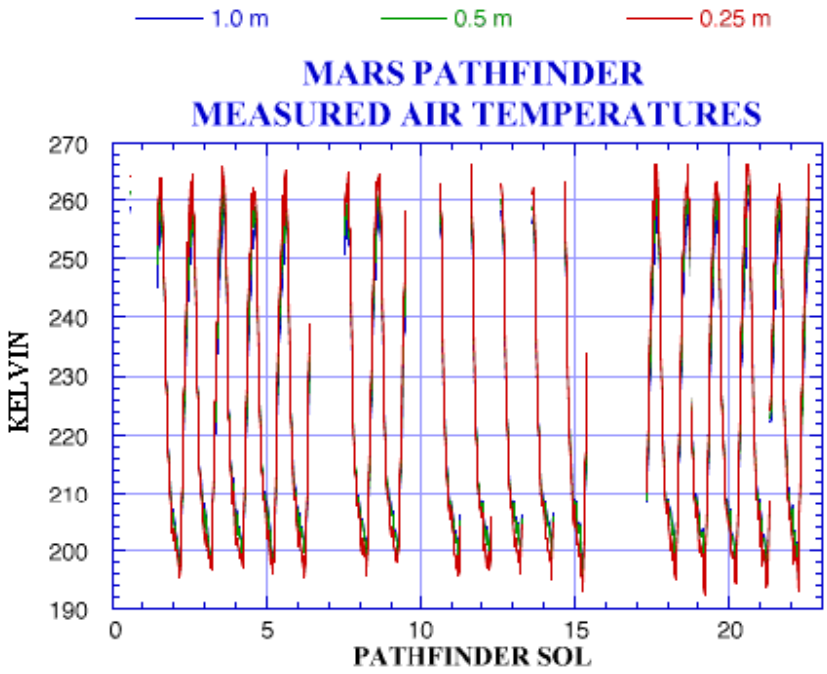

Fig. 38. Measured Mars air temperature. [37]

Reference [2] illustrates calculations of temperatures for sky, air and ground for two cases that are hot and cold (depending on day of the year and location on Mars surface). For the hot case Ls = 180° and latitude = 45°, for the cold case Ls = 270° and latitude = 45°. See Fig. 39 and Fig. 40.

The graphs indicate that significant diurnal fluctuation of temperature could be utilized to generate energy on a daily cycle. Also temperature difference between air and ground could be utilized for energy production.

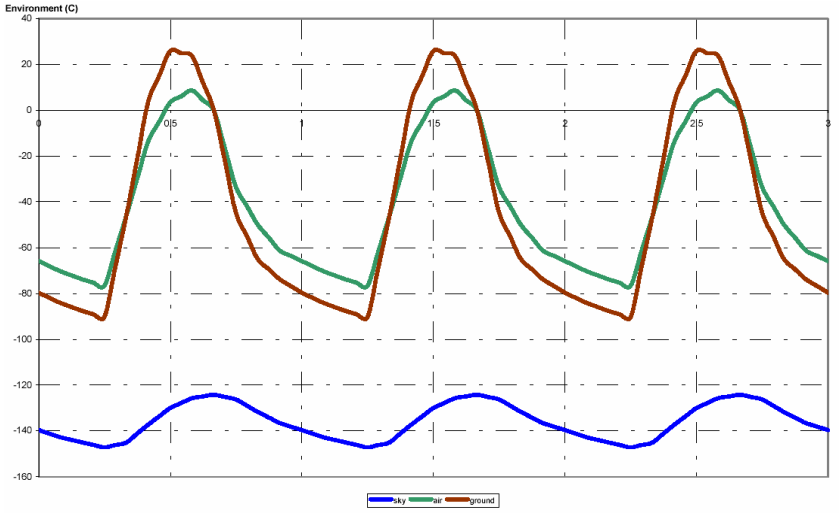

Fig. 39. Temperature of Martian Hot Case over 3 Days; sky (blue), air (green), and ground (red). [2]

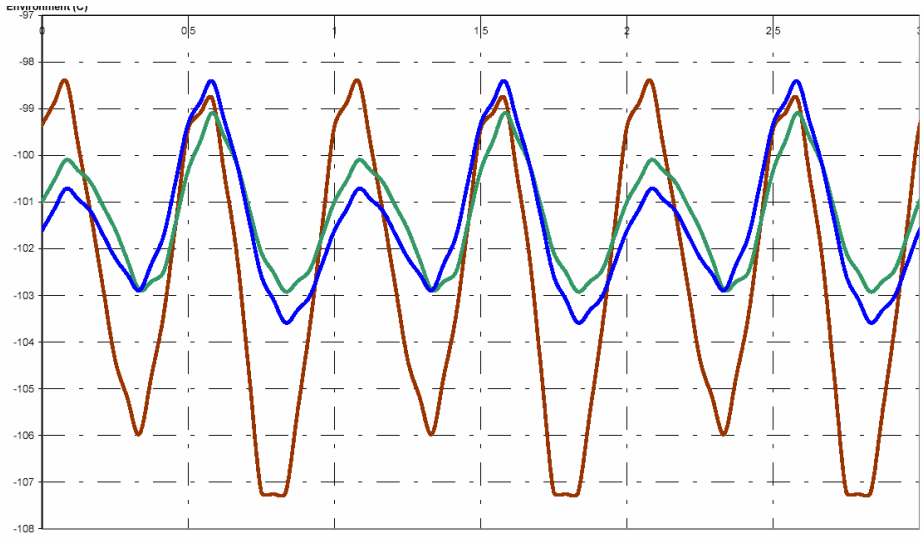

Fig. 40. Temperature of Martian Cold Case; sky (blue), air (green), and ground (red) [2]

8 Mission requirements

8.1 Mission description

When landed the mission would start by deployment of the Mars rover from the lander or from the landing configuration and preparation for operation. After deployment the rover can immediately start the first science cycle making the desired measurement and/or sampling procedures and transmitting the data. After the science phase the rover can enter to locomotion phase that lasts until the next science phase. The locomotion and science phases would be repeated until the end of mission.

Length of locomotion and science phases depends on area to be explored, number of measurements to be performed and time needed for analysis and communication. Also some time for household keeping and possibly for battery re-charging may be required.

Survival in harsh Martian environment may become a challenge. Viking Lander 1, landed on July 20, 1976, ceased operation after 2,245 sols (2,306 days) on Mars. The Viking landers were powered by radioisotope thermal generators (RTG). Pathfinder lander was operational for 90 days, and the Sojourner rover lived 84 days. Limited –but still much longer than designed- life time of Pathfinder mission is related to depletion of the spacecraft's battery and a drop in the spacecraft's operating temperatures due to the loss of the battery. For a new long-term exploring mission a few terrestrial-months could be expected, six months would be a significant extension, while terrestrial 1-2 years for a mobile robot would be desirable.

So far the distance that has been explored on surface of Mars has been tens or a few hundred meters. Scientific interest would extend the distance to be traveled to several kilometers, if not tens or hundreds of kilometers. However, in this case a question rises if the roving system needs to communicate directly to an orbiter traveling around Mars, or directly to Earth since connection to the lander may be lost due to long distance.

The Table 2 below from ExoMars09 CDF Study Report [2] presents an anticipated scenario for European drilling mission. Length of locomotion, sampling and communication cycle is six days. In this scenario two days is reserved for traveling 20 km, one day for drilling and one day for sample analysis. Additional two days are needed to transmit all the collected data (680-690 Mbits).

A new long-range Mars rover probably will not carry a drill, but will aim to long-distance traveling with low-mass instrumentation. Thus the drilling phase may be replaced with another analysis-phase, or sampling and data-collection may even be performed during rover locomotion. However, amount of accumulated data with respect to data-transfer capabilities must be considered carefully. Even though the rover transmits data in every possible occasion (twice a day), it takes total of six days to transmit expected 680 Mbits of data. Further, the rover must stop all the other actions for the period of transmittal, for energy reasons and for data-link quality reasons. Thus it is worth considering carefully which kind of measurements shall be performed and resulting effect on cycle length.

Table 2. ExoMars09 drilling cycle. [2]

#	Phase	Description	Subsystems on	Subsystems off	duration	time counter (days)	note
1	Rover overall initialisation	After landing, all equipments are checked, payload and navigation is initialised, "Alright" signals are sent to Earth	Power, DHS, payload (except drill), payload electronic, comms (only during windows), navigation, Locomotion unit (only partially)		10 hours. (assumption the useful illumination time in one day is 10	0.50	1 day is needed in order to catch the comms windows. This phase is not dimensioning
2	Night	The rover goes in sleeping mode	RHUs, power, DHS (only wake-up unit), comms during the visibility windows (0.8 h)	Payload, locomotion unit, navigation	14 hours	1.00	
A first measurement is performed at the landing site. Afterwards the rover moves to the other measurement points							
The cycle starts							
3	Drill	The rover drills	Drill unit, power, DHS, comms during the visibility windows (0.8 h)	All the rest of the payload, locomotion unit, navigation	30 min to 10 hours (1 day)	0.50	Depending on the soil
4	Night	The rover goes in sleeping mode	RHUs, power, DHS (only wake-up unit), comms during the visibility windows (0.8 h)	Payload, locomotion unit, navigation	14 hours	1.00	
5	Measurements	The rover measures the sample and trasmit to the orbiter the data during the comms window	All payload (except drill), DHS, power, comms (only during windows)	Locomotion,navigation	1 day	1.50	Can be combined with the drill in case of short drill duration
6	Night	The rover goes in sleeping mode	RHUs, power, DHS (only wake-up unit), comms during the visibility windows (0.8 h)	Payload, locomotion unit, navigation	14 hours	2.00	
7	Moving	The rover moves at 100 m/h. To scroll for 2 Km 20 hours (2 days) are needed	Locomotion unit, navigation (initially and every 5 m), power, DHS, payload camera and computer (only few minutes), comms during the windows	Payload (except camera and computer)	2 days (10hX2,shorter phases are possible if the measurement points are closer)	3.00	Assumptions: max distance between measurement points: 2 Km, Part of the day with sufficient illumination: 10 hours. When the orbiter is visible (0.8 hours per day) the rover stops and transmits
8	Night	The rover goes in sleeping mode	RHU's power, DHS (only wake-up unit), comms during the visibility windows	Payload, locomotion unit, navigation	2 nights (each of 14 hours duration)	4.00	
9	Comms	Additional 2 days are needed to download all the data volume required (TBC). The rover just waits for the comms windows and transmits during those	Power, DHS, payload camera and computer (only few minutes), comms during the windows	Payload (except camera and computer), locomotion unit, navigation	2 days	5.00	6 days in total are needed to send all the data volume to the Orbiter. This fixes the cycle duration
10	Night	The rover goes in sleeping mode	RHU's power, DHS (only wake-up unit), comms during the visibility windows	Payload, locomotion unit, navigation	2 nights (each of 14 hours duration)	6.00	
End of one cycle							
Repeat the cycle up to 180 days (nominal endlife due to dust degradation)							

The several Mars Tumbleweed studies referenced earlier very often propose also a mission scenario where no specific landing system is included, or the ball would land separately from the lander. After final approaching suspended by a parachute the ball would be released and it would land and bounce on its own, as the airbags of conventional landing systems. This way valuable mass and space can be saved on spacecraft, or the ball can travel as a piggy-back on a larger exploration vehicle.

8.2 Locomotion requirements

Requirements on mobility are directly derived from the scientific requirements. The required distance between measurement points drives the design of the locomotion system and, in particular, its speed. This latter, in turn, together with the minimum number of measurements, drives the minimum time of presence on the surface needed to accomplish the scientific goal. According to [2] minimum distance specified is 0.5 km, and maximum is 2 km, and number of samples is 10, which makes minimum travel

distance 5 km, in case the system does not return to the lander at all, but acquires and sends the data autonomously. Maximum distance would be 20 km. A 100 m/h traveling speed would then call for 200 hours or 20 days traveling time, which is in line with anticipated 2-3 months life time, since traveling can take some 30% of total time, while the rest of the time is spent on communications, scientific measurements and sleeping over night. The requested traveling speed should be reached over a rocky surface described in the previous paragraph.

If robot swarms would be used locomotion distance can be reduced as the robots would be initially distributed over a large area. This way also locomotion speed can be reduced. Distribution of scientific instruments among several robots would add redundancy and also decrease size of each robot. Added redundancy may allow acceptance of robot loss, which would relax obstacle overcoming capability and thus would allow smaller, lighter, simpler and cheaper robots. Tumbleweed swarms and their behavior are explained in [39].

8.3 Scientific payload requirements

A recent initiative of the European Space Agency was concerned with the identification of specific objectives in the search for life on Mars. It aims to develop a set of imaging and spectroscopic systems which will facilitate a search for evidence of extinct microbial life at all scales down to 0.01 μm. These systems should also provide for the study of the mineralogy and petrography, as a function of depth, in the near subsurface region of Mars. Microfossils are most likely to be found in rocks that have been buried to a considerable depth and have resurfaced due to impact ejection or are exposed on canyon walls. The scientific instrument package is currently known as ‘the Pasteur package’.

The scientific objective of the Pasteur package is the search for signs of past and/or present life on Mars. To fulfill this mission, the package must be able to characterize the organic and inorganic composition of Martian deposits of exobiological interest. The package will be mounted on a rover, and must conduct measurements of multiple samples from surface rocks and the Martian subsurface. The Pasteur package is still at the conceptual design stage. However, some of the instrument components rely on previously developed payloads. [2]

Table 3. Recommended Analytical Instrument for 'Pasteur'-Package [28] [2]

Recommended Analytical Instrument 'Pasteur' Package [28] [2]	
Microscope: for examination of samples • 3 micron resolution • mass, 250-500 g • expected power, 3-6 W *Infrared spectroscopy*: molecular analysis of minerals and organics (with Raman) • expected mass, less than 1 kg • expected power, 3-4 W *Raman spectroscopy:* molecular analysis of minerals and organics (with IR) • expected mass, 1-1.5 kg • expected power, 2.5-3.5 W *Life marker chip:* Compare residues with known organic compounds • expected mass, 3 kg • expected power, 3-20 W	*APX-Spectrometer* (elemental analysis, detection limit: a few .1%) • mass, 570 g • power, 340 mW *Mössbauer:* quantitative analysis of Fe • mass, 500 g • power, 1.5 W *Pyr-GC-MS system:* isotopic, elemental, organic and inorganic molecular composition, and chirality measurements • total mass, 5.5 kg • power, 10-20 W *H_2O_2 and other oxidants dedicated sensors:* • expected mass, 100g
Drill and Sample Distribution System: This is an important feature of the Exobiology Package and will utilize various European technological developments in drills, moles, penetrators and sample distribution systems. • expected mass, 11 kg • expected power, 10-100 W	

The Pasteur-instrument package presented in Table 3 aims merely on search for signs of life from and below planet surface. Mass estimation has been done on the basis of realistic data for the instruments (already existing or in advanced design status): Instruments weight 32 kg. [2]. The package is very large and may not be applicable for future novel locomotion methods that are designed merely to cover large distances and utilize quite limited local energy sources. A very large roving vehicle, walking machine or a balloon might be able to carry all these instruments, but a small flying, gliding or jumping instruments may adopt only some of these instruments. Alternative -smaller and less heavy- scientific instruments may include –a shown in Table 4- thermometers, gas analyzers, cameras, electrical resistance meters and other simple instruments to study atmospheric and surface properties.

Table 4. Possible Analytical Instruments for Thistle Rover Science Package.

Possible Analytical Instruments for new Thistle Rover Science Package	
LOW-MASS INSTRUMENTS: *Microscope:* for examination of samples • 3 micron resolution • Mass 250-500 g • Power 3-6 W *H_2O_2 and other oxidants dedicated sensors:* • expected mass, 100g *Wind speed measuring sensors* *Optical cameras with dedicated filters* *Thermometers* • Masses 10-100 g	**POSSIBLE INSTRUMENTS WITH CHALLENGING MASS:** *Life marker chip* • Mass, 3 kg • Power 3-20 W *Panoramic camera* • Mass 2 kg • Power 8 W *Subsurface Electromagnetic Sounder* • 1.5 kg • 10 W *APX-Spectrometer* • Mass 570 g • Power 340 mW *Mössbauer:* quantitative analysis of Fe • Mass 500 g • Power 1.5 W *Rock surface drill:* A small surface drill, similar to one carried by the Beagle lander. • Mass 400 g • Power 2 W

8.4 Household and auxiliary payload requirements

In addition to scientific instruments also a certain number of housekeeping, navigation, communication and power equipment are needed. The ExoMars09 CDF Study Report [2] describes rover sub-system mass and energy requirements that are collected in Table 5 below.

Table 5. ExoMars09 rover sub-system requirements [2]

Subsystem	Mass	Power
Communication system	6.3 kg	16.5 W
Solar Array	11.25 kg	
Power unit	2.15 kg	6 W
Data handling	4.4 kg	
Attitude control system	0.9 kg	
Harness	1.00 kg	
Battery	6.60 kg	
Thermal control	5.9 kg	

8.5 Energy requirements

As for power system solar panels, batteries and radio-thermal generators can be considered. Practically when considering novel systems, one should consider power generation methods that would utilize local power generation resources like wind or heat. Some of already consumed energy can be re-gained with novel solutions during atmospheric descent or rolling down the dynes, as for an example.

The ExoMars09 CDF Study Report [2] presents a 6-wheeled 58 kg rover chassis, total mass with payload ~190 kg. Thermal control is realized with Radioisotope Heater Units and passive methods and does not call for external energy. The power budget for the rover is presented in Table 6.

Table 6. ExoMars09 CDF rover power budget [2]

Subsystem	Power
Navigation	10 W
Locomotion	30 W
Sensors for locomotion	5 W
Power system	6 W
Computers	12 W
Wake-up system	1 W
Communication	16.5 W
Scientific instruments	203 W

The Thistle Rover can be assumed to have similar requirements for the household and communication systems, while locomotion, navigation and instrumentation needs will depend on selected architecture and scientific instruments. Further it is possible to switch between locomotion, science and communication phases so that the maximum power requirement will stay within reasonable limits. Thermal control will again depend a lot on selected architecture and passive methods should be preferred to save energy. Anticipated Thistle rover energy budget is presented in Table 7.

Table 7. Anticipated Thistle rover energy budget

Subsystem	Power
Locomotion	0-30 W
Navigation	0-15 W
Household	19 W
Communication	17 W
Instruments	5-20 W
Thermal control	TBD

8.5.1 Energy philosophy

Independent from possible novel technologies for locomotion and power generation; communications, system control and instruments will need some electric power in every case.

> As an interesting exception on the statement above, one could imagine a completely passive research device that would travel carried by local energy sources (like wind), and would passively react on certain environmental parameters (temperature, humidity, air pressure, electric conductance) with the aid of smart materials (bi-metals, shape memory alloys, electro-actuated polymers). The materials that react on parameters would also participate directly to communication by passive means, like tilting a mirror or releasing a target. [1]

However, if restricting to conventional communications and research instruments, a conclusion is, that some electricity will be needed.

With current technology mobility and guidance is most easily realized with electric actuators, which –however- consume a great deal of systems energy budget. If passive locomotion means could be adopted then less electrical energy would be needed and system size and mass may be reduced. Also alternative, possibly less efficient, energy production methods can be developed and utilized.

8.6 Folding for flight

As vehicle size and/or mass become higher, a question rises whether the launch system and lander system are capable to adopt it. One should aim towards systems that are low in weight and can be folded in a very small volume for the time of interplanetary flight. The LaRC, TTU and NCSU deployable Tumbleweeds described earlier present several novel mechanisms to realize a foldable rover structure.

8.7 Landing on Mars

The latest Mars-landers have relied on airbags, illustrated in Fig. 41 below. So far the airbags have been unnecessary and -if not successfully retracted, even harmful after landing. Mass and volume the airbags take is a penalty for the scientific instruments.

As an opposite approach the flexible gas-filled surface structure could function as a structural and active element for the roving vehicle. In that case no separate lander nor a separate landing system would be needed at all, which would save a significant amount of mass and volume, which has been also noted by the JPL Tumbleweed team [30].

The image below, presenting the Pathfinder airbags, shows approximate size of the airbag needed to land 360 kg onto surface of Mars. This in turn gives a hint of a size of a flexible-structured Mars-rover that would not need a separate landing system at all. (Naturally, the heat shields, parachutes and retro-rockets are needed anyway.)

Fig. 41. Mars Pathfinder airbag system in the Mars Yard at JPL.
Image: NASA/JPL / The Planetary Society. [3]

8.8 Deployment

Before deployment any landing systems possible obstructing rover transfer from the land onto Mars surface (like remnants of airbag) are retracted or by other means removed form the rover's path. Driving ramps, if necessary, are lowered onto ground and surface conditions are checked for safe deployment. In case of integrated landing structure / rover structure none of these actions are necessary. Rover health and computer- and power systems are checked. Necessary aerials, cameras etc. are extended and deployed, after which the roving vehicle can either move onto surface or start making scientific measurements immediately.

9 Biologically inspired locomotion concepts

When considering the past and planned robotic missions, quite often a biological inspiration can be recognized, -except for the wheeled vehicles; The Phobos hopper imitates locomotion of a grasshopper or a flea, Soviet Mars 2 and Mars 3 –crawlers move in a similar manner as seals on dry ground, Pluto digs into ground like a mole or a earthworm, origin of the JPL Tumbleweed is clear, airborne balloons resemble soap bubbles, and swarms duplicate spreading of dandelion seeds. As an exemption to wheeled devices in general, the Russian Marsokhod rover possesses a biologically inspired locomotion sequence where it can move by extending and retracting its body in a similar manner to an inchworm.

9.1 Russian Thistle

The robotic tumbleweed would imitate natural tumbleweed and would travel along Martian surface driven by the wind or by its internal motor, or rolling down the slopes.

9.2 Motivation

As several six-wheeled vehicles have already been exploring Mars surface, a short discussion on motivation of a ball-shaped roving vehicle is justified.

The main goal on Thistle development is to at least partly utilize local energy sources (wind or heat) for locomotion. Direct wind propulsion on a wind-borne ball appears to be the most simple and efficient method to utilize local energy sources. Locomotion of the Thistle is aimed to be autonomous and mostly lacking any kind of external control or guidance, and goal is to cover a long distance during a lengthy time.

Diameter of the ball exceeds wheel diameter of a four- or six-wheeled rover of a similar mass. Although body structure of the rover allows overcoming obstacles whose height exceeds the wheel diameter (while the ball can only overcome obstacles smaller than 50% of ball diameter), energy efficiency of a large sphere on smooth terrain is probably better than that for a small-wheeled rover.

In this sense the Thistle is not to replace roving vehicles that travel accurately short distances to desired destinations, but the Thistle is to be dropped on surface and then autonomously cover a long distance with locally available energy.

10 Local energy sources

Rover power-supply sub-systems play a significant role in rover mass and lifetime. Lately solar cells and batteries have been used in conjunction, while older Viking landers –as for an example, and some future designs rely on radio-isotope thermal generators (RTG). Some old rovers were even tethered to the lander. Especially batteries and solar cells suffer from limited life and harsh environmental conditions.

Utilization of local energy sources that would free the rover from batteries would provide the rover better autonomy and possibly a longer life time and operation range.

Local energy sources on Mars could be direct solar electricity, thermal energy and wind power, -all originating from Sun radiation. Direct solar electricity is already familiar and its limitations are known. So far wind-energy has been studied, and some prototypes have been operating on Earth. Utilization of thermal energy has not been apparent up to date on roving vehicles, while some passive temperature control systems use it. Energy sources not listed yet might include chemical energy stored in Martian soil or atmosphere, and potential energy of slopes and hills (however, one needs first to get on top of the hill), or potential energy of the lander while still at the orbit. How could we store the huge amount of energy that is wasted into atmosphere in the form of heat during spacecraft descent and landing? Abundance of carbon dioxide and solar radiation opens an interesting possibility to utilize biological photosynthesis for energy production.

10.1 Wind

Martian wind is in the public probably the best-known phenomenon of planet Mars. Atmospheric density on Mars surface is very small, only 1.6% of that on Earth. However, despite of low density, high wind speeds carry a significant amount of energy. Theoretical energy content may be calculated by the speed and mass ($E=½*m*v^2$) flowing through a defined area. The area could be defined by diameter of a windmill, as for an example. The Table 8 below presents energy content of wind flowing through three different areas at two different speeds. Maximum collected energy is limited by Betz-limit to approximate 60% and real windmills on Earth operate at 40% or 20% efficiency depending on rotor type. [34]

Table 8. Energy content of Martian wind.

Air density: r = **0.02 kg/m^3** **Kinetic power: P = dE/dt = 0.5 x** r **x** p **x R^2 x v^3**		
Generator diameter 2R (m)	**Wind speed v (m/s)**	**Kinetic power P (W)**
1	**7**	**2.7**
6	**7**	**97**
30	**7**	**2 423**
1	**30**	**212**
6	**30**	**7 630**
30	**30**	**190 755**

Since household energy requirement alone has been estimated to be around 20 W, and in addition is needed either for locomotion, communication or science power; -if not them all simultaneously. Peak power will then be around 40-50 W, some of which may be, however, drawn from a temporary storage like batteries. Average power generation should then be around 30-50 W, which indicates at 40% efficiency a 70-125 W kinetic wind power. A 6-meter windmill operates in this range during reasonable Martian wind conditions.

In addition to windmills the energy of wind can be utilized also in some other ways. One method could be to generate drag-force with a kite or sails, or let the wind push a ball like a Russian Thistle; -just to mention a few options.

10.1.1 Wind mills

Windmills for a large-scale Martian energy production, in the range of kilowatts and hundreds of kilowatts, has been studied widely already, as for an example in [34]. These cannot be considered as a solution for mobile roving systems, but only for stationary power plants.

However, a small-scale windmill designed for a rover power-source was presented in [40]. Here a 1 m diameter windmill was considered for a Venusian rover as shown in Fig. 42. (Venusian atmospheric density is 64 kg/m^3). Expected collected windmill power was 1.8-15 W at 0.5-1 m/s wind speed. Corresponding power on Mars with Martian atmospheric density and wind speeds 10-30 m/s would be 4.7-127 W.

The windmill power was utilized in two ways. In one solution the windmill was mechanically connected directly to driving wheels (with sufficient gear ratio) and the mill practically drove the rover. There is also possibility to collect surplus wind energy with a generator and store it in batteries. An alternative method is to use the mill power to charge batteries and drive the rover with electric motors, which provides easier control and more simple mechanical solution.

Fig. 42. A wind-mill powered rover. (RCL-company). [40]

A drawback of using a windmill for a novel biologically inspired roving system is that the mill needs a proper alignment and a steady base to be operative. A large six-wheeled rover can provide this platform, but any kind of hopping or rolling devices may not be suitable solutions.

10.1.2 Direct propulsion – A Russian Thistle

Direct wind propulsion here means, that the kinetic momentum of moving air mass directly and without any energy conversion or transfer mechanisms causes the rover to move. One example is the Russian Thistle that is blown forward by the wind. Alternative solutions could use sails, kites and wings, which –thanks to aerodynamics- in principle can provide traveling velocities exceeding the wind speed.

The Russian Thistle appears very attractive due to its simple structure and mobility concept. Similar Tumbleweed-designs have been studied closely as discussed before. The following sections present an analytical study on expected traction force on Russian Thistle placed on Martian surface. In addition effect of re-shaping the Thistle surface to imitate a wind-turbine is discussed.

The tangential blades associated with the wind-turbine–like layout, shown in Fig. 43, may have also several other functions to assist Thistle motion on surface. The blades add ball diameter and they add flexibility, -both features assist in overcoming obstacles. The blades may also collect some wind-borne sand that causes an off-balance that makes the ball to rotate. The sand falls back onto ground as the ball rotates.

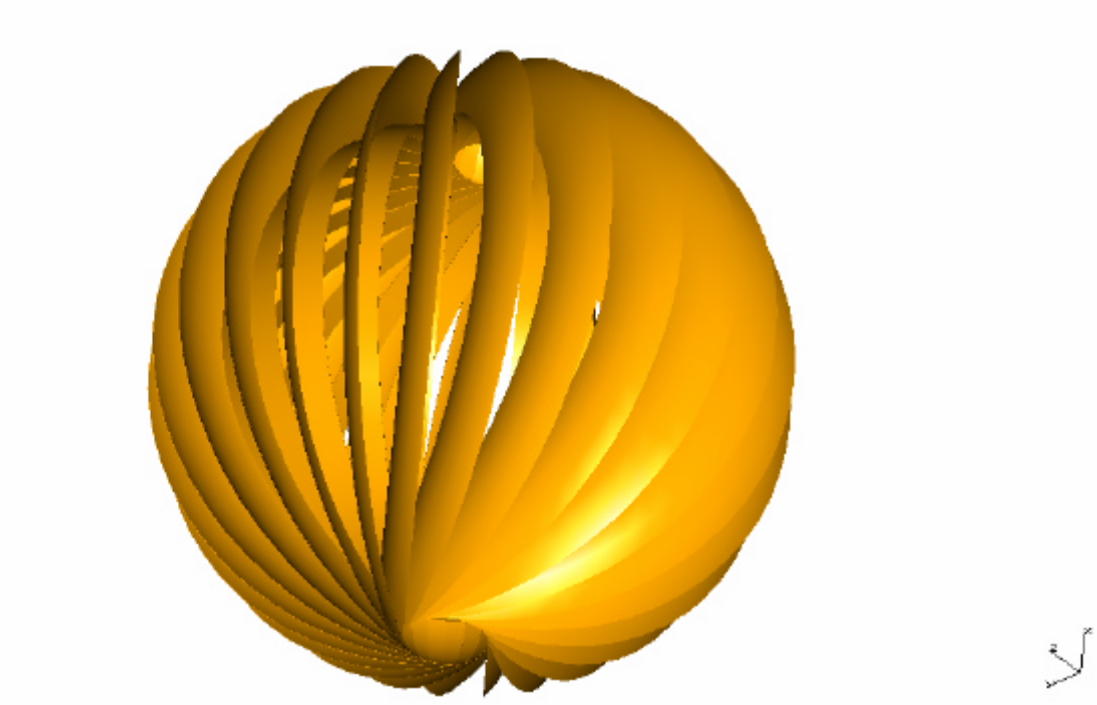

Fig. 43. An artistic view of a Robotic Russian Thistle
with a wind-turbine layout

10.2 Solar energy

10.2.1 Solar panels

Currently on Mars surface, the Opportinity and Spirit rover solar arrays –when fully illuminated- generate about 140 watts of power for up to four hours per sol (a Martian day) [6]. The solar panels deploy to form a total area of 1.3 m^2 (14 ft^2) of three-layer photovoltaic cells. The array can produce nearly 900 watt-hours of energy per Martian day, or sol. However, by the end of the 90^{th} sol, the energy generating capability was estimated to be reduced to about 600 watt-hours per sol because of accumulating dust and the change in season. [41]

For a moderate scaled 50 W roving system a 0.5 m^2 panel area would be sufficient. However, as mentioned above, lifetime of the solar panels is limited due to dust accumulating onto panel surfaces, if no device for dust removal is implemented. After 180 days the power availability is reduced by almost half. [2] The Fig. 44. below presents a reduction factor as a function of time of presence on the surface. The first curve, based on Sojourner data, gives a reduction rate of 0.3% for the first 30 days and a slower rate of 0.1% in the following days. The second one, more conservative is based on a constant reduction rate of 0.3%. [2]

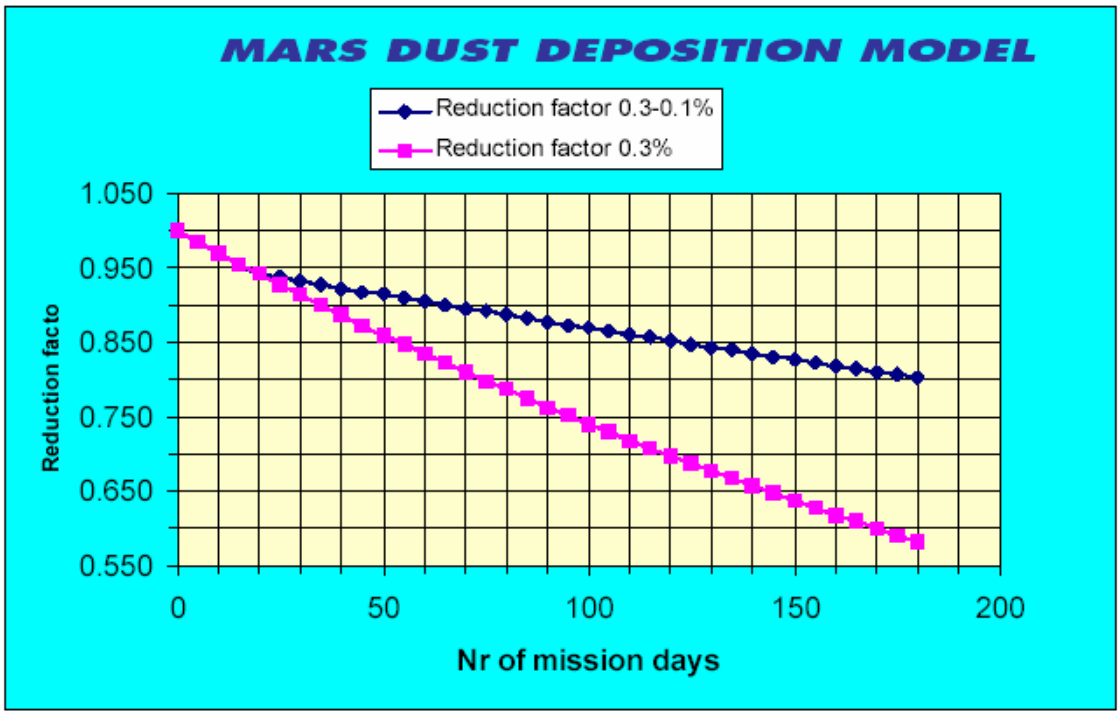

Fig. 44. Solar panel efficiency reduction due to dust deposition. [2]

The solar panels also require proper alignment with respect to sun direction to operate properly. Hence a steady platform, like a big-wheeled rover, is needed to carry them. Availability of solar energy is also dependent on the season of the year.

NCSU has demonstrated flexible photovoltaic silicon cells mounted on sails of a Tumbleweed with encouraging results. In future integration of cells into sail material can turn the complete Tumbleweed into a mobile solar power plant. [23]

10.2.2 Other methods using solar light

Abundance of carbon dioxide and solar radiation opens an interesting possibility to utilize biological photosynthesis for energy production. In practice photosynthesis turns solar energy into chemical energy that must be converted further into electricity or other forms of energy to be utilized. Fuel cell technology could be a method to produce electricity. Photosynthesis, however, relies on activity of living life forms, and sustaining life on Martian environment is a challenge alone.

10.3 Heat

Heat on Martian surface is one form of solar energy. Heat is produced by absorption of solar radiation. Collecting heat-energy is in principle quite easy; with a properly designed surface properties absorption can be maximized and reflection/emission minimized. In practice heat energy can be collected with passive components, while active components (like heat pipes) can be used to transfer energy. Also storing of heat is possible with passive means; a simple well-insulated mass can be used. Active systems, based on phase transformation –as for an example- can be used for a more efficient energy storage. As like solar cells, also heat-absorbing surfaces may suffer from dust deposition or other changes on surface properties. However, this effect can be expected to be of less importance. Dust deposition and surface ageing can be expected to reduce reflective properties of bright surfaces, which is only beneficial for heat collecting surfaces.

In general utilization of heat energy relies on temperature difference, not on absolute temperature alone. Thermal engines -like Stirling engine-, peltier elements, and smart materials -like bi-metals and shape memory alloys-, all generate mechanical or electrical energy from temperature difference. Temperature difference may exist either in time (sequential heating and cooling) or in place (other end in hot and other end in cold).

Diurnal variation in Martian air and soil surface temperature is 80-100 ℃ in hot case, as presented earlier. Similar changes in rover surface temperature can be expected with a proper design. This temperature variation can be utilized to produce energy on a daily cycle. In cold case and in winter time the variation is much less.

Localized temperature difference can be found between air and ground. However, the difference changes during the day so, that in the morning the ground is colder than air, while in the evening ground is hotter than air. Localized temperature difference can be also found over different parts of the rover. Sunny side of the rover might be hotter than the side in shadow, or exterior parts can be hotter/colder than the interior parts. A rotating wheel transfers its surface continuously from sunny side to the shadowed side.

A hot surface would be constructed of hot thermal blanket (absorption factor 0.28 and emissivity 0.02). In stationary state absorbed energy equals to emitted energy:

$$se \cdot \left(T^4 - T_2^4\right) = aB$$
$$where:$$
$$s = 5.67 \cdot 10^{-8} \frac{W}{m^2 K^4}, a = absorbtion, e = emissivity \quad (2)$$
$$T = object\ temperature$$
$$T_2 = environment\ temperature$$
$$B = Energy\ \ flow\ onto\ surface$$

If emitting area is double of the absorbing area (like a sheet that is illuminated from one side), the left side of the formula can be multiplied by two. For given emission and absorption factors, assumed 320 W/m^2 sun radiation (example peak 480 W/m^2 [2]) and –140 °C (133 K) sky temperature we get T = 446 K (174 °C). This applies for vacuum. In Martian atmosphere transmission losses and convection decreases the stationary state surface temperature.

Upper limit on thermal efficiency μ is set by the Carnot law μ=dT/Tcold. The Table 9 below shows some values for Carnot-efficiency on possible Martian temperatures. With moderate temperature difference at Martian average air temperature a 15 % Carnot efficiency can be calculated. If we assume 0.28 absorption factor for Sun energy (320 W/m^2) and Carnot efficiency 15%, energy to be collected remains 0.28 * 320 * 0.15 or 13 W/m^2. Real efficiency depends on properties of energy collection system.

Table 9. Example values for Carnot-efficiency on Martian temperatures.

Carnot-efficiency (Martian hot season.)				
Tc (°C)	**Th (°C)**	**DT**	**eff**	**Note**
-130	**-40**	90	**39%**	Tc = sky temp.
	0	130	**48%**	
	20	150	**51%**	
	50	180	**56%**	
	100	230	**62%**	
-80	**-40**	40	**17%**	Tc = low air temp.
	0	80	**29%**	
	20	100	**34%**	
	50	130	**40%**	
	100	180	**48%**	
-40	**-40**	0	**0%**	Tc = average air temp.
	0	40	**15%**	
	20	60	**20%**	
	50	90	**28%**	
	100	140	**38%**	
Tc = Cold temp. Th = Hot temp. DT = Temp. difference, eff. = Carnot efficiency				

If on purpose generating thermal gradients over mechanical structures of the roving system, one needs to make sure that thermal gradients and thermal variation do not endanger operation and durability of the system.

In the following sections some methods to utilize thermal energy are discussed.

10.3.1 Peltier elements

For many space exploration missions the light from the sun is too weak to power a spacecraft with solar panels. Instead, the electrical power is provided by converting the heat from a heat source into electricity using thermoelectric couples. Such Radioisotope Thermoelectric Generators (RTG) have been used by NASA in a variety of missions such as Apollo, Pioneer, Viking, Voyager, Galileo and Cassini. With no moving parts, the power sources for Voyager are still operating, allowing the spacecraft to return science data after over 25 years of operation. [44]

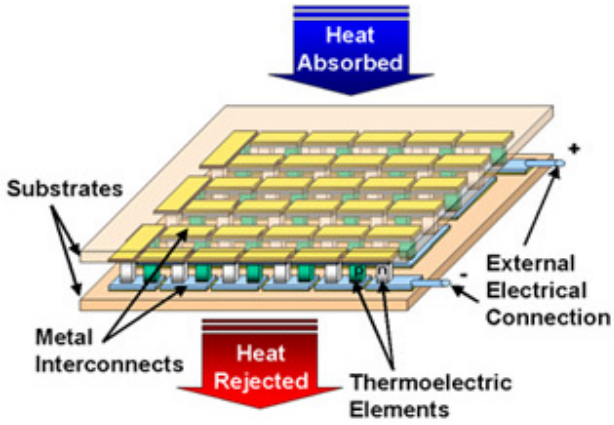

Fig. 45. Thermoelectric Module (JPL) [44]

A thermoelectric converter consists of several n- and p- type semiconductor thermoelements, which are connected electrically in series and sandwiched between two electrically insulating but thermally conducting ceramic plates to form a module. Upon a temperature difference across the module electrical power will be delivered to an external load and the device will operate as a generator. Conversely, when an electric current is passed through the module, heat is absorbed at one face of the module and rejected at the other face; thus, the device operates as a cooling element.

The JPL Thermoelectrics Website [44] presents a new branch of miniature thermoelectric modules based on MEMS-technology, see Fig. 45. Thermoelectric microdevices can convert rejected or waste heat into usable electric power, at moderate (200-500K or -73 – 227 ℃) temperatures and often with small temperature differentials.

Miniature Radioisotope Thermoelectric Power Cubes, developed at JPL [45] would be heated with 4.2 W radioactive-decay energy up to 200 °C. A 0.2 cm^3 cube would have dimensions 0.58 cm x 0.58 cm x 0.58 cm, or 6 faces 0.34 cm^2 each totalling 2.05 cm^2. Each face holds 50 thermocouples and the 300 thermocouples together generate 240 mW

of power (12 Volts, 20 mA). Overall thermal-to-electrical energy-conversion efficiency is between 5 and 6 percent. (5% of 320 W/m^2 Sun flux on Mars would be 16 W/m^2.)

Assuming a 5% efficiency for a Peltier-element on Thistle surface, approximately 1 m^2 for each subsystem (Locomotion, Navigation, Household, Communication, Instruments) would be needed. Efficient area being heated by the Sun would be less than a hemisphre; assume 1/4 of the ball surface being efficiently heated (45 degrees angle of view, allows 29 % reduction in heat radiation intensity). For a 1.5 m sphere this would make 1.8 m^2, for a 3 m sphere 7 m^2 and for a 6 m sphere 28 m^2. Obviously a 3 m Thistle would have sufficient surface area to carry enough Peltier-elements for Thistle power generation –if utilizing power density familiar from JPL miniature power cubes.

Since the Thistle moves by rolling, the Peltier elements must be placed all over the ball surface. It needs to be studied how much weight such a Peltier-blanket would have. The MEMS-Elements can provide a mass-effective solution. Another topic to consider is availability of required temperature difference. The ball surface can become very hot under Sun radiation, but where we can find the cold side? The commercial Peltier elements require the hot side on the other side of the element, and cold on the other. This would mean that interior of the ball should be cold and exterior hot. It can be a challenging task to maintain interior cold temperature under continuous Sun heating.

10.3.2 Fluid circulation

In nature thermal circulation of fluids is a common phenomenon. Winds originate from heating of air on certain parts of Earth, hot smoke raises upwards from the candle, hot water rises above cold water, a hot-air-balloon floats carried by colder air. Energy of fluid flow can be transformed into electrical energy with turbines and generators. Also mechanical motion can be generated from fluid flow; if considering a wheel or a ball –as for an example, fluid flowing from one part to other part moves mass and so changes location of mass center. This may cause an unbalance which in turn makes the system rotate to restore the balanced position.

In the following sections utilization of fluid flow is discussed, as a means to provide electricity and as a means to generate direct mechanical motion by unbalancing a wheel or a ball. Then some methods to generate desired fluid flow are discussed.

10.3.2.1 Radial flow

In the radial-flow concept heat makes the fluid -gas or liquid- flow from outer surface of the wheel or ball towards interior parts. As the heating energy comes from the sun, only half of the ball is illuminated and heated. From these parts the fluid flows towards inner parts. Energy can be collected from a gas flow by using turbines and generators; mechanical motion develops when mass of liquid moves from outer surface closer to the ball center. Resulting unbalance makes the ball to rotate and expose new surface area for sun heating.

10.3.2.2 Tangential flow

In the tangential-flow concept the ball –or a wheel- is divided into several tangential sections. Sun radiation heats up a limited number of sections while the rest remain in cold state. Resulting temperature difference generates a fluid flow that in turn can be transformed into electrical energy or mechanical motion in a similar manner as above.

10.3.2.3 Heat induced gas flow

Utilization of Martian atmosphere –mainly carbon dioxide- as an active element of the power system is an interesting option since this gas is available all the time. In case some gas should be lost during operation, new can be always pumped from atmosphere.

Heat induced gas pump would operate in a following manner (see also Fig. 46):
The ball surface is divided into several gas containers. Each container extends radially through a valve into internal parts of the ball. The valve is also equipped with a microturbine and generator. In initial condition the ball is in uniform temperature and gas pressure is even in all parts of the gas container. As sun radiation starts to heat the ball surface, the gas also heats up and pressure develops in the outer container. When pressure is high enough the valve is opened and gas flows through the microturbine into inner container of lower pressure. Gas flow continues until pressure difference is zero, and energy is collected with a generator connected to the microturbine. Before evening the valve is closed and high pressure remains in all parts of gas container. During night ball surface cools down faster than internal parts of the ball, and pressure in outer gas container drops. The valve is opened and gas flows through the turbine back to the outer gas container.

The sequence can take place on a daily basis when the ball is parked, and more frequently when the ball is rotating, provided that the heating and cooling speed is high enough compared to ball rotation speed.

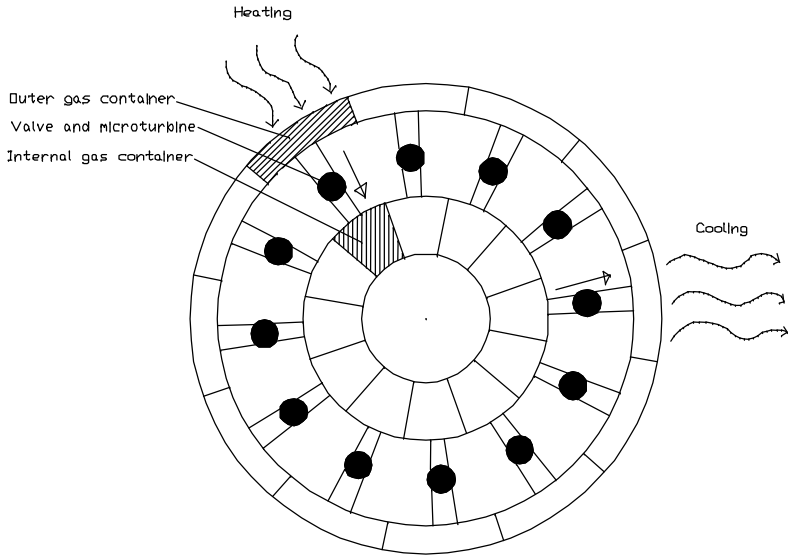

Fig. 46. Heat induced radial flow of gas.

An alternative and a simpler method would utilize complete ball volume as a gas container. However, this concept cannot utilize rotation of ball, but relies solely on diurnal temperature variation; during the day the gas inside the ball is heated and pressure develops. In the evening the pressure is released through a microturbine. When pressure difference has disappeared a valve is closed. During the night gas cools down and underpressure develops. In the morning the valve is opened and pressure difference is released through a microturbine.

Energy available for this kind of system can be estimated by calculating energy content of the gas flowing through the microturbine. First we calculate the pressure increase in a closed container as it is being heated by sun radiation:

$$p_1 = p_0 \cdot \frac{T_1}{T_0} \tag{3}$$

Where p_0 is initial pressure, T_0 is initial temperature, T_1 is final temperature and p_1 is final pressure. Volume of the hot gas, when released to outer pressure is:

$$v_2 = v_0 \cdot \frac{(p_1 - p_0)}{p_0} \tag{4}$$

Where v_0 is volume of gas container, v_2 is volume of released gas in outer pressure, p_0 is outer pressure, and p_1 is pressure inside container. As gas flows from higher pressure p_1 to lower pressure p_2 and expands simultaneously to volume v_2, it has an energy content *Wex* as follows:

$$Wex = p_2 v_2 \cdot \ln \frac{p_1}{p_2} \tag{5}$$

As the gas expands, it performs work *W2* against external pressure p_2:

$$W2 = p_2 v_2 \cdot \left(1 - \frac{p_2}{p_1}\right) \tag{6}$$

Maximum energy to be collected from gas is in theory *Wex*-*W2*.

Making the following assumptions:

Container volume	113 m^3	Volume of a 6 m ball
Initial pressure	700 Pa	Mars atmosphere
Initial temperature	223 K	Cold air temperature
Hot temperature	293 K	Hot surface temperature

We can calculate the energy available from gas flow. Most of the energy is lost in expansion of gas, and amount to be collected is 847 J. In order to calculate energy content of in-flowing gas as the ball cools down, the initial values can be changed and energy to be collected becomes 491 J.

Total amount of energy to be collected during one complete cycle is 1338 J. If we assume 20% gain of turbine and generator in transformation to electric energy and 48% efficiency of motor and gearbox, available mechanical energy becomes 128 J or 2 W-min per cycle.

Amount of energy collected is very low. Reasons for low energy gain lie in small heat-induced pressure difference and low gas pressure. If we choose the first option and use a pressurized system we can increase energy gain significantly. If we assume that the pressurized system functions as described in formulas above, we can make new calculations with added pressure. Assumption can be realized with very large or flexible containers, or cylinders which provide a variable volume. The latter case would represent a type of a Stirling heat engine. Assuming 1 bar operation pressure we can recalculate the energy to be collected and we get 18350 J or 306 W-min. This is, a 1-Watt motor can run with this energy for 5 hours, or a 20-W communication system can operate 15 minutes. For 2 bars pressure the result is double.

Heimendahl in [26] proposes use of liquid/gas phase change of propane or propene to activate a wind-driven Soft-ball. With this approach also significant amount of gas could be generated upon heating to flow through the turbine. As volumetric change of agent during phase change is very large, the limiting factor would be the volume and pressure where the gas would be stored during the day. When the night falls the gas should cool down, condensate and flow –driven by the gravity- passing the turbine back to container to wait for the new expansion to happen in the morning.

Drawback with pressurized system is that high pressure and large variation can cause gas leaks, which must be compensated by pumping new gas in. This would decrease system efficiency. Also gas flow and gas expansion must take place in closed volumes which causes higher resistance for gas expansion and smaller energy gain. Variable volumes realized with cylinders and pistons can give a solution, but with added mechanical complexity and mass. However, replacing the turbine with a Stirling-engine it can be possible to increase total efficiency in transforming the heat energy into mechanical motion.

10.3.2.4 Micro turbines

The MIT Micro Gas Turbine Engine Project has the goal of using MEMS fabrication technologies to construct compact electric power generation systems from a gas turbine generator comprising a compressor, combustor, turbine and electric generator. Another system under development is a stand-alone turbine/generator. Detailed models of the electric induction machine have been developed and used to design an optimized 6-phase machine having a 4 mm diameter. Operated as a generator, this machine is expected to output 0.5 W at 300 V and 1.5 MHz. An initial set of motor/generator devices have been built; see Fig. 47 below. [46]

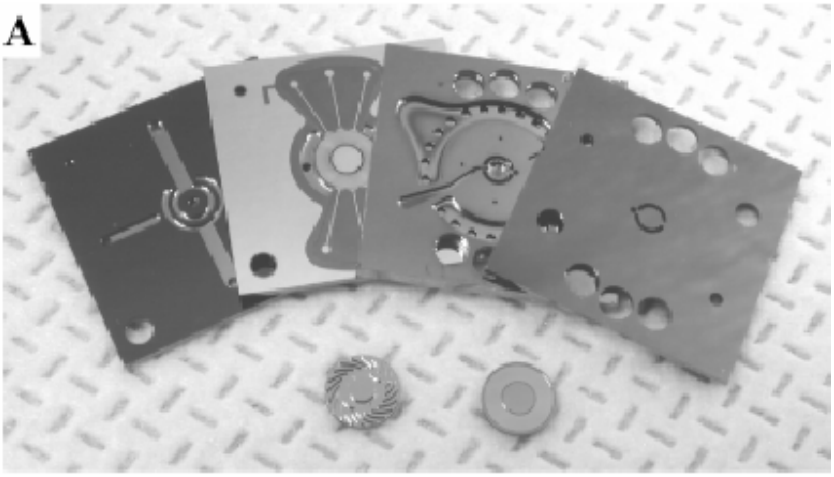

Fig. 47. A Micro Gas Turbine (4 mm dia.)
developed at MEMS@MIT. [46]

10.3.2.5 Heat induced liquid flow

Transfer of gas does not easily generate significant off-balance due to low mass of gas. On the contrary, transfer of liquid would move much higher mass. However, thermal expansion of liquid is much less than that of a gas. A solution could be phase transformation of liquid into gas upon heating. Operation of liquid/gas torque wheel would be like the following (see also Fig. 48):

Fluid containers would be constructed in a tangential series around the ball or wheel. The containers are separated from each other with a valve, so that fluid can circulate only in one direction. When cold the fluid remains in liquid state. Upon heating the liquid vaporizes and expands. Expansion generates a pressure that pushes liquid in other containers in the direction stated by the valves. The section being heated remains with less mass, while some mass in liquid form moves to opposite side. Resulting off-balance makes the wheel to rotate and exposes new sections for sun heating. Already heated part rotates into shadow and starts cooling and changes state back to liquid.

The tangential container system must have some structural flexibility to allow circulation and uneven accumulation of the liquid, as the liquid is non-compressive by nature. The valves are equipped with socks that allow expansion of gas, but prevent gas from flowing from one compartment to another. If the gas would be able to flow freely, it would find

its way to uppermost part of the wheel, and would not generate any off-balance to rotate the wheel. The wheel tends to rotate away from the Sun. As the Sun moves from one side of the wheel to the other side, the wheel changes its direction of travel.

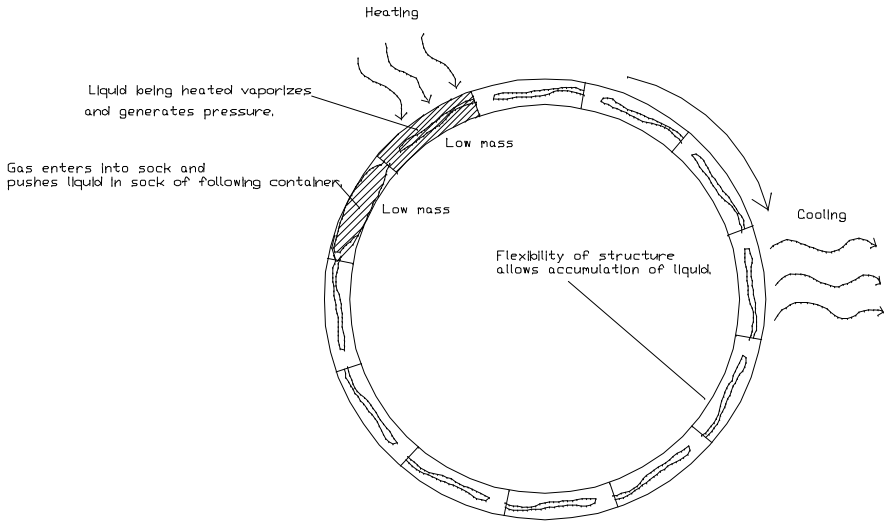

Fig. 48. Heat induced vaporization and tangential flow of liquid.

10.3.2.6 Osmosis

Other biological methods to generate fluid circulation are osmosis or diffusion. Here fluid flows autonomously through a semi-permeable membrane, driven by different concentration of fluids on both sides of the membrane. Large trees elevate water from roots to the uppermost leaves with this method. In order to utilize external energy source (heat) we need to find a way to control this diffusion flow with external heat. One option could be to develop such a fluid that would change its concentration upon heating/cooling. The fluid could be nearly over-saturated. Upon heating the fluid can dissolve more of this component which causes fluid to flow through a membrane.

Operation of the wheel/ball would be similar to one illustrated above. Fluid containers would be constructed in a tangential series around the ball or wheel, as shown in Fig. 49. Tangential flow of fluid would cause an off-balance on the wheel and would make the wheel to rotate. Rotation of the wheel would expose a new fluid container for heating and the process repeats. The tangential container system must have some structural flexibility to allow circulation and uneven accumulation of the liquid, since the liquid is non-compressive by nature.

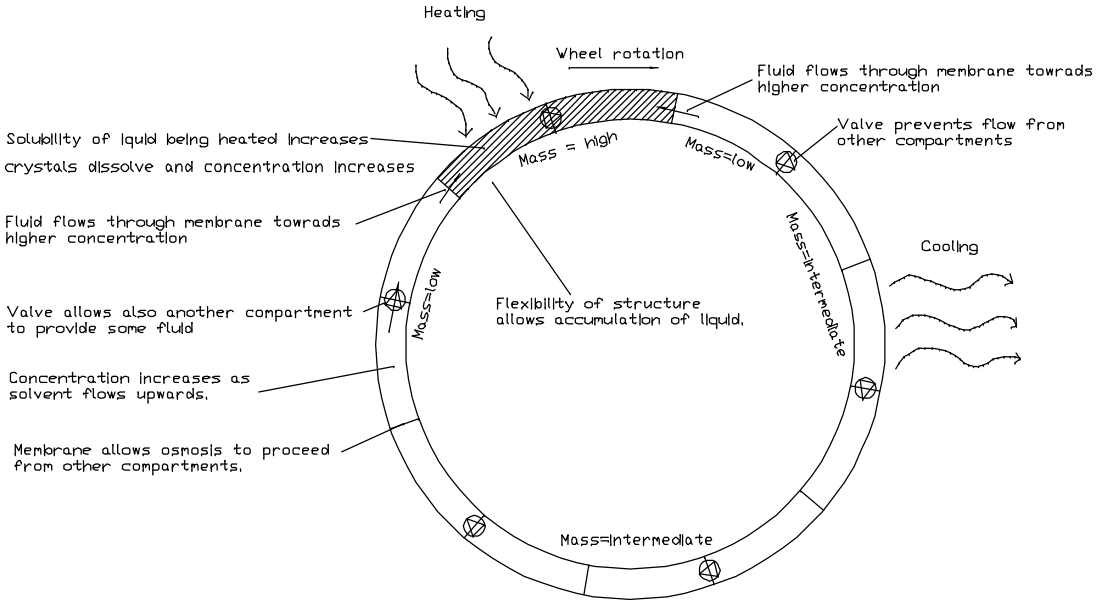

Fig. 49. Heat induced osmosis driven fluid flow.

Considering the concept of tangential flow and vaporization, the Fig. 48 shows a design where vapor generated in one container flows into two containers, and fluid of one container is divided by the rest 10 containers. Hence the two containers will have a total mass of one container, and the 10 containers will have a total mass of 11 containers. If we assume that ball diameter is 6 meters, tangential length of container is 30 degrees i.e. 1.57 m and effective width of containers (area to be heated) is 90 degrees i.e. 4.71 m. Assume container thickness 0.01 m. Volume of one container is then approximately 0.074 m^3 or 74 liters. Total volume is 12-fold i.e. 0.887 m^3 or 887 liters.

Assuming (just for an example) that the containers are filled with water, then total mass would be 887 kg and one container would weight 74 kg. Resulting off-balance would depend on the angular position of the area being heated. Maximum radius of moment would be 3 m and minimum radius 0 m. Off-balancing force would equal to weight of one container that has been removed by vaporized gas. Thus maximum off-balance torque would be 74 kg x 3 m x 3.7 kgm/s^2 = 821 Nm. Practical off-balance could be roughly 1/3 of this i.e. 273 Nm.

Resulting off-balance seems attractive, but a severe penalty is the total mass of the system. Utilizing a smaller amount of liquid or liquid with smaller weight would reduce the total mass, but also the torque would be reduced respectively. It is possible to make larger containers and use total of 8 instead of 12 containers, but still the resulting torque with respect to total mass would not reach a favourable ratio. A concept to collect all of the liquid into one location could save a lot of mass.

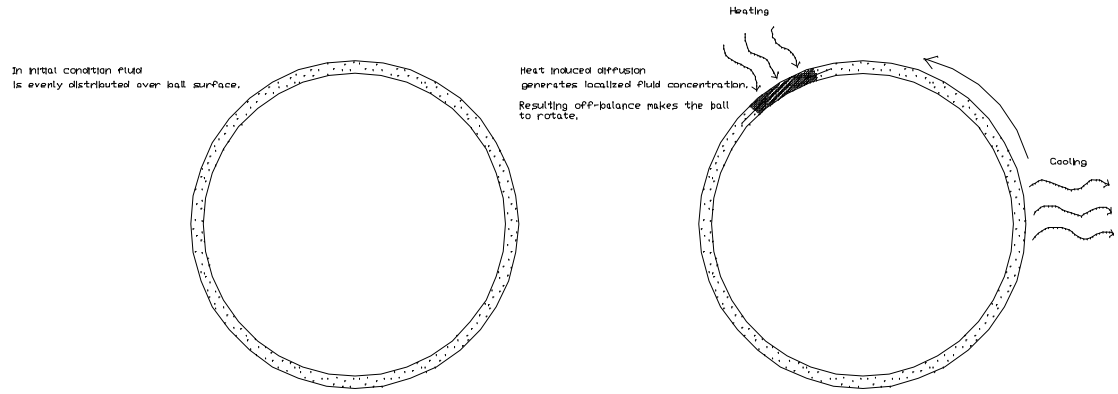

Fig. 50. Heat causes fluid concentration in a sponge-like material.

Osmosis or diffusion could perhaps concentrate the fluid on the area being heated, and leave the other parts dry. The wheel/ball surface could be constructed of a sponge-like material, like in Fig. 50. Another solution could be a sort-of shrink-tube that shrinks in cold and expands when hot. In cold areas of the ball the tube shrinks and pushes the fluid into hot areas, where the tube expands. With these solutions we can produce similar un-balance as above, but keep the ball mass low at the same time. The shrink tube would be preferably constructed of some plastic material with low mass and high coefficient of thermal expansion. A woven net-like exterior structure can improve volumetric changes as temperature varies. Also bi-metals and shape-memory alloys can be used to construct a shrink-tube, but with some added mass.

10.3.2.7 Discussion on fluid circulation

The radial gas flow appears quite straightforward solution. Its only drawback with respect to other two solutions is that it needs additional actuators to generate motion. The two other solutions would provide autonomous rotation without any actuators. However, due to control and navigation needs the actuators may be required anyway.

The tangential liquid-flow that is based on vaporization appears quite challenging when considering handling of vapor and liquid in the same volume. The biologically inspired option to use diffusion, osmosis or dialysis to cause fluid flow provides another operation principle. Also thermally actuated shrink-tubes can be used to concentrate the fluid on the hot areas.

The concepts presented above utilize a tangential mass to generate a locomotion torque. This fluid would be only a ballast mass (several tens of kilograms) and it would be more useful to utilize some active and useful mass that would be carried along in any case. This could include batteries and other structural mass. This option is to be discussed later.

Heimendahl in [26] proposes also use of liquid/gas phase change to activate a wind-driven Soft-ball. Here propane or propene are proposed as for an active agent that would

evaporate for the day and inflate the ball to be driven by the wind. During the night the gas would condense and allow the ball to flatten and rest still in place.

10.3.3 Direct conversion to mechanical motion

Smart materials, like bi-metals and shape memory alloys, react to temperatures or temperature variations by changing their shape. This change can be used to perform some work and propel a rover into motion.

Operation of bi-metals is based on different thermal expansion of two tightly bonded metal strips. The structure bends as the other metal expands/shrinks more than the other. One example is an old-time thermometer or car thermostat. As thermal expansion alone is usually small, the difference between two materials along a long joining seam can produce large variations in curvature and large movements in the end of a beam. Energy can be collected, or work performed, upon heating and/or cooling of the system.

Operation of shape memory alloys is based on change in crystal structure of the alloy. There are several commercial alloys and the Nickel-Titanium is largely used and possesses good technical properties. Ni-Ti alloy can reproduce (recover) geometrical variations of 5-8% in dimension. Force to be generated depends on amount of material being heated. Recommended recovery stress for Ni-Ti alloy is 170 MPa. It is evident that geometrical variations are small in general, but great forces can be generated. With certain mechanical solutions, like springs, levers or pulleys, geometrical variation can be enlarged but respectively output force is reduced. [42]

There are two types of shape memory effects: one-way and two-way. One-way effect needs to be restored (deformed) after heating into shape it was having before heating. This deforming operation for Ni-Ti alloy requires 70 MPa stress. Two-way effect regains the as-cold geometry autonomously, but available output force becomes low. Recovery temperature of Ni-Ti alloys can be adjusted to any temperature between –60 and +100 centigrade, so it suits well on Martian environment. [42]

Typical for bi-metal or shape-memory actuators is that the resulting motion is limited and a continuous motion must be generated with several sequential and repetitive motions. Then the actuators must heat up and cool down in a sequential manner. In order to maintain reasonable locomotion speed heating and cooling can not be tied to diurnal variations, but it should rely on rover motion or other external motion that would re-direct heating to the desired actuators in a desired manner. Obvious approach would use direct sun light for heating and cold Martian air for cooling. Utilization of heat stored in Martian surface can be difficult since in the morning it is colder than air, and in the evening it is hotter than air. Also contact to the ground cannot be predicted due to distribution of rocks and boulders.

10.3.3.1 Continuous acting SMA-heat engines

There exist several solutions to produce continuous motion with SMA-engines, two of which are presented in Fig. 51. However, currently their efficiency is quite low and their

design and operation is quite complicated regarding the distribution of hot and cold energy in Martian conditions. [43]

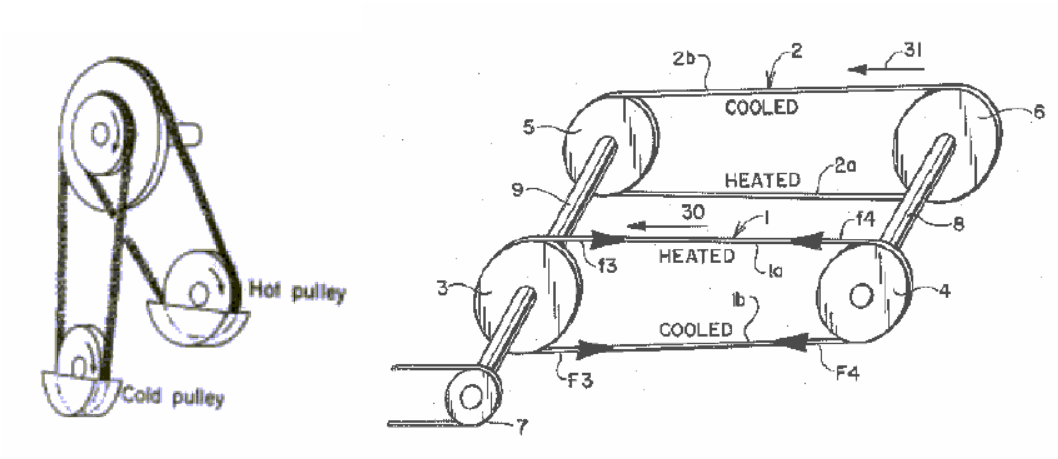

Fig. 51. Some early SMA-heat engines. [43]

10.3.3.2 Heat-induced structural deformation

Structural deformation could be used to deform the ball or wheel structure to cause off-balance that would in turn to make the ball/wheel roll. (See Fig. 52.) This approach suits only on areas/times where sun shines from a low angle. If the sun should shine from a very high angle, the top part of the ball/wheel would deform, and the resulting off-balance would not cause any motion any more.

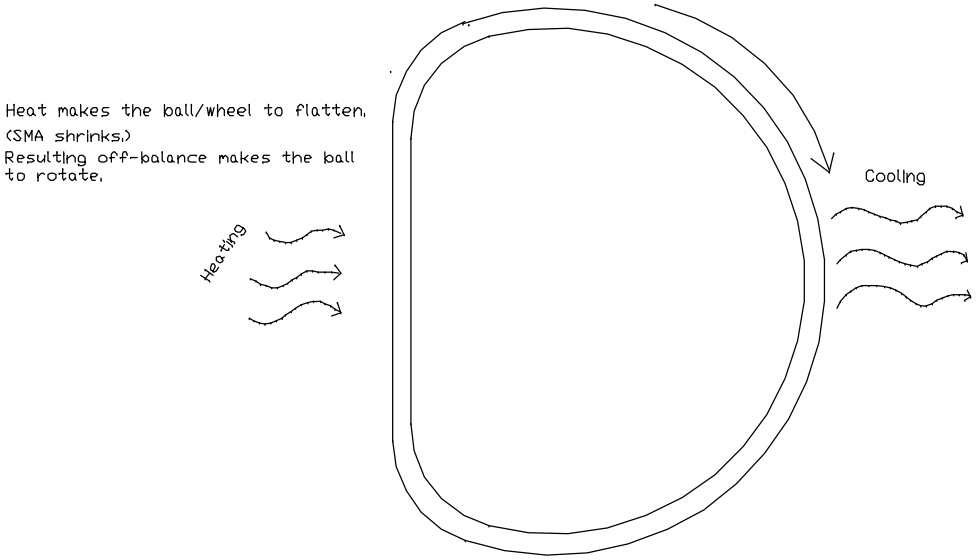

Fig. 52. Heat deforms a SMA-constructed ball/wheel surface.

Heat could also cause some protrusion with a ballast to move and so cause un-balance. It would be beneficial to let the protrusion extend inside the ball (as in Fig. 53), so that any

external protrusions would not prevent ball rotation, or would not stick to any stones or holes around. A 6 m diameter ball would provide enough volume for this.

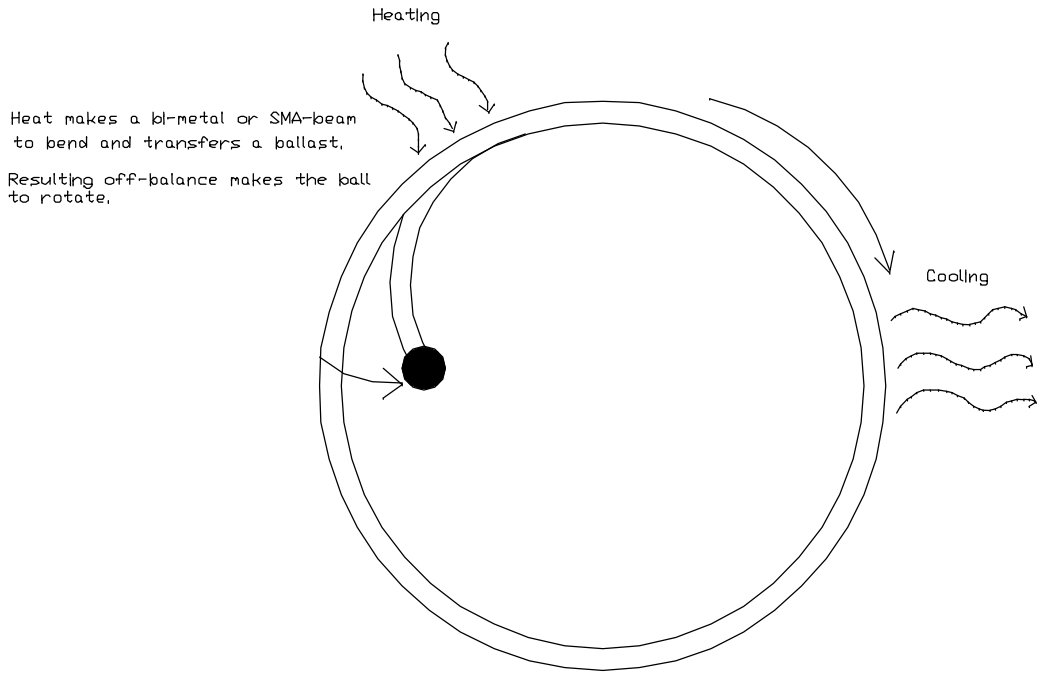

Fig. 53. Heat moves a ballast inside the ball/wheel.

Considering the image above, we can assume that the beam holding the ballast has a length of 1 m, and it bends so that the ballast moves radially 200 mm inwards. If the ballast has a mass of 2 kg (a battery, as for an example), relocation of the mass causes an unbalance that has a magnitude of mass times radial dislocation, i.e. 2 kg * 0.2 m = 0.4 kgm or 1.5 Nm in Martian gravity. Torque can be increased by adding number of beams and ballast being active. Considering a 18.8 m perimeter of a 6 m ball, possibly 90 active ballasts can be considered –some in parallel-, and the torque can be increased to 130 Nm. The ballast must be present all over the surface, for example18 units in line and possibly 15 units in parallel, giving total of 270 units. If each weighs 2 kg, total mass of ballast only is then 540 kg.

Estier and Heimendahl in [26] introduce a SMA-activated Hardball, that would upon Sun heating adopt a spherical shape and so be driven by Martian wind. In the cold of the night the ball would flatten and remain steady on the surface. Also the TTU-Box-Kite concept could be deployed by using SMA:s. In both cases, however, the SMA would not provide the active motion, it would only deform the structure to be driven by the wind.

Sugiyama and Hirai present in [49] working concepts of a SMA-actuated rotating wheel and a jumping ball. Fig. 54 presents the wheel rolling up-hill (left) and a deformed ball just before a 15 cm high jump. Diameter of the wheel is 4 cm and roughly 5 cm for the ball. Motion of the wheel may be considered similar to that of the Arizona University Mars ball in Fig. 27.

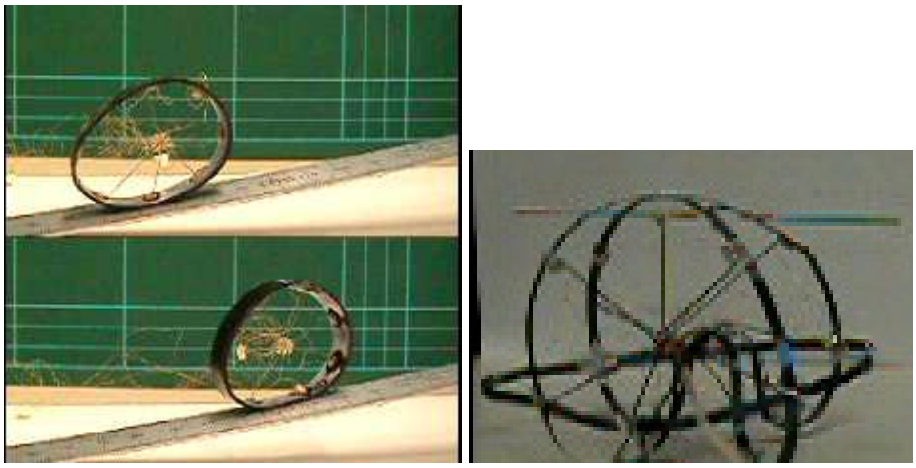

Fig. 54. SMA-actuated elastic wheel and ball. [49]

10.3.3.3 Internal parts as a ballast

The examples above indicate that if using ballast located on ball outer surface to generate rolling torque, overall mass versus torque –ratio becomes poor. The reason is that, as the sphere rotates, the ballast must be available on all parts of the sphere. An exemption is the concept of collecting small amount of fluid into one single location, leaving all other parts of sphere surface dry.

An alternative solution is to use one single ballast inside the ball and let the ball rotate around it. The ballast would then be carried by and hinged to sphere axis of rotation. The ballast would construct of rover payload: batteries, computers, structural parts etc. So it would not add any dummy mass for the system. If assuming a 40 kg mass for the parts being used as a ballast, a 1 m off-centred distance would generate a 40 kgm or 148 Nm torque in Martian gravity. (1 m off-centring equals to 40 degrees tilt with 1.5 m radius.)

In order to utilize structural mass, batteries, or other active components as a ballast mass (as in Fig. 55) external energy should be transferred into internal parts of the wheel/ball, where all the active components are located. There rotation of the components around an axis would generate rolling torque. However, task of conducting heat or heat-induced motion from ball/wheel surface into internal parts is not an easy one. A solution might be to generate electricity on ball/wheel surface (with Peltier elements or micro-turbines) and utilize electric motors inside the ball/wheel to generate rolling torque.

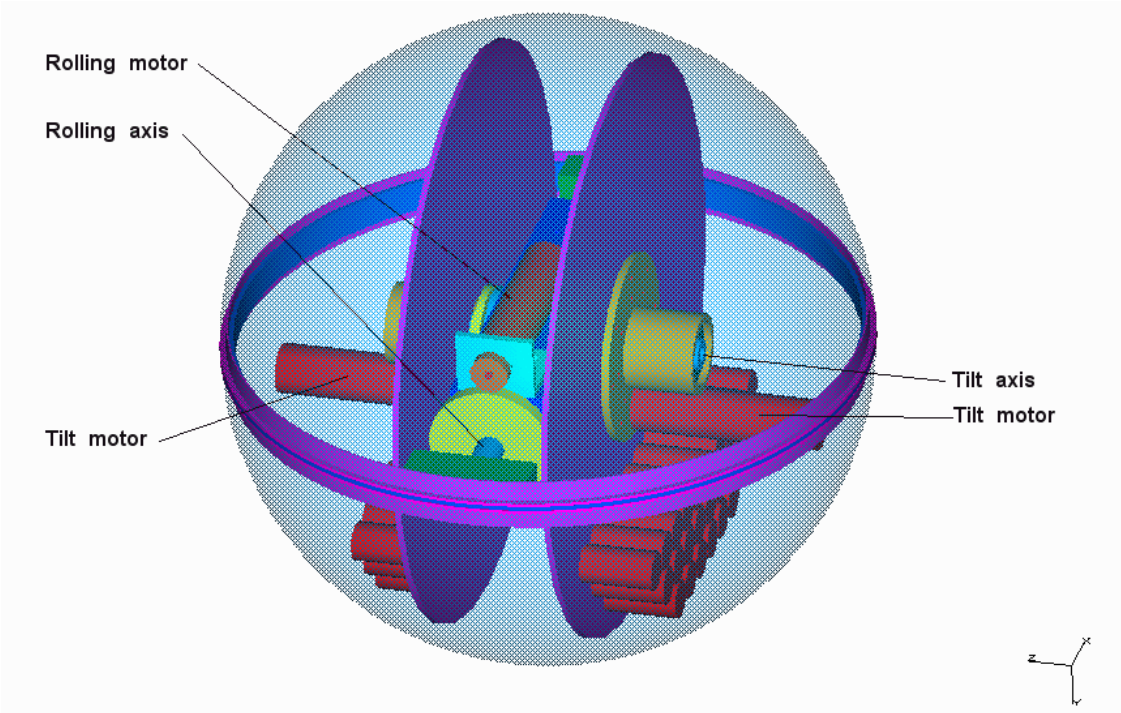

Fig. 55. A concept of internal ballast hanging on rolling axis and using electric motors.

10.3.4 Discussion on heat as a local power source

Considering the several conceptual methods presented above, the most simple, robust and reliable solutions deserve a closer attention. The heat induced radial gas flow with microturbines provides a mechanically simple and electrically flexible power source.

Using liquids as a moving ballast appears to cause a high mass-penalty and a challenging task to control fluid flow inside ball/wheel structure. In a similar manner also the mechanical concept to transfer ballast from outer surface radially, even though simple and reliable solution, suffers from the fact that the ballast must be present all over the surface. The consequence is that total mass becomes high and ratio between mass and locomotion torque is not sufficient.

A concept that collects all of the fluid into one location at the time could be a suitable solution when considering the resulting off-balanced torque and total mass. A challenge is to find working concepts to collect the fluid into desired location against Martian gravity and thermal variations.

A competing concept using ballast is the internal off-centering of system instrumentation that can generate high torque with little added mass. A challenge is to utilize external energy sources to relocate internal ballast for locomotion.

10.4 Slopes, wind and re-charging of batteries

Slopes do not provide any energy; unless always rolling downwards. However, some potential energy is being collected as the Thistle drives onto a hill. The ballast motors can be used as generators while rolling down the slope, and some of the energy can be restored in the batteries. In a similar manner wind can be used to re-charge the batteries while rolling along with a high-velocity wind.

10.5 Discussion on local power sources

Two locomotion principles have been discussed for the Thistle-rover. It can be either propelled by wind, or it can roll driven by un-balanced ballast. Un-balancing energy source varies largerly. The Table 10 below presents utilization of local power sources for Thistle locomotion. Performance of these options is discussed in the following sections after mobility considerations.

Table 10. Utilization concepts of local energy sources.

Utilization concepts of local energy sources					
Locomotion method	**Power source**	**Power conversion method**	**Power carrying system**	**Used form of energy**	**Locomotion generating system**
Wind propulsion	**Wind**	None (direct)	Martian wind	Wind kinetic energy	None (direct)
Un-balancing ballast	**Wind**	Wind mill	Martian wind	Electricity	Electric motor
	Heat	Micro-turbine	Thermal expansion of gas	Electricity	Electric motor
		Evaporation	Fluid phase transform	Gas pressure	Fluid container as a ballast
		Osmosis	Fluid concentration	Osmosis-pressure	Fluid container as a ballast
		Bi-metal	Thermal expansion of metal	Bending stress of beam	Beam + ballast
		Stirling engine	Thermal expansion of gas	Mechanical motion	Piston + pinion assembly
	Sun radiation	Solar cells	Solar energy	Electricity	Electric motor
	Heat	Peltier element	Temperature difference	Electricity	Electric motor

In the Table 11 below the energy sources used for production of electricity are compared separately. The ‘Notes’-column lists several assumptions that had to be made in order to perform the power and energy calculations. Performance of solar panels is clearly above others, although power from Peltier elements is still sufficient. A wind-mill solution could work if enough wind is present and some time can be reserved to charge batteries. Power gain from thermal expansion of gas inside the ball appears to be very small.

Table 11. Electricity production from local energy sources.

Electricity generation comparison			
Method	**Power**	**Energy**	**Notes**
Solar Panels	271 W (38 W/m^2)	130 080 W-min / sol	3 m ball, 25 % surface illumination, 8-hr sun visibility, 12 % efficiency, solar flux 320 W/m^2
	1 084 W	520 320 W-min /sol	6 m ball
Peltier elements	113 W (16 W/m^2)	54 200 W-min / sol	3 m ball, 25 % surface illumination, 8-hr sun visibility, 5 % efficiency, solar flux 320 W/m^2
	452 W	216 800 W-min / sol	6 m ball
Gas turbine + thermal expansion of air in ball	30 mW	2 W-min / sol	700 Pa, 6 m ball, 9.6 % efficiency from gas energy to electricity, assume flow time 1 hr
	5 W	306 W-min / sol	1 bar, 6 m ball
	10 W	612 W-min / sol	2 bar, 6 m ball
Wind-mill	1.08 W	777 W-min / sol	1 m mill, 7 m /s, 40% efficiency, 12 hrs wind / sol
	9.7 W	6 998 W-min / sol	3 m mill, 7 m /s, 40% efficiency, 12 hrs wind / sol
	38.8 W	27 936 W-min / sol	6 m mill, 7 m /s, 40% efficiency, 12 hrs wind / sol

11 Mobility considerations

Before we can compare the performance of different energy sources, we have to consider mobility requirements and also size of the system. Mobility and rolling torque for three different sizes of Russian Thistle –type balls are studied, and needed wind-force or ballast loads are calculated.

As the Thistle hits an obstacle, it adopts a new point of contact. If we wish to overcome the object the needed torque must be calculated according to this new point of contact between the ball and the object. As the contact point moves from ground to the obstacle, also the torque caused by vertical ballast force or horizontal wind-load changes.

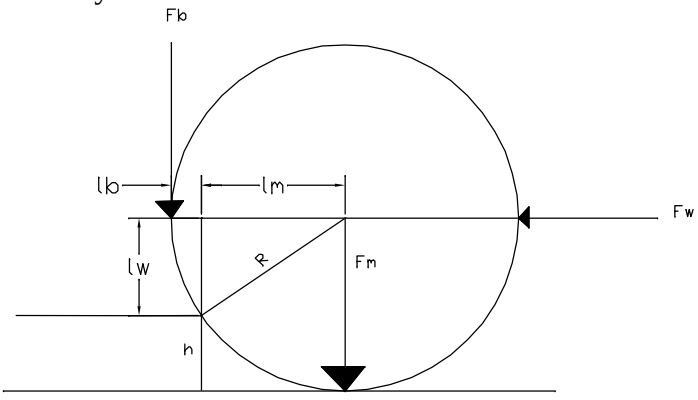

Fig. 56. Loads acting on a sphere overcoming an obstacle.

11.1 Wind propulsion

Consider the Fig. 56 above. If the rolling Thistle meets an obstacle of height h, mass load of the Thistle F_m generates a resistive torque T_m with moment arm l_m.

$$T_m = F_m \cdot l_m \tag{7}$$

$$\begin{aligned} &\textit{by geometry :} \\ &T_m = m \cdot g \cdot \sqrt{2 \cdot R \cdot h - h^2} \\ &\textit{where :} \\ &g = \textit{gravity}, m = \textit{ball mass} \end{aligned} \tag{8}$$

If wind load F_w is used for locomotion, the resulting torque T_w with wind-load arm of moment l_w must overcome the resisting torque. We make an assumption that wind load center goes through the center of the sphere.

$$Tw = F_w \cdot l_w \tag{9}$$

$$\begin{aligned} &\text{by geometry:} \\ &T_w = Fw \cdot (R - h) \end{aligned} \tag{10}$$

The needed wind force F_w to overcome an obstacle can be calculated by setting $T_w = T_m$, from which follows:

$$F_w = m \cdot g \cdot \sqrt{\frac{2 \cdot R \cdot h - h^2}{(R - h)^2}} \tag{11}$$

Next we will calculate the F_w in general and in section 11.1.4 we determine the needed wind velocity to overcome a defined obstacle.

11.1.1 Atmospheric drag

Drag means a force developed on an object subjected to a fluid flow. Granger in [48] (pp. 398) presents two formulas to define friction drag and pressure drag. From these the pressure drag is dominant for a blunt and smooth object, while friction drag increases as surface gets more rough. For the case of the Thistle pressure drag can be used;

$$
\begin{aligned}
&D_p = C_{Dp}(\tfrac{1}{2} d U^2 A_p) \\
&\quad where: \\
&D_p = drag\ force \\
&C_{Dp} = drag\ coefficient \\
&d = fluid\ density \\
&U = flow\ velocity \\
&A_p = cross-sectional\ area
\end{aligned}
\tag{12}
$$

Defining the drag coefficient is not a straightforward procedure. It depends greatly on geometry, surface properties, wind velocity and air density. Reynold's number R_d is used to define the circumstances where a certain C_D can be considered applicable. The issue is discussed in [23], [29], [39] and [48]. Granger in [48] (pp. 381) presents a formula for R_L:

$$
\begin{aligned}
&R_L = \frac{UL}{n} \\
&\quad where: \\
&R_L = Reynold's\ number \\
&U = flow\ velocity \\
&L = specific\ dimension\ (e.g.\ sphere\ diameter) \\
&n = kinematic\ viscosity\ of\ \ fluid
\end{aligned}
\tag{13}
$$

On Earth kinematic viscosity of air is 1.8E-5 m^2/s, on Mars it has been estimated to be 8E-4 m^2/s. Assuming a Thistle model diameter range 0.1 m – 1.5 m and wind velocity range 1 m/s – 10 m/s on Earth we can calculate a corresponding R_D range to be 5 556-833 333. On Mars, assuming Thistle diameter range 1.5 m – 6 m and wind velocity range 5 - 30 m/s we can calculate a corresponding R_D range to be 9 375 – 225 000. Granger in [48] (pp. 790) presents a graph showing C_D for a smooth sphere over a large range of R_D. When R_D is in range 100-100 000 the C_D falls between 0.9 and 0.4 respectively. Literature gives a C_D 0.4 for rough surfaced sphere when Re is 10^6, or C_D is 1.17 for a flat square plate. [47]. It is worth to note that between $R_D = 10^5$ and $R_D = 10^6$ there happens a quick drop in C_D. When operating in this area the aerodynamic properties of the object must be studied very carefully.

Two conclusions after several wind-tunnel tests on several models are presented in [26] and [21], see Fig. 57. The tests have been carried out with terrestrial air in atmospheric pressure. It has been shown that for the applied ball properties and wind velocities the Reynold's number stays both on Earth scale model and on Mars application in such an interval that the test results are representative. Hajos et.al. present the drag coefficient as a function of angle-of-attack, i.e. from different wind directions. Heimendahl shows dependency on wind velocity at the given range, and the Hardball is also tested in different angles of incidence. Wind velocity at Hajos tests (12 m/s) is 50% higher than

the maximum in Heimendahl test (8 m/s), but still on a reasonable level if considering daily wind conditions on Mars.

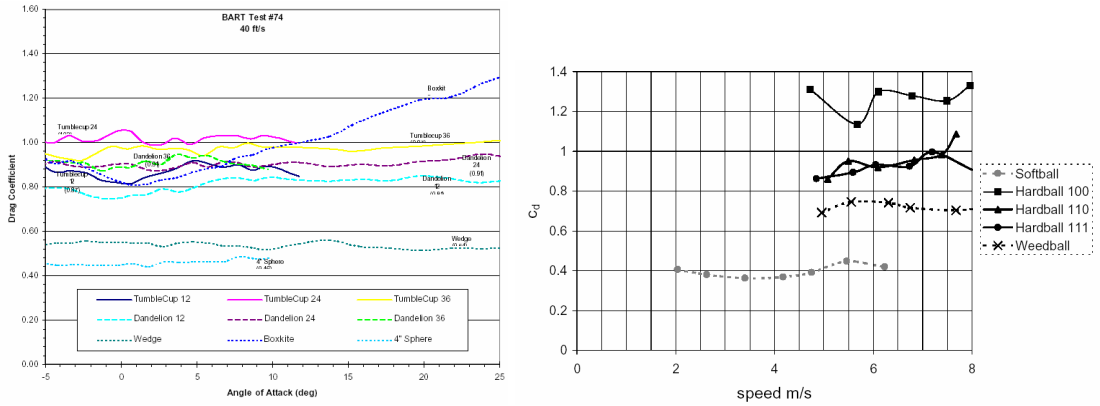

Fig. 57. Measured drag coefficients by Hajos et.al. (left) [21] and Heimendahl (right) [26].

The Box-Kite is in practice a set of flat plates and upon proper angle of attack the C_D indeed exceeds the value 1.2, as does also the Hardball. An inflatable ball is rough enough to produce the right drag coefficient according to common table information, C_D is roughly 0.4 in both tests. Other spherical objects with less pronounced flat surfaces and still without a smooth surface seem to produce a drag coefficient falling between 0.8 and 1.0.

It appears reasonable to assume that a smooth ball on Mars would have a drag coefficient of 0.4, while with some added structural complexity in can be elevated up to 0.8, still being on conservative side. Exceeding 1 would require accurate design and testing of a structure consisting of plate-like structures. The air density is 0.02 kg/m^3 for Mars, and 1.29 kg/ m^3 for the air on Earth.

11.1.2 Test setup

In order to experimentally compare performance of a turbine-type ball with respect to a plain ball a simple test set-up was constructed. The test-items were two 32 cm beach balls, one of which was equipped with turbine blades or pockets. Six pockets were constructed of plastic sheet and taped on surface of the ball. Pocket height was 35 mm at maximum, and zero at poles.

Plastic poles with pin-holes were glued on balls to provide a support point and rotation axis. The ball was then assembled on a pivoted jig. The jig was supported by an electronic letter scale that allows read-out of force acting on the ball. The turbine ball pole was also equipped with a short lever arm (55 mm long) and a piece of thread and counter-weight, which with a properly positioned letter scale allowed measurement of torque acting on the ball.

Wind load was generated with two parallel-mounted blowers. Intensity of wind was varied by adjusting power input to the blower, and also by selecting two different

distances from the blower (0.83 m and 1.66 m). Actual wind speed and wind profile was measured on both locations with an electronic wind speed metering device.

The Fig. 58 and Table 12 below present the balls and the complete test set-up.

Fig. 58. Test set-up for a comparative wind force measurement.

Table 12. Some properties of test set-up.

Test set-up properties		
Test ball diameter	320	mm
Turbine pocket height	35	mm (in center line, zero at poles)
Turbine pocket cross-section area	8797	mm2
Number of pockets	6	
Ball cross-section area	80424	mm2
Single pocket area/ball area	0.11	
drag force / scale readout ratio	2.22	(mechanical amplification of support system)
Torque arm length	54	mm (to measure turbine torque)
Read-out accuracy	10	Gramms (scale read-out variation)
Scaled read-out accuracy	0.22	N (drag force variation)

The wind velocity was measured at free-flowing arrangement (without ball or fixture) with a hand-held wind-speed-meter. The speed was measured at two different distances, with three blower power levels and at three different heights (ball lower edge, middle height and ball upper edge). The results (shown in Table 13) indicate one clearly unsuccessful speed measurement (circled) that causes an undesired peak in graphical presentations. Reason for the inaccurate result is that blower levels 2 and 3 happened to be so close to each other that wind velocity difference was lost in read-out accuracy. The same applies in measured drag force.

Table 13. Wind velocity measurement.

	Measured wind velocity (m/s)					
Distance from blower (m)	**0.83**			**1.66**		
Measurement height (mm)	**160**	**320**	**480**	**160**	**320**	**480**
Blower setting						
Level 1	3.2	3.7	3.4	2.6	2.4	2.1
Level 2	3.5	4.6	4	3.2	3.2	2.6
Level 3	4	4.6	4.1	3.2	3	2.6

The graphs of Fig. 59 below present the wind-velocity vertical profile. Maximum velocity affecting in the middle of the ball was used in the following calculations.

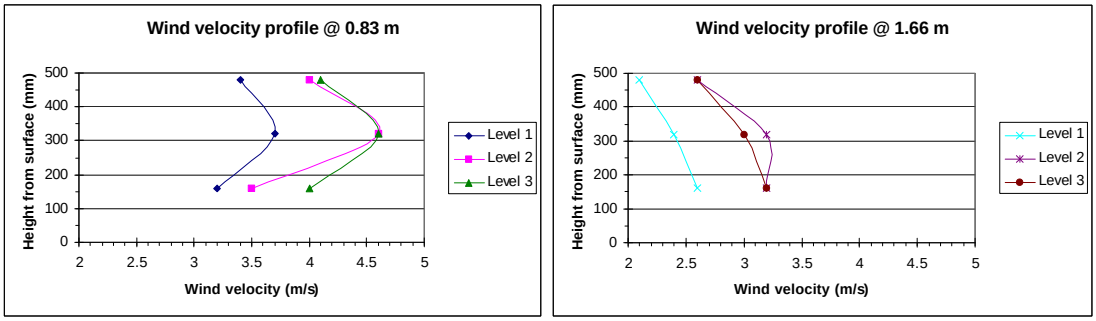

Fig. 59. Measured wind velocity profile.

11.1.3 Test results

The test was run with three different blower power setting and at two different distances from the blower. The Table 14 and Fig. 60 below show the results. In close distance (0.83 m, high wind velocity) the turbine ball appears to generate 66% higher thrust than the one without turbine pockets. In larger distance (1.66 m, low wind velocity) the benefit of the turbine lay-out appears even more favorable exceeding 70%. Resulting torque on the turbine ball appears quite low; if the torque is translated as an point-load on a single turbine blade, the theoretical wind force (0.19 N) on the blade is only 7.2% of total push force (2.6 N at Level 3, 0.83 m distance). Reynold's number R_D under test conditions is in the range of 50 000.

Table 14. Test results.

			Measured drag force (N) and calculated C_D								Measured torque (mNm)	
			Turbine ball				Round ball				Turbine ball	
Distance from blower			0.83		1.66		0.83		1.66		0.83	1.66
Blower setting	Measured wind speed											
	@0.83 m	@1.66 m	F	C_D	F	C_D	F	C_D	F	C_D		
Level 1	3.7	2.4	0.58	0.82	0.27	0.89	0.35	0.50	0.15	0.52	4.24	17.48
Level 2	4.6	3.2	1.06	0.97	0.49	0.92	0.64	0.58	0.27	0.50	9.54	30.72
Level 3	4.6	3	1.10	1.01	0.53	1.00	0.66	0.60	0.30	0.57	9.54	30.72

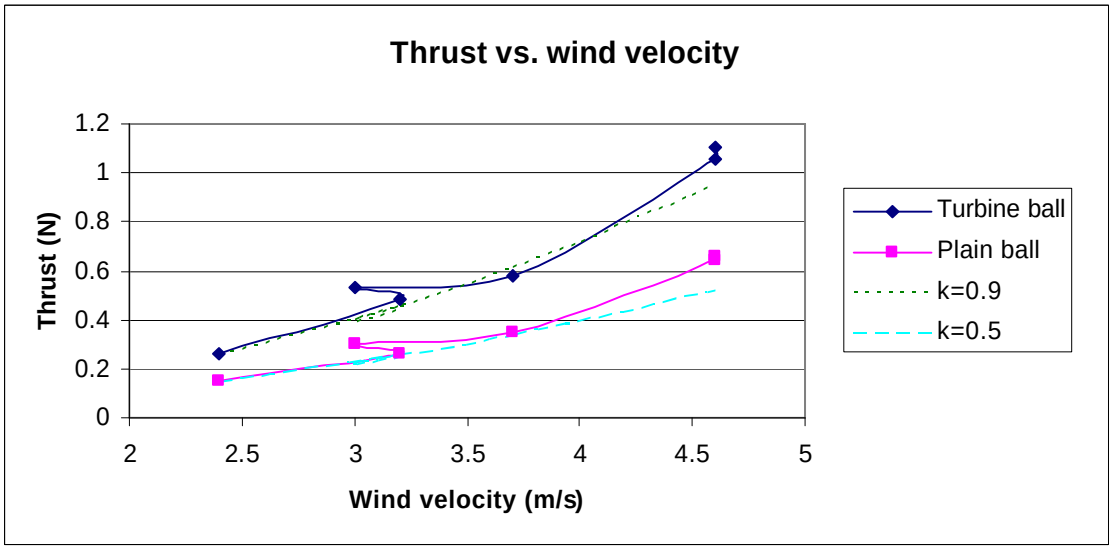

Fig. 60. Test results graphical presentation.
(Note the peak resulting from a measurement error.)

The C_D was calculated using the maximum measured wind velocity affecting on the centre of the ball. However, overall average velocity is less than that and therefore the calculation reveals a lower C_D than it in reality would be. The calculated drag coefficient also seems to have a dependency to wind velocity. At least at short blower distance it is clearly visible that also shape of the wind velocity profile changes as velocity is increased. This change may affect on calculation of the C_D. Despite of this the calculated C_D appears to fall very well in expected range.

The graph above presents also analytical curves to describe ball drag force. For this case apply quite well $C_D = 0.5$ for a plain ball and $C_D = 0.9$ for the turbine ball. Further the drag force appears to depend on wind velocity with a higher ratio than expected, which may, as stated above, be caused by properties of the test set-up.

11.1.4 Required wind velocity

Performance of the sphere increases if the mass can be kept low. The Fig. 61 below shows the needed wind velocity for low-mass spheres. Performance of the 1.5 m sphere is still poor. A 3 m sphere would have a good locomotion capability under strong winds, and a 6 m sphere would travel over most of obstacles without difficulty already driven by light winds. Only a 6 m ball would have any performance if the ball mass is to be increased to 50 kg as shown in Fig. 62.

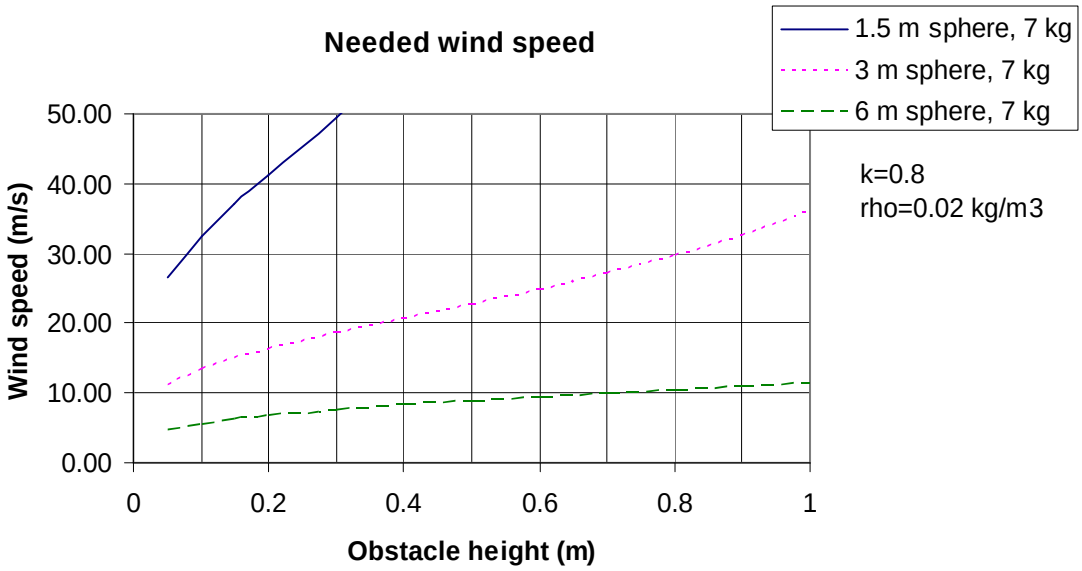

Fig. 61. Needed wind speed for a low-mass sphere.

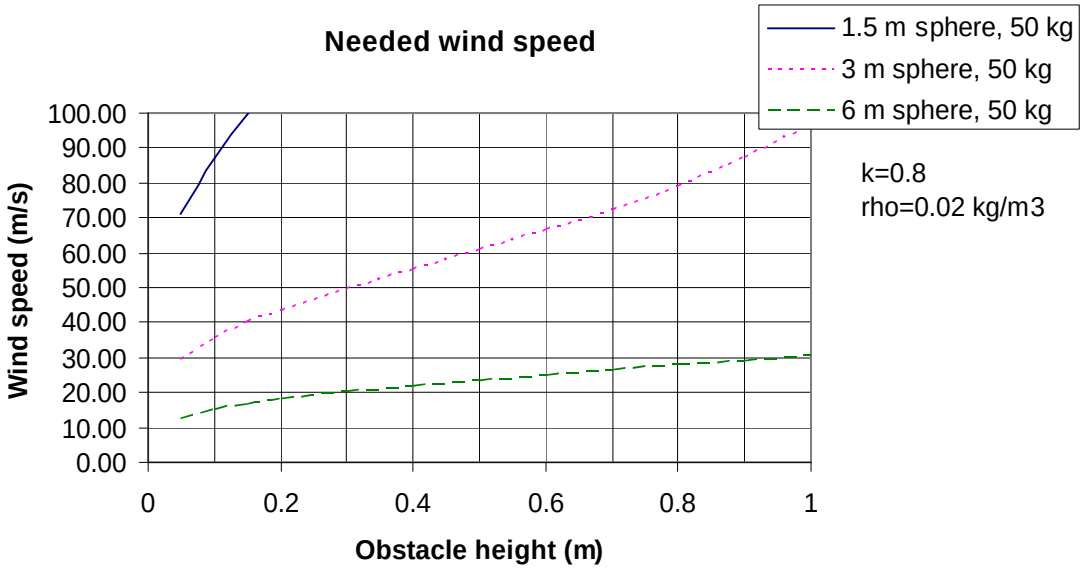

Fig. 62. Needed wind speed for a high-mass sphere.

For the interest of the reader the following graphs in Fig. 63 show how required wind velocity depends on ball mass and obstacle height.

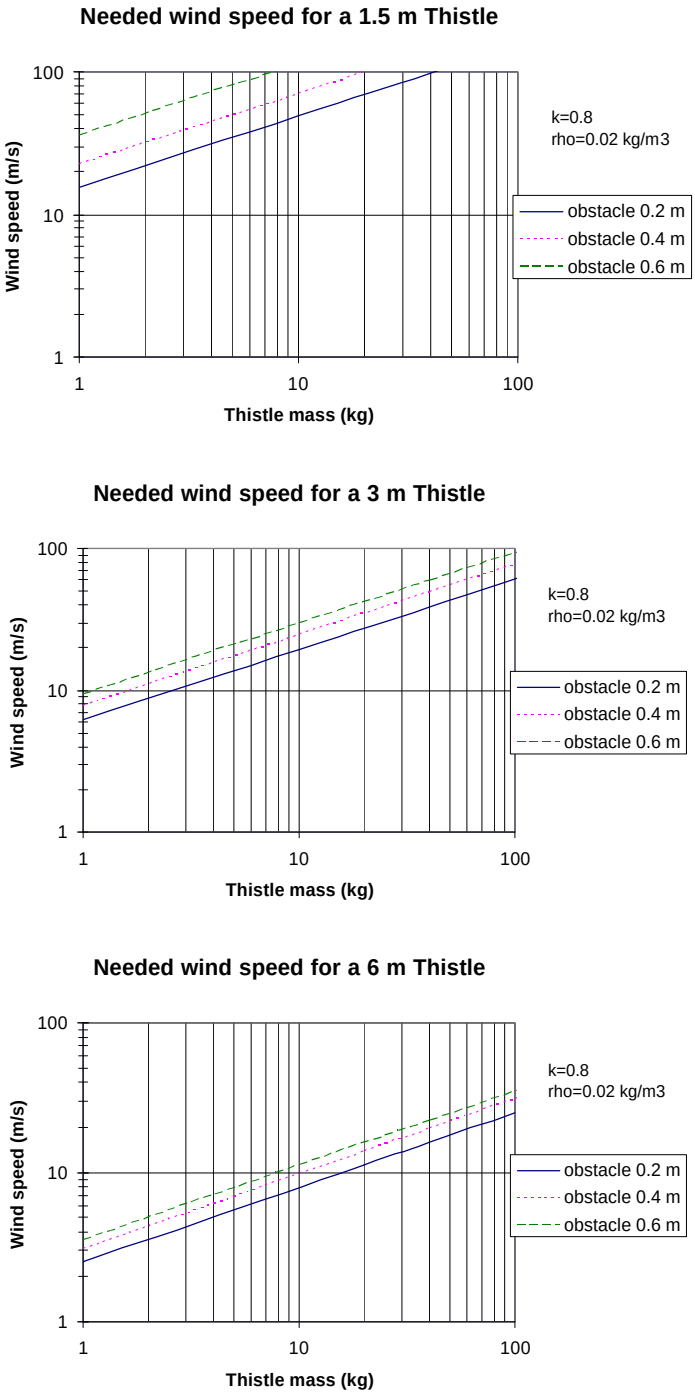

Fig. 63. Wind speed requirement as a function of mass.

11.1.5 Conclusions

Wind load on turbine-shaped ball appears very promising compared to a plain ball, although wind-generated torque remains negligible. Definitely ball shape and surface structure deserve more close study in order to maximize wind resistance of Thistle-type wind-driven planetary rover.

11.2 Ballast mass

Study the Fig. 56 again; if using un-balanced ballast mass for locomotion the sphere mass must be divided in two portions: an evenly distributed structural mass acting through the center and resulting in resistive torque, and the ballast mass causing F_b and having moment of arm l_b. The figure shows the ballast mass to be located exactly on the outer surface, i.e. $l_b+l_m = R$. In reality this would not be the case.

Length of moment arm *lb* depends on mechanical structure and Thistle size. For small spheres ratio $(l_b+l_m)/R$ could be roughly 0.5, while the ratio approaches to 1 as the sphere diameter increases. For a 6 m Thistle $(l_b+l_m)/R$ could have an estimated value 2 m / 3 m or 0.66. In the following calculations the value 0.66 is used for $(l_b+l_m)/R$. Now the resulting driving torque from ballast load F_b is F_b*l_b or $F_b*(0.66*R-l_m)$. This geometric 'inefficiency' was not considered in [1] and thus the results presented here differ from the results shown in the mentioned reference.

The figures below show the needed ballast mass to overcome an obstacle. Sphere masses are similar to ones used for wind-velocity calculations. Sufficient locomotion capability could be achieved only for a 6 m sphere.

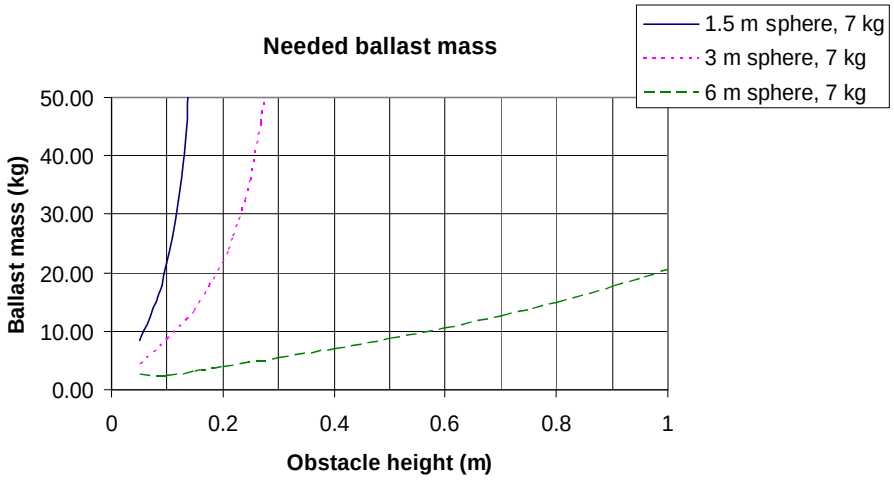

Fig. 64. Ballast mass for a low-weight sphere.

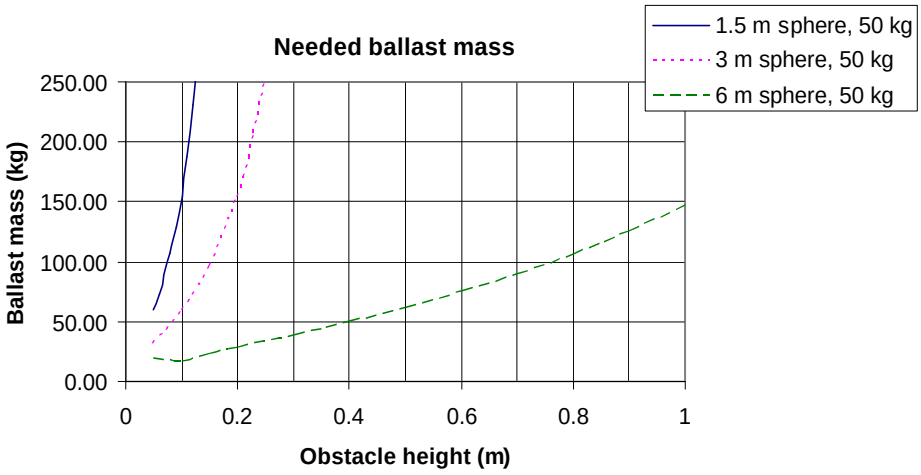

Fig. 65. Ballast mass for a heavy-weight sphere.

For the interest of the reader the following graphs in Fig. 66 show how required ballast mass depends on ball mass and obstacle height.

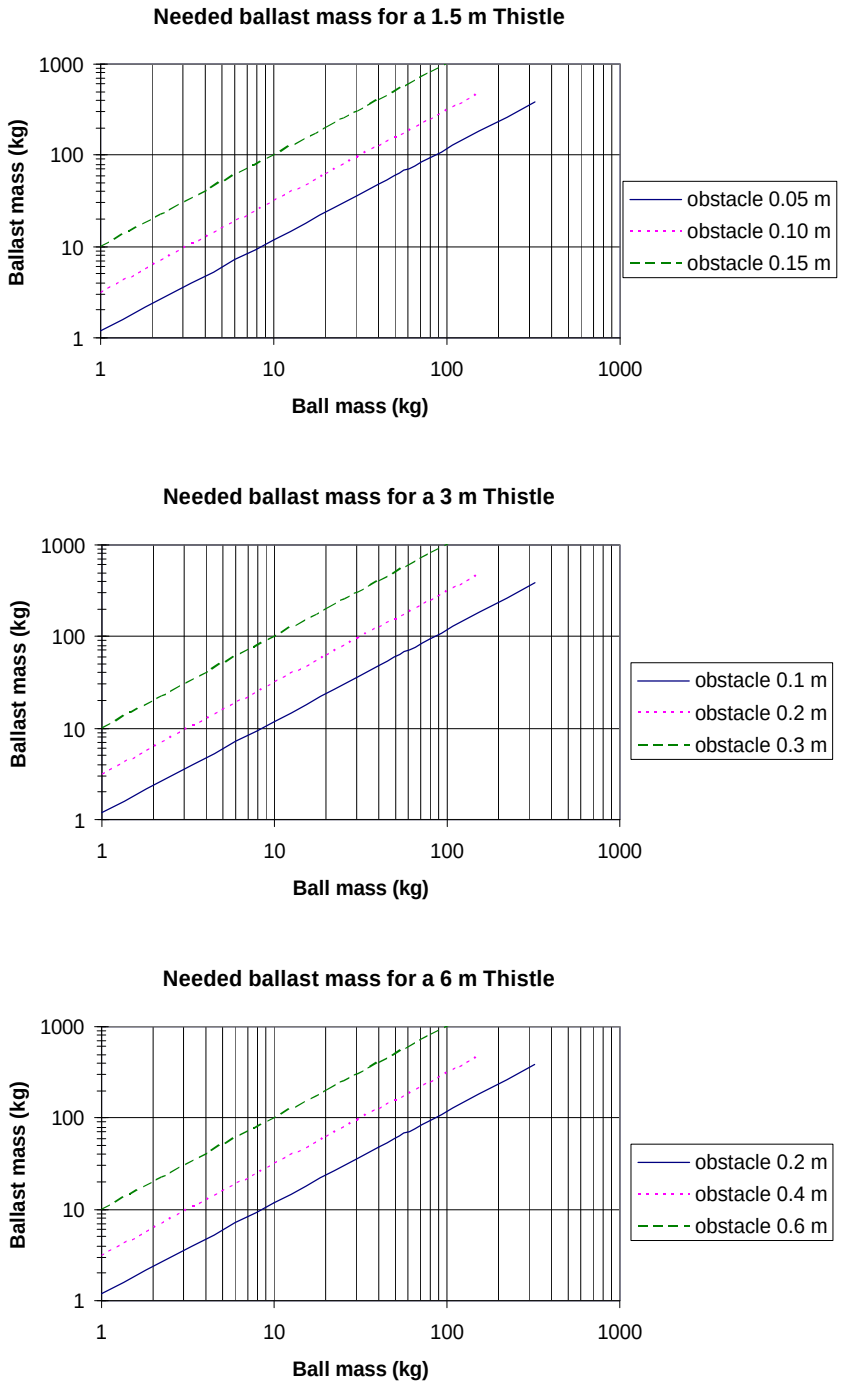

Fig. 66. Ballast mass requirement as a function of mass.

11.3 Discussion on mobility and dynamics

In above calculations, -wind propulsion and unbalanced drive, a static analysis has been performed. The cases do not consider dynamic effects of a moving ball which may help in a great extent in overcoming obstacles. The issue has been discussed also in [20]. It is worth to note that effect of dynamic properties increase as gravity decreases.
Also only step-shaped obstacles have been considered. Often a slope is of an interest, and the presented calculation models are applicable also for those. In practice the slope angle can be calculated as a tangent at the point where the ball touches the corner of the step.

11.4 Comparison of wind propulsion and ballast drive

In order to compare wind-propulsion and ballast-drive the previously-presented graphs can be collected into one table. The table below presents as a function of Thistle total mass the needed wind velocity or alternatively the ball mass and the needed ballast mass.

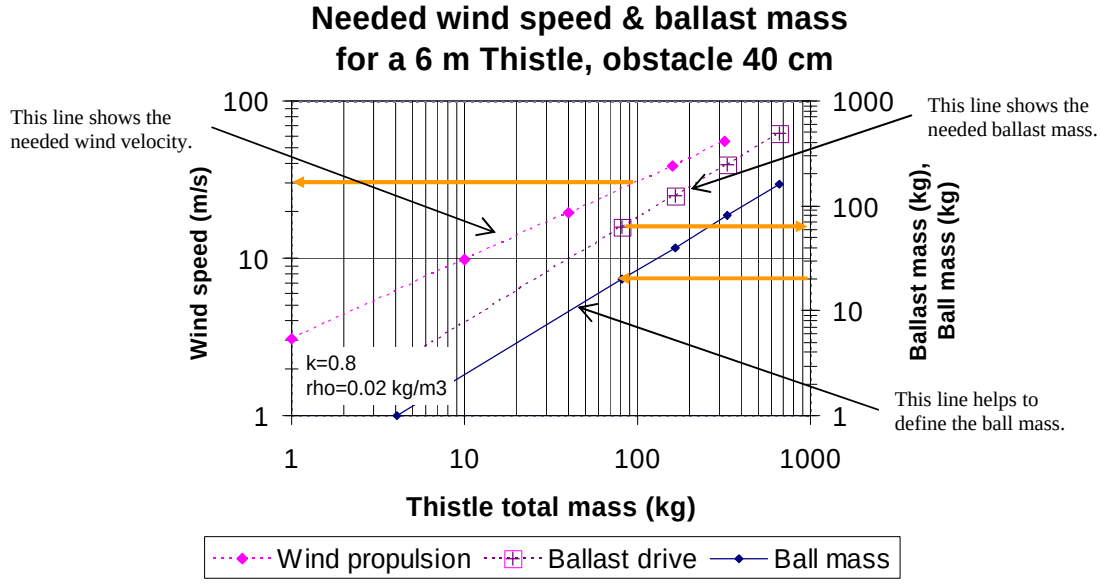

Fig. 67. Wind velocity and ballast mass as a function of Thistle total mass and obstacle height. (6 m Thistle)

The graph can read so, that when looking for the needed wind velocity, one first selects the total mass of the Thistle from X-axis and then follows vertical line to the uppermost tilted wind-velocity line. Elevation shows the needed wind velocity on left-hand Y-axis. When looking for the ballast mass, one first selects the sphere shell mass from the right-hand Y-axis and then follows a horizontal line to the lowermost tilted line. Now the value on X-axis below tells the Thistle total mass. Continuing upward to the middle tilted line one can finally read the needed ballast mass from the right-hand Y-axis.

Conclusions made by the graph rely on three additional numerical values which are: the maximum (or operational) expected wind velocity, the obstacle height to be overcome, and estimated shell mass of the sphere. Naturally the sphere diameter affects too.

It can be seen from the graph that with certain assumptions there does exist a range where similar locomotion performance can be achieved with a reasonable wind speed and also with reasonable ratio of ballast mass / total mass. The assumptions made are: max wind velocity 30 m/s, obstacle height 40 cm, Thistle total mass approx. 95 kg and Thistle shell mass 20 kg. This kind of 6 m diameter Thistle could utilize both methods of locomotion, but with limited 40 cm obstacle size. Both methods could be implemented for redundancy and versatility.

If we wish to modify Thistle total mass, we see from the graph that on the left side the total mass becomes so low that mass reserved for the sphere shell becomes very small and ballast-drive can not be realized. On the right side the total mass of the Thistle becomes so high, that unrealistic wind velocity would be needed for locomotion and a ballast drive would provide a better alternative.

A 20 kg shell mass appears quite low for a 6 m ball and can be considered probably only for inflatable structures. If we up-scale the existing 1.3 m and 4 kg prototype shell assuming that the mass is proportional to surface area (square of the diameter), we may assume a 85 kg shell mass for a 6 m sphere. The Fig. 68 below shows that in this case there is no more an overlapping area, but the wind propulsion is limited to 100 kg Thistle while ballast drive becomes effective only above 300 kg total mass. Effect of shell mass is very strong.

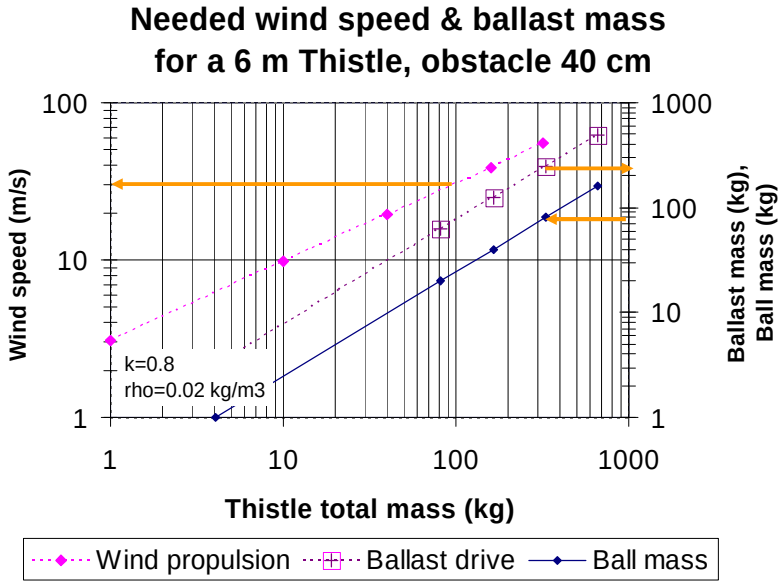

Fig. 68. A 6 m, 300 kg Thistle with a 85 kg shell.

Alternatively we may study effect of the obstacle size. When the size is decreased from 40 cm to 20 cm, the wind propelled ball mass can be increased up to 150 kg. Since the obstacle is smaller, the ballast mass becomes smaller and total mass approaches the shell mass. Now a 20 kg shell would call less than 30 kg ballast and total mass stays at 50 kg.

A 50 kg ball would be propelled already by a 20 m/s wind velocity. Alternatively a 85 kg shell would call for a 100 kg ballast, see Fig. 69. below.

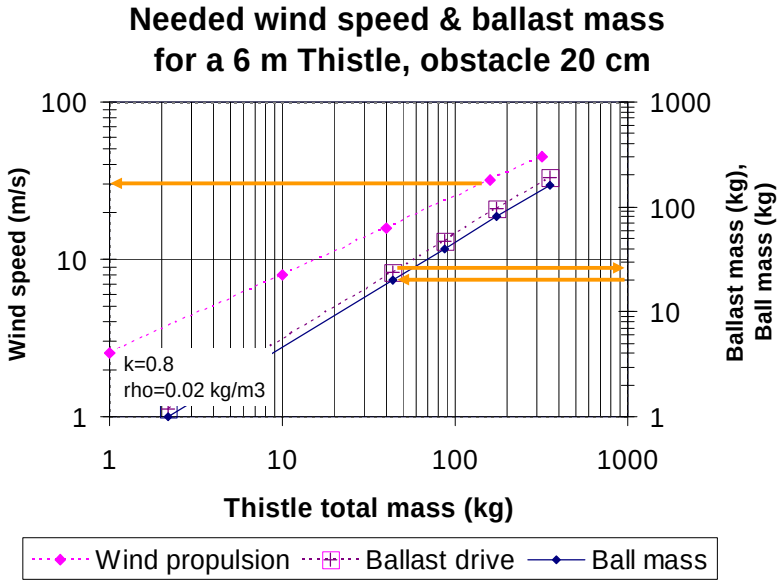

Fig. 69. Performance at reduced obstacle size.

A similar comparison as presented above can be conducted also for 3 m and 1.5 m Thistles. See Fig. 70 and Fig. 71 below. Neither of the smaller Thistles indicate a common region of operation. Wind-propulsion of a low mass (inflatable) 3 m sphere is limited to rough 20-kg mass and 0.2 m obstacles. Also ballast-drive of a Thistle with a reasonable 20 kg sphere mass calls for a ballast mass exceeding 60-kg to overcome 20 cm obstacles. The 1.5 m Thistle would be wind propelled up to 4-kg mass overcoming only modest 10 cm obstacles. Total mass of a ballast-driven Thistle starts from 22-kg (4 kg sphere mass, 18 kg ballast) and continues upwards.

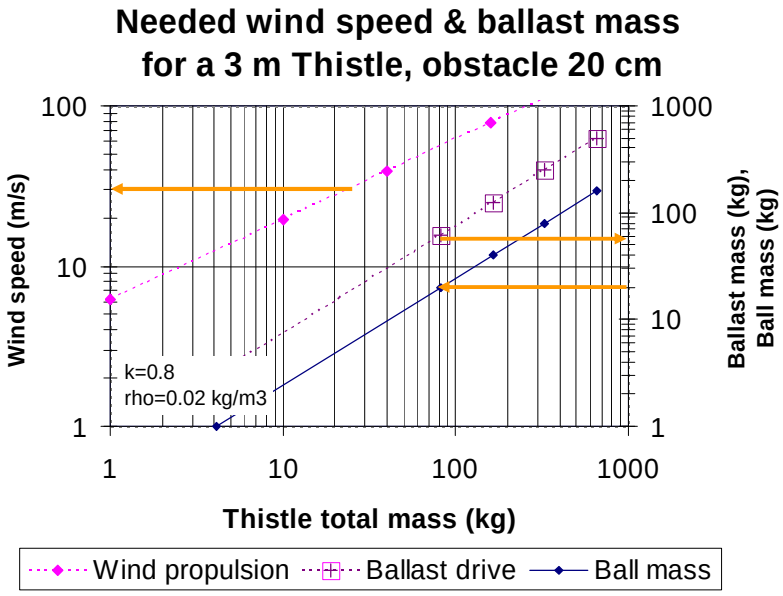

Fig. 70. Wind velocity and ballast mass as a function of Thistle total mass and obstacle height. (3 m Thistle)

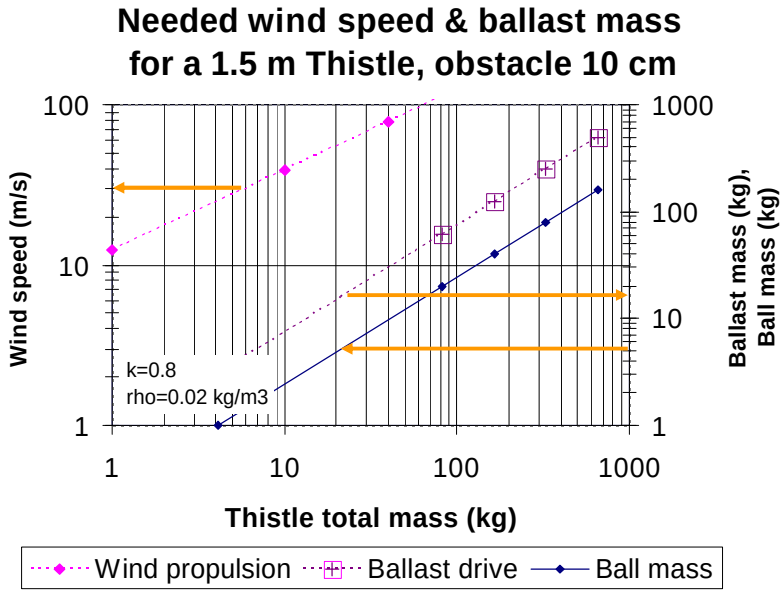

Fig. 71. Wind velocity and ballast mass as a function of Thistle total mass and obstacle height. (1.5 m Thistle)

11.5 Conclusion of mobility considerations

As we have now calculated the basic criteria for the mobility, realized with wind thrust or ballast mass, we can collect the data into the Table 15 below and perform a comparison between different concepts. Comparison is not quite straightforward, as performance

depends strongly on ball diameter and mass. Therefore some alternative values are presented in order to indicate preferred direction of development.

Table 15. Comparison of wind/ballast-propulsion performance; some examples.

Comparison of propulsion performance						
Concept	**Ball dia. m**	**Ball mass kg**	**Ballast mass / wind velocity**			**Notes**
			Small obstacle 0.2 m	**Medium obstacle 0.4 m**	**Large obstacle 0.6 m**	
Wind propulsion	1.5	1.5	19 m/s	27 m/s	44 m/s	Very-low-mass solution.
	1.5	4	31 m/s	45 m/s	72 m/s	Low-mass solution.
	3	5	14 m/s	18 m/s	21 m/s	Very-low-mass solution.
Note: Different	3	10	20 m/s	25 m/s	31 m/s	Low-mass solution.
Wind conditions	3	20	28 m/s	35 m/s	41 m/s	Medium-mass solution.
	3	30	34 m/s	43 m/s	52 m/s	High-mass solution.
	6	30	14 m/s	17 m/s	20 m/s	Low-mass solution.
	6	80	23 m/s	28 m/s	32 m/s	Medium-mass solution.
	6	150	31 m/s	38 m/s	43 m/s	High-mass solution.
Wind propulsion with turbine-design	As above	As above	As above 11 % less velocity expected			25 % higher wind resistance expected (k = 1)
~~**Tangential fluid flow; vaporizing or osmosis**~~	~~6 m~~	~~900 kg~~	~~N/A~~	~~N/A~~	~~N/A~~	~~Assumes water density.~~ Total mass out of scope.
~~**Tangential ballast and deformation**~~	~~6 m~~	~~540 kg~~	~~N/A~~	~~N/A~~	~~N/A~~	~~Assumes 200 mm radial displacement of ballast.~~ Total mass out of scope.
Internal ballast; includes also tangential fluid flow; mobile fluid ballast.	1.5	N/A	N/A	N/A	N/A	Mobility limited to 10 cm obstacles
	3	5	16 kg	N/A	N/A	Very-low-mass sphere
Note: different	3	10	31 kg	N/A	N/A	Low-mass sphere
Structural ballast	3	20	62 kg	N/A	N/A	Medium-mass sphere
mass						
	6	30	36 kg	93 kg	300 kg	Low-mass sphere.
	6	80	96 kg	248 kg	800 kg	Medium-mass sphere.
	6	150	179 kg	465 kg	1500 kg	High-mass sphere.

Solar cells, Peltier elements and Micro turbines all produce electrical energy that can be transformed in locomotion torque with electric motors. In case of Thistle-rover the internal ballast is the method to utilize these energy sources.

As we at this moment do not know physical properties of the Thistle-rover to be constructed, we need to consider a few options. Note that internal ballast and tangential

fluid ballast do not differ from each other in terms of mobility. Only the method to produce the off-balance is different. The ones to be taken into consideration from the sections above could be the ones presented above.

With proper mass distribution between ball structure and ballast the obstacle overcoming capability can be similar for ballast-driven and wind-driven locomotion. If the instrument mass can be used as a ballast, adding a ballast-driven system to a wind-propulsion would improve operational capabilities of the Thistle. It is necessary to include a mechanism to locate ballast in a favorable orientation inside the ball for wind-driven rolling. However, if the ballast mass is a dummy mass without any scientific reasoning, pure wind-propulsion would be more beneficial due to smaller system mass.

For a purely wind-driven Thistle any ballast would add mass and thus reduce performance. However, adding the ballast would add a steering capability and independence of wind conditions. A possible ambitious ballast-driven Thistle design could have a 3 m diameter, 18 kg ballast and 6 kg ball equipped with wind-turbine design. Obstacle overcoming capability would be 20 cm with internal ballast drive or with 30 m/s wind. A 6 m 24 kg Thistle with a 74 kg ballast would still have a good locomotion performance and capability to overcome obstacles 40 cm high with ballast drive or with 30 m/s wind velocity. Requirements for low shell mass are very high. In case shell mass increases the mobility performance either of the ballast drive or wind propulsion must be compromised.

Use of a liquid-ballast is justified only if autonomous locomotion independent from wind-conditions is desired. This is because the liquid adds mass and so reduces performance of a wind-driven Thistle. Liquid is a dummy mass that can be replaced with useful payload for a lever-ballast or rail-ballast.

12 Mechanical Thistle concepts

12.1 Wind turbine

The wind turbine would be completely driven by the wind with little possibilities for steering. The turbine-shaped Thistle would resemble the JPL-developed Tumbleweed, except that the turbine-shape can improve response to wind load by approximately 25% (11% less wind velocity is needed). The Thistle need not necessarily be of an open-section, as illustrated in artistic drawings in Fig. 72 below, but it can construct also of a closed volume (a balloon or similar) to protect the instruments from Martian environment.

Additional functions that can be installed for the Thistle would include re-orienting the ball with a movable mass inside the instrumentation tube, and anchoring the thistle on ground to be used as a wind mill. A movable mass would turn the Thistle and instrumentation tube into vertical position, and the anchoring system in the end of the tube would enter into ground. Now the turbine can rotate around the instrumentation tube and electricity can be produced with a generator. Energy production capability of a such Thistle can be significant.

Caution must be paid for the mass of the system since added mass rapidly decreases locomotion capability of the Thistle. Also anchoring of the ball to the ground would be a challenging task. A sort of drill or harpoon should be considered and added mass would be several kilograms, unless there is a scientific drill already included in the system.

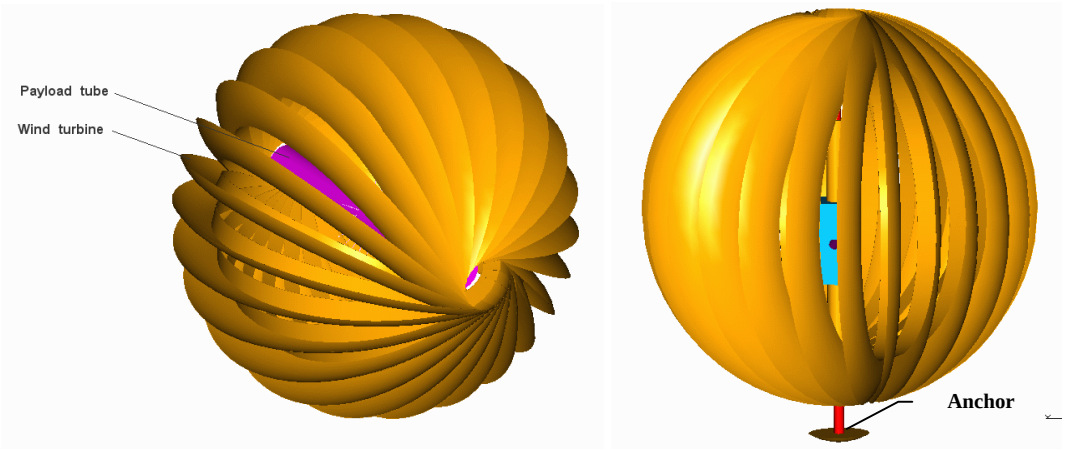

Fig. 72. Wind-turbine Thistle rolling (left)
and anchored for a wind mill operation (right).

12.2 Fluid ballast

The fluid ballast constructs of a series of circumferential shrink-tubes filled with fluid. Amount of fluid is 20-200 kg depending on Thistle mass and diameter. The shrink tube is constructed so that it shrinks in cold, and expands in hot, as shown in Fig. 73. So the fluid inside the tube is collected on hot part of the tube, and off-balance develops. The resulting off-balance makes the ball to rotate and the rotation turns the heated part into shade and reveals a new part of surface to be heated. Shrinking and expanding of the tubes drives the fluid again towards the heated part of the tube.

The fluid itself should remain liquid in temperature range –80 C to +100 ℃ and in Martian atmospheric pressure 700 Pa. The tubes can also be pressurized, but then leaks to atmosphere are more evident. Silicone oils and other synthetic oils, like lubricants developed for space use, can fulfill these requirements.

If we assume that fluid (20 kg) is to be collected on 90 deg. high illuminated area of a 3 m ball (10-kg sphere), tube length of this portion would be pi/2 * 1.5 m = 2.36 m. If we assume expanded tube diameter 3 cm and fluid density 0.9 g/cm3, one tube would hold in the hot part 1665 cm3 or 1499 g fluid. Hence number of tubes in parallel should be 13 which, when 3 cm in diameter, would take 40 cm width or a 15 degrees wide sector, as illustrated in Fig. 74. 13 tubes 1.5 cm in diameter in initial condition would hold the needed amount of fluid, but require complete shrinkage in cold and expansion to 3 cm diameter in hot to push all fluid into desired location. A larger tube with less shrinkage can be used, but then some fluid will remain in cold parts of the tubes as an unnecessary weight.

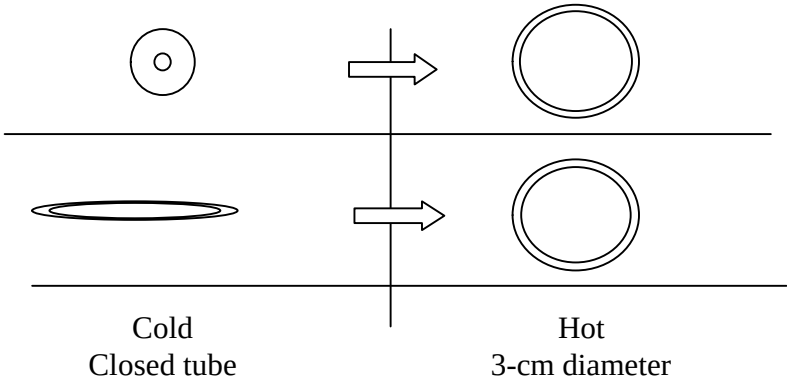

Fig. 73. Operation of a shrink-tube pushing the fluid into hot areas (two options).

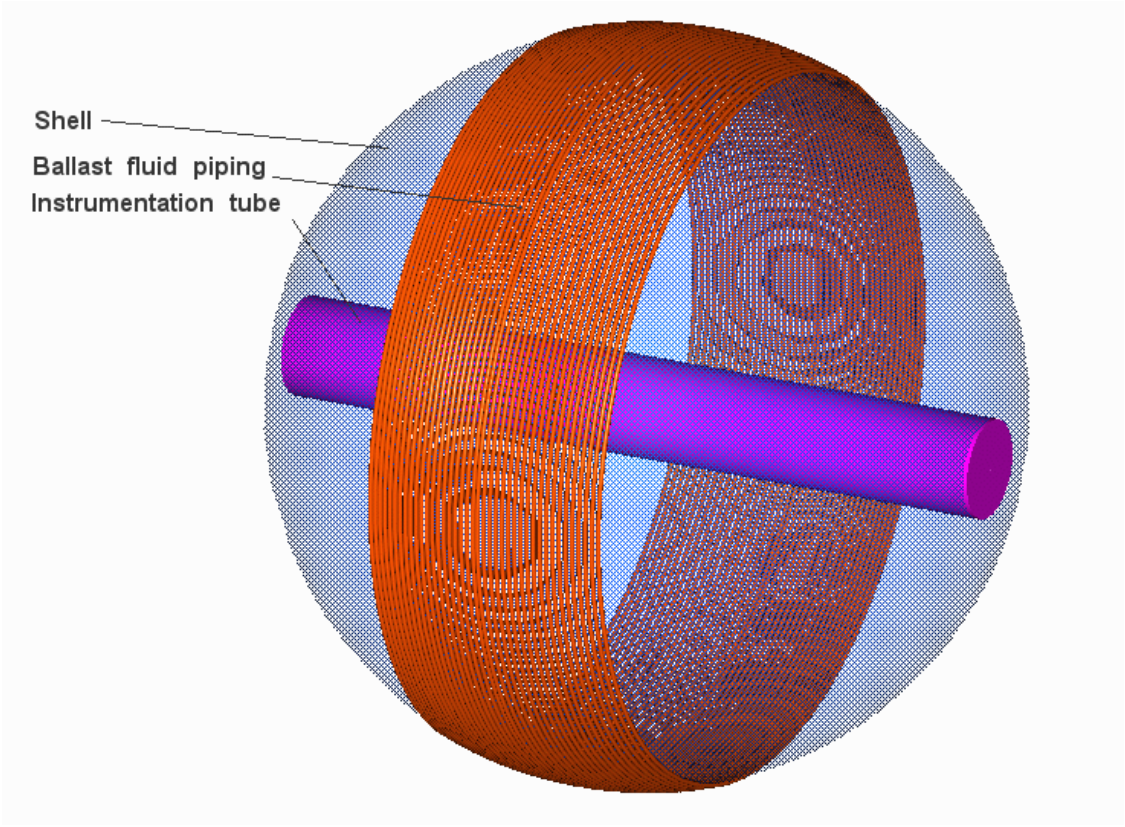

Fig. 74. Fluid-ballast -type Thistle.

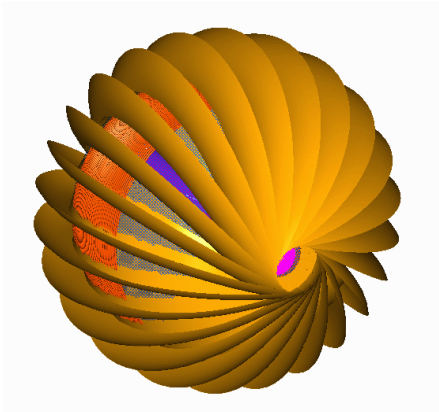

Fig. 75. A combined wind-turbine / fluid ballast Thistle.

It is not evident how this kind of a rover could be guided. The payload inside the instrument tube could be made movable, and so balance of the ball can be disturbed and it could be stopped by turning the tube into vertical position (the tangential fluid tubes in horizontal plane then). Even if there exists some ways to select orientation of the ball, it will in any case always roll towards the Sun.

Mobility of the ball can be assisted with added wind-turbine lay-out, as illustrated in Fig. 75 above.

12.3 Lever ballast

In this concept a rolling axis runs through the ball. A lever is mounted to the axis with bearings and a drive gear. A ballast mass mounts to the end of the lever, as shown in Fig. 76. In steady position the ballast hangs right below the axis. As the roll motor is activated the ballast tries to elevate which makes the ball to roll around the rolling axis.

The concept would be most suitable for small-sized balls (0.5-3 m). A 3 m ball is already quite big since the lever needs to be already roughly 1.5 m long. A long lever would ask for high motor torque and may also induce undesirable bending, flexibility and vibration into system.

The design does not include any means for steering. For steering purposes additional freedoms (and motors) must be implemented.

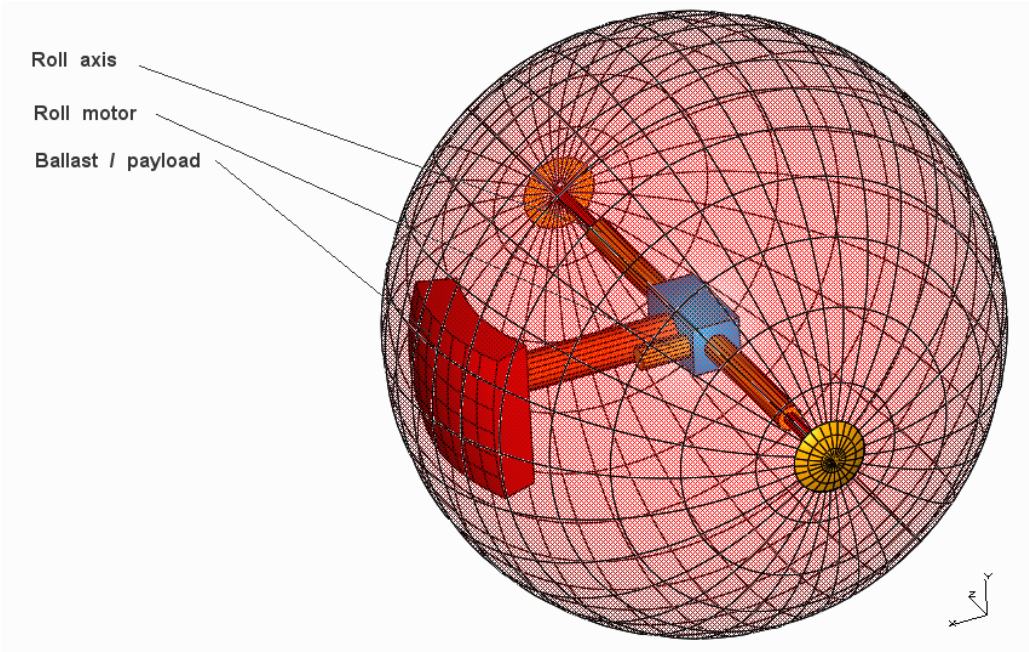

Fig. 76. A Thistle with a lever ballast.

12.3.1 Double lever ballast

Steering capability can be implemented by dividing the ballast into two parts and adding another degree of freedom in the end of the lever. Now the angle between the lever and rolling shaft can be adjusted. See Fig. 77 below.

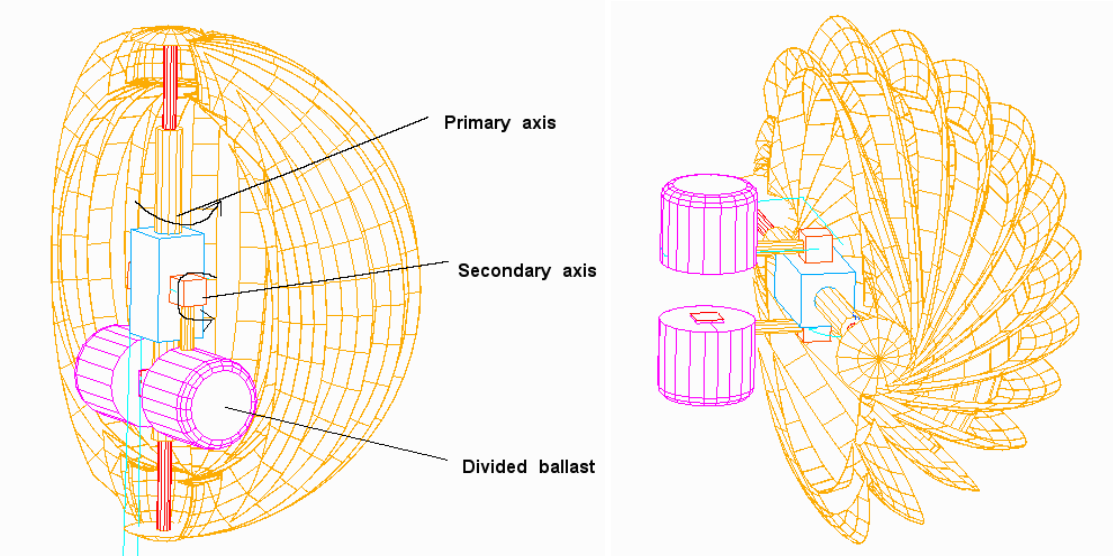

Fig. 77. A Thistle with a steering ballast; turning position (left), rolling position (right). (Cut-away views).

When the lever is turned to be parallel with the roll shaft, the ball adopts a position where the roll shaft stands in vertical direction. Now the desired rolling direction can be selected by rotating the roll motor. As the lever is rotated to be in straight angle to the roll axis, the ball sets the roll axis into horizontal position. Now the roll motor rotates the ball into direction orthogonal to roll axis. Also two orthogonal rolling directions can be achieved by rotating either the rolling motor (primary axis) or the lever motor (secondary axis).

12.3.2 Lever ballast motor torque and dynamic behavior

A fundamental property of ballast arm system is the way it stresses the ballast motor. The ballast motor is located in the center of the ball (mounted on ball axis of rotation). The ballast mass is located in the end of the ballast arm.

As shown in Fig. 56, Length of the ballast arm is *lm+lb*. As the ball hits an obstacle with height *h*, the ball mass generates a resistive torque (*Fm* x *lm*). The ballast mass generates an opposite driving torque (maximum possible illustrated in drawing Fig. 56) (*Fb* x *lb*). The ballast motor torque, however, is much larger than the driving ballast torque: motor torque is [*Fb* x (*lb+lm*)]. It can be noted that motor torque is inefficiently used. This torque also stresses the ballast arm requiring reasonable strength and also stiffness to avoid unwanted vibrations.

Instead of using constant motor torque to drive the ballast, also dynamic behavior of the ballast as a pendulum can be utilized. By a sequential correctly timed power input the oscillating ballast pendulum can collect a sufficient amount of energy to elevate into required height, but requiring less motor torque. The oscillating motion would also cause the Thistle to move back and forth in front of the obstacle which can help in overcoming the obstacle by utilizing dynamic inertia of the Thistle motion.

As a solution for a more efficient motor use the ballast arm can be removed completely, the ballast mounted on a rail running along ball outer surface and the motor being a part of the ballast mass.

12.4 Rail ballast

In order to avoid long levers inside the ball, the ballast can be mounted on a rail running around the ball inner surface. See Fig. 78 below.

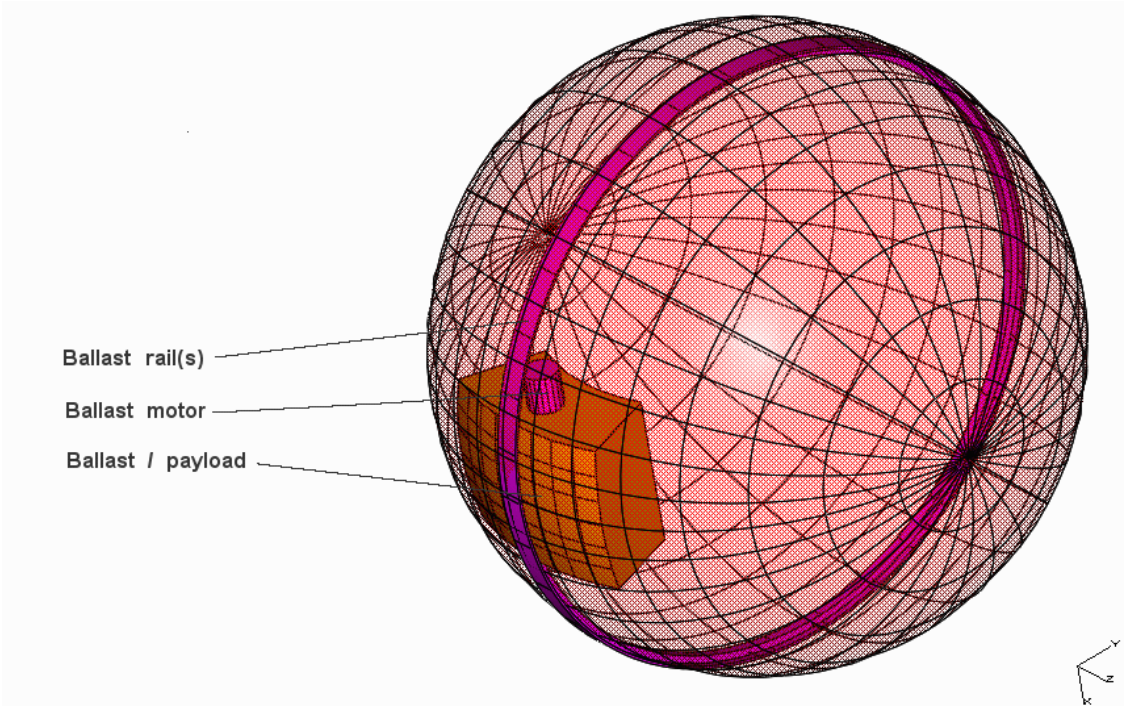

Fig. 78. A ballast on a rail.

The concept resembles a guinea pig running wheel and several other old designs to develop torque from inside a wheel. Also the ball resembles a tracked vehicle, as it carries the pavement (the track, or the sphere in this case) along with it. Here the track maintains the spherical shape instead of running around two wheels. Like the single lever-concept this design does not include any means for guidance. A design with two ballasts on a single rail could be guidable.

12.4.1 Velcro-ballast

In order to avoid challenges caused by rigidity and accuracy requirements of a circumferential rail running on ball surface some additional constructions may be considered. One evolution of the previously-mentioned Rollo-robot consisted of a smooth ball and a 2-dof. roving vehicle running inside it. The vehicle had 4 wheels and it generated traction on ball inner surface purely based on friction. The vehicle, and so also the ball, had complete 2 independent degrees of freedom and it was easily rideable. A similar solution can be considered also for a larger ballast-driven ball. A 2-dof. rover can travel freely inside the ball and so guide the ball direction without limitations. The design is sometimes called also as a ‘Hamster ball’.

A flexible structure, beneficial for a light system with large diameter, can not provide a good surface for high-friction wheel drive. Instead, the rover wheels could be coated with hooks of the Velcro-tape, and the ball inner surface with the loops containing fabric. Thus the rover with large flexible wheels could travel along flexible ball inner surface at high levels and so generate a high rolling torque. A challenge would be to choose proper materials to generate high enough holding force between the wheel and ball, but not too

high to tear the system apart or to consume too much energy in breaking the bond between the wheel and ball surface.

12.4.2 Lever ballast on rail

Imagine now that the two ballasts are connected to each other with a roll axis. A lever ballast is then hanging on this axis. We get a rail-carried lever ballast with two degrees-of-freedom. This steerable design has been developed and tested at HUT Automation technology laboratory for years already, see Fig. 19.

12.5 Energy collection for ballast-concepts

The examples on ballast locomotion discussed above rely on electric motors. If we wish to utilize external power sources, we should transfer the collected energy for the motors. The sphere surface has a large area that would carry a large solar panel or array of Peltier elements. Energy from the panel or elements could be transferred for the control electronics and motors via slip-rings or current tracks and brushes mounted on axis-joints or rails. However, since the ball moves by rolling, the solar arrays and Peltier elements are endangered by Martian dust and external damages from terrain contact.

12.6 Science instrument positioning

The Thistle is expected to study Martian soil and atmosphere. Gases in atmosphere can be conducted inside the central tube through the poles of the open- or closed section Thistle. Thus the gas analyzing instruments may be located on/in the central tube. In open-section Thistle the atmosphere is available also inside the Thistle and the instrumentation can be placed in the end of the ballast arm. Also gas line with a rotary joint between the central tube and ballast arm can conduct the gas to the ballast mass of a closed-section Thistle. Additional atmospheric sensors can be mounted on Thistle outer surface with electric lines running via central tube and ballast arm to the electronics.

For soil sampling an open-section Thistle with a ballast arm can lower the instrumentation against the ground with a telescopic arm. (See Fig. 79 below left.) Additional sensors measuring soil surface properties can be mounted on running surface of the Thistle, being connected to the electronics as the atmospheric surface sensors. A 2-dof. ballast lever Thistle can be rotated so that the central tube ends into vertical position, another end lying against the ground. Now the instruments placed to the end of the tube can study the soil or anchor the Thistle for operation as a wind mill (see Fig. 79 below right).

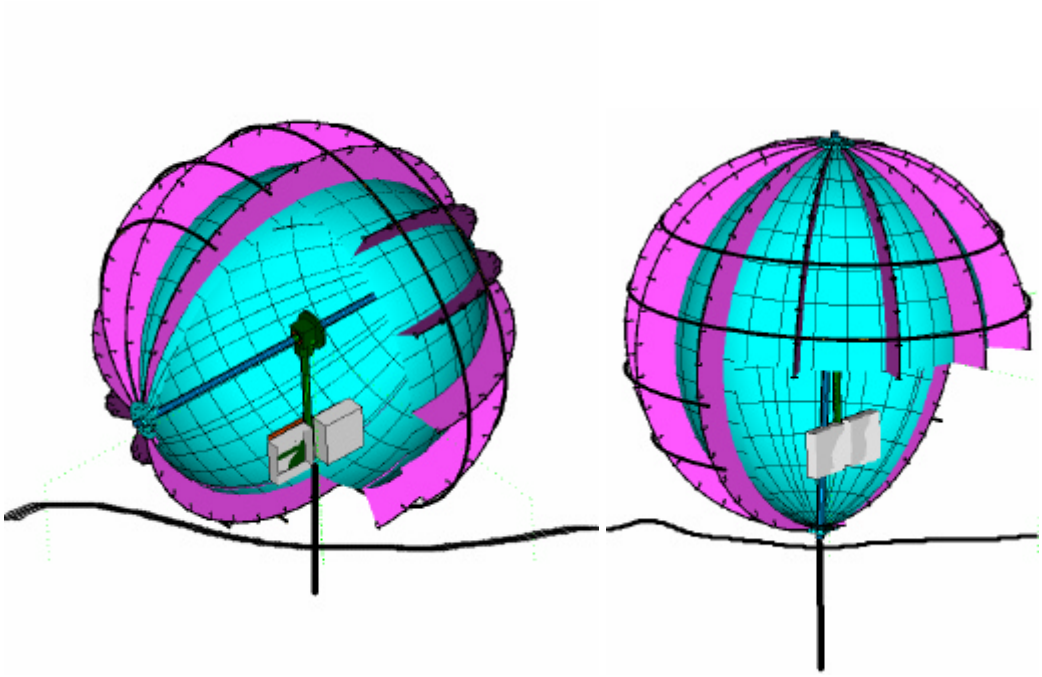

Fig. 79. Cut-away views of a 2-dof. ballast Thistle
in two possible soil sampling positions.

12.7 Pressurizing

Pressurizing of a closed-section Thistle adds rigidity of the structure. One solution could be to add the turbine blades on a pressurized closed-section Thistle. See Fig. 80 below.

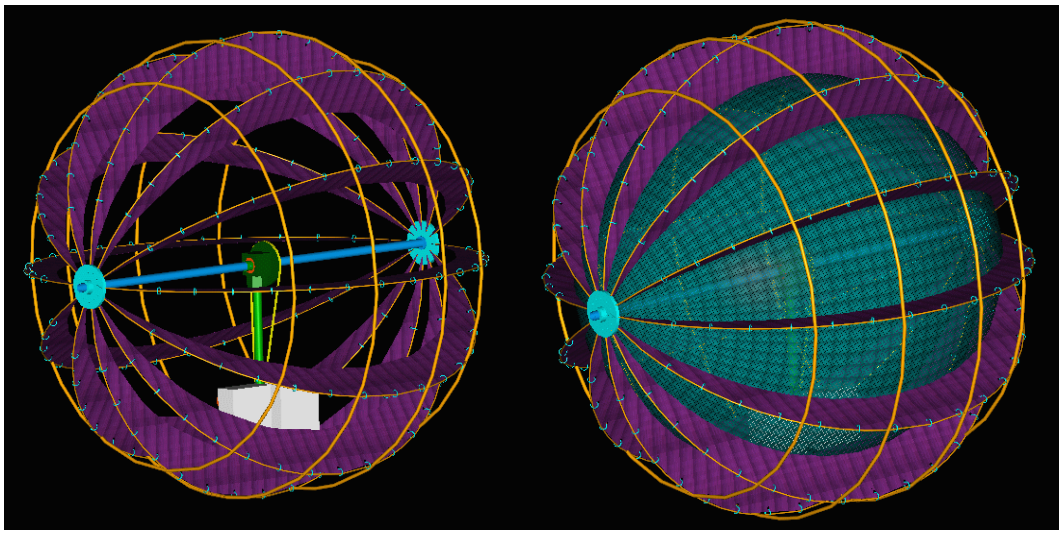

Fig. 80. An open-section model (left) and a pressurized closed-section Thistle (right) with turbine blades and external skeleton.

12.8 Effect of spikes

Further improvement in propulsion efficiency and mobility can be achieved by adding spikes into the sphere [1], as seen in a biological inspiration in Fig. 81.

Fig. 81. A natural spiked Thistle.

The Fig. 82 left illustrates how a passive Spiked Thistle with spring loaded spikes adapts to surface geometry. With properly dimensioned spikes also obstacle overcoming capacity can be improved. If the Thistle would be propelled by wind, some linear generators (magnet and coil) in the spikes could be used to produce energy. The illustration on the right shows how an epicentric rotating mechanism extends the spikes in a sequential manner and thus makes the Thistle to roll actively. The spikes could be activated also with some other means, like air or hydraulic pressure or linear motors. If heat energy could be guided in a controlled manner from Thistle surface to the individual spikes then bi-metals, shape memory alloys or linear wax actuators (based on melting and expansion of wax) could be used to produce motion from local energy sources.

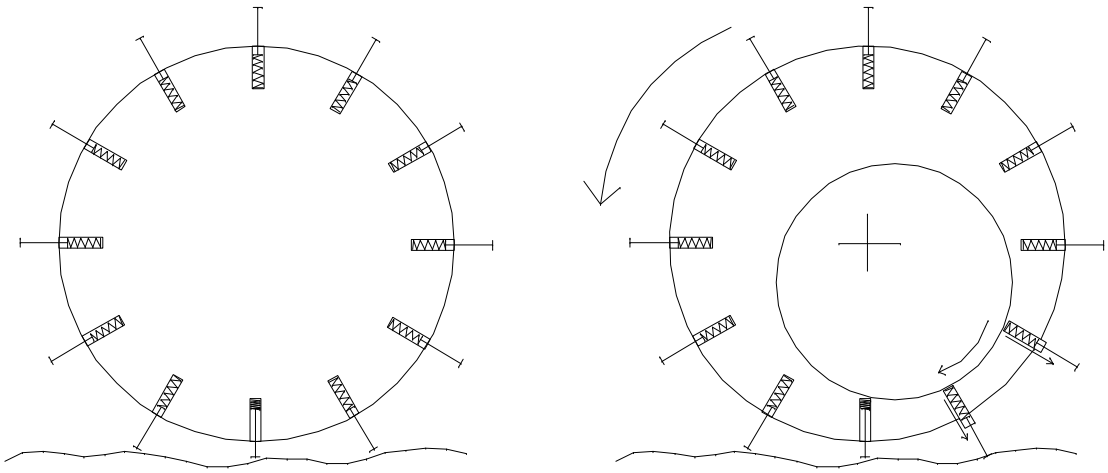

Fig. 82. A passive (left) and an active (right) Spiked Thistle.

13 Proposed Russian Thistle System description

13.1 Mechanics

The proposed Russian Thistle concepts is a combination of ballast drive and wind propulsion. The Thistle consists of a central tube, an inner sphere of fabric (pressurization as an option), radial carbon fiber arcs for turbine blades (also from fabric), and tangential carbon fiber circles for added rigidity and smooth rolling. On the central tube is mounted a 2-dof. lever ballast, or alternatively a double-rail ballast runs along inner surface of the ball.

The lever ballast allows better control, operation as a generator and folding, but projects very high torque on the motor and lever. On Earth a 43-kg ballast mass with a 1.5 m lever would provide a 633 Nm torque on the ballast lever joint, the same torque also bending the lever and twisting the central tube. On Martian gravity the torque would be 240 Nm. This would require quite strong structures and target mass for the ball structure may become a limitation. In case torque requirement becomes intolerable the double rail ballast (or velcro-ball) provides an alternative solution. The double rail ballast requires advanced rail structure which may prevent use of telescopic central tube and thus affect on folding.

Proposed Thistle properties are:

- Diameter 3 m.
- Ball mass 5 kg,
- Ballast mass 16 kg
- Total mass 21 kg

A larger 6 m Thistle would provide a better mobility and higher wind-resistance, but would require more demanding mechanical solutions.

13.2 Obstacle overcoming capacity

- 0.2 m obstacles with ballast drive
- 0.4 m obstacles with 35 m/s wind (assumes drag factor 0.8)

A larger Thistle would have better locomotion capability. A 6 m Thistle with a 30 kg sphere and 36 kg ballast (total mass 66 kg), would overcome 20 cm obstacles with ballast and 60 cm obstacles with a 32 m/s wind thrust.

13.3 Scientific and payload instrumentation

Ballast mass (16 kg or 36 kg) allows a large number of instruments, also some heavy ones. A more strict limitation is the power requirement that limits to 10-30 W average. Some light-weight instrumentation can be mounted inside the central tube.

If ballast drive is omitted and the Thistle relies on wind propulsion only the sphere mass becomes critical (30 kg max.) and small and low-mass instruments should be selected.

13.4 Energy

- A 10-30 W average (8 hours per day) power production is expected with the aid of solar cells, Peltier elements or wind-mill operation (optional).
- Local energy sources:
    - Advanced thin membrane solar cells
    - Advanced MEMS-Peltier elements
    - Collection of wind energy while rolling (using arm ballast and the motor as a generator).
- Batteries or RTG as an alternative for local power sources

13.5 Options

- Telescopic central tube
- Pushing mechanism
- Anchoring mechanism for operation as a stationary wind mill (possibly in conjuction with a drilling system.)

13.6 Operational capabilities

- Travel over smooth terrain and overcome obstacles propelled by wind
- In absence of wind travel with ballast drive
- Change traveling direction with a 2-dof. ballast drive
- Re-orient central tube in vertical position with the aid of 2-dof. ballast
    - In vertical position: examine soil, operate drill, anchor for wind mill operation, activate push stick for escape from a cavity (optional), extend an antenna

- With a telescopic central tube (optional) allow parking (tube contracted in vertical position) and/or folding (tube extended in horizontal position).

14 Prototype

In parallel with the Ariadna-study the Automation Technology Laboratory with its own funding produced a 1.3 m-prototype to demonstrate operation and performance of the Thistle. The drawings in Fig. 83 present anticipated construction of a simple 1-dof. Thistle.

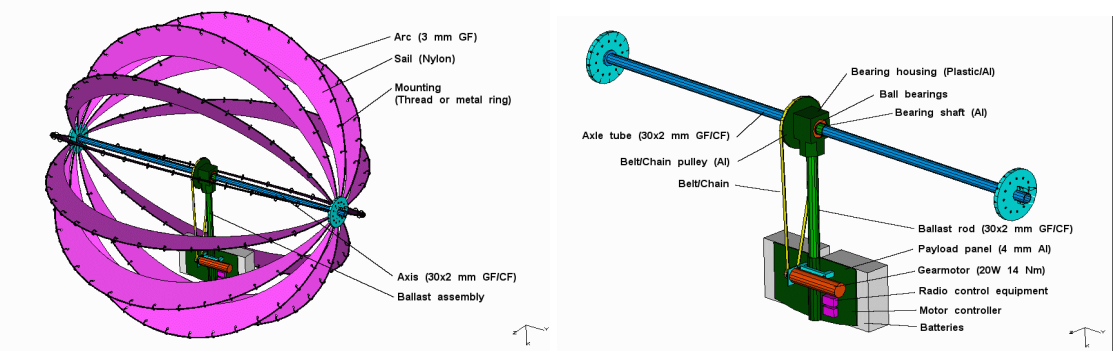

Fig. 83. Possible configuration of a 1-dof. ballast lever Thistle prototype.

14.1 Construction

Due to limited resources materials and structures were selected to allow low-cost components and easy manufacturing. The central tube is made of a 32 mm diameter glass fiber tube attached with two PVC-disks on both ends. The arcs were made of 18 pieces of 2 m long 8 mm diameter glass fiber rods. The rods were sold in 6 m poles. Wind sails were sewn of nylon fabric intended for clothing.

As the Thistle has an open structure its wind drag is expected to be smaller than that for a closed ball. The open structure, however, provides better view and access to mechanisms inside. In later phases, if so desired, the interior can be closed with an inflatable ball. The ball and sails alone weight 4.5 kilograms, but significant mass savings can be achieved by using advanced materials like carbon fiber rods and axle, and mylar sails. The photograph in Fig. 84 presents the 1.3 meter diameter Thistle prototype, in this stage intended for wind propulsion only. So far the locomotion properties have not been studied widely. In an experimental test the Thistle was set outside during a windy day, and its tendency to catch the wind easily was noticed. However, lacking any guidance the Thistle tends to roll downwards along any slope. Further, possibly due to flexible structure and non-perfect spherical shape the Thistle tends to change its rolling direction autonomously. Clearly this tendency decreases the effectiveness of wind propulsion. As the ball is constructed of 18 separate arcs, it does not roll completely smoothly. Deviation from a perfect sphere, however, equals to 1 cm high obstacle only. On soft surface (like snow or fine sand) the discrete Thistle surface effectively makes the ball to ‘walk’ on the surface instead of rolling. This means that the ball does not push any material in front of

as the rolling wheels do. Naturally this is of advantage on soft terrains but is not important on hard and smooth surfaces. Flexibility of the structure introduces additional features that prevent a smooth rolling. However, as mentioned also in several other studies, irregular shape of the Russian thistle-plant may in fact generate a favorable bouncing motion that may assist in over-passing obstacles. This could be the case also for the Thistle.

Fig. 84. The wind-propelled Thistle prototype.

14.2 Steering

In the second phase of prototype development a steerable motor drive was introduced. A pivoted lever was mounted with a sliding bearing in the middle of the rolling axis. In the end of the lever was mounted a battery and an electric motor. A tooth-belt runs between motor pinion and a larger drive gear mounted on the rolling axis. A special guiding system was mounted to guide the belt past the lever pivot joint. The Fig. 85 below shows the drive assembly: rolling axis and drive gear on top, the driving motor and battery at bottom. Also the steering motor and mechanism is visible on the left side of the lever. Lever pivot joint is located inside the lever upper part, just behind the two rollers that guide the belt in between. Pivot joint axis runs orthogonal to paper plane.

The Thistle is driven remotely with a Futaba radio-control system adapted from RC-toys. Motors are conventional Maxon A-Max 12 V 32 mm diameter motors, rated power approximately 15 W. The drive motor is controlled with a commercial Aeronaut Multi 20 RC-motor driver designed for RC-car, airplane and boat use. The driver gives a possibility for continuous speed control in both directions. The steering motor is driven with a home-made switch –connected to the RC-receiver- that allows to drive the steering motor back and forth with a pre-set velocity.

Before introducing the steering system the motorized Thistle was first experimented with a passive pivoted drive mechanism. Idea behind the test was to see, if passive freely hanging mass would allow the Thistle tilt (the axis of rotation deviates from horizontal

direction) and run past (not over) obstacles more easily. In earlier stage the lever was made stiff, without a pivot. Then the hanging mass quite strongly defined the rolling direction of the Thistle and in case an obstacle was introduced to partly block the way, the Thistle was not able to tilt and go around the obstacle but stopped immediately. However, a freely hanging pivoted mass introduced similar problems that were encountered with the pure wind-propelled Thistle: it would follow the slopes and wander around without a tendency to follow any path. Therefore an active steering system was introduced.

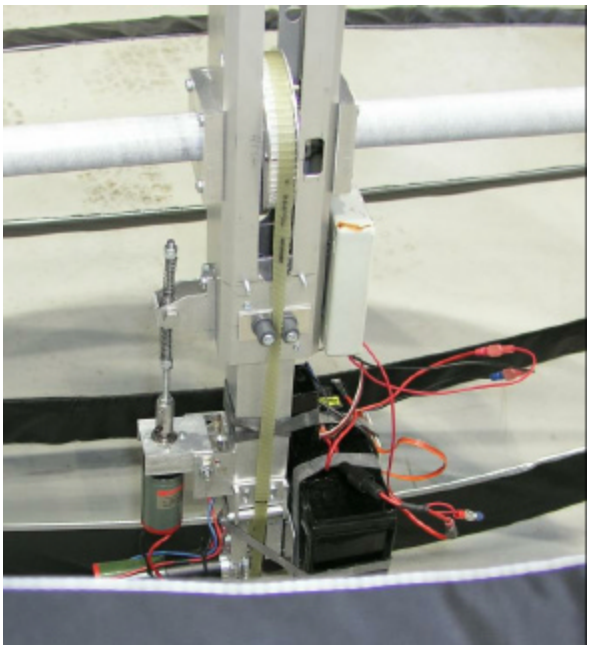

Fig. 85. The motorized drive and steering system.

In addition to the steering motor described above, the steering system contains a linear drive realized with a conventional M3 thread screw and nut. The screw mounts directly to the output shaft of the steering motor, that is mounted with a pivot to allow operation of the linear drive. The nut is also pivoted and mounted with an extension to the upper part of the complete lever system. When the linear drive is operated the lower part of the lever rotates around the pivot joint, as may be seen in Fig. 86. There is no position sensing nor any kind of feedback in this very simple system. In order to protect the linear drive the thread is removed from the screw outside the safe range of operation. This stops the linear drive motion at the limits but still allows the steering motor to rotate safely causing no harm to the mechanism. Upon change of motor running direction the nut – aided with external push-spring- encages again to the threads and the linear drive and steering system re-enters in operation. The operator can only command rotation direction of the motor. In practice the operator tells the Thistle to change its tilt angle. When the operator thinks the angle is suitable and stops driving the steering motor, the Thistle maintains this angle. Commercial RC-servos with a continuous feed-back were not used due to high force needed for steering.

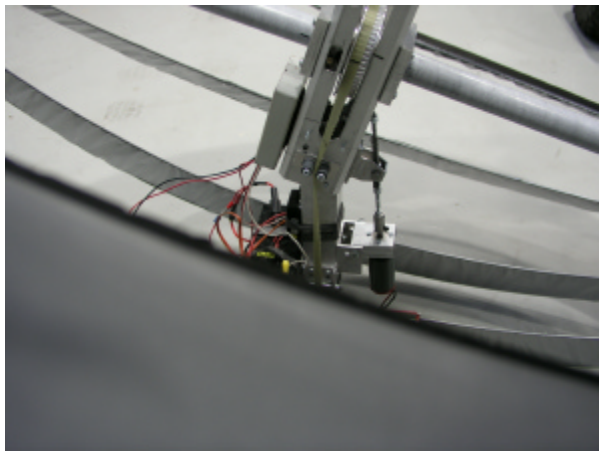

Fig. 86. The steering system has tilted the axis of rotation from horizontal plane.

14.3 Behavior

Driving tests with the Thistle show that locomotion is quite clumsy and somewhat chaotic. Structural flexibility and sectional circumference make the ball to precede in short bursts. First the ballast mass (the battery) elevates until resisting forces are exceeded, then the Thistle rotates almost a half revolutions and stops. While Thistle stands, the ballast again steadily elevates towards the point when the Thistle would take another burst. If a tilt angle is introduced with the steering system, during rolling the Thistle follows a spiral-like path in which the radius of curvature decreases towards end of the motion. After stopping, the Thistle remains wobbling and finally sets close to pre-set tilt angle. Structural hysteresis allows the tilt-angle to change time-after-time. In practice it is possible to make the Thistle to turn in a very limited space, but controlling the length of the turn is more difficult.

Weight of the drive- and steering system –including the battery- is 5 kilograms and length of the lever (to the middle of the battery) is 40 cm. Assuming total ballast mass of 5 kg to be located at this distance, and knowing total mass 9.5 kg and overall diameter 1.3 m we can calculate the maximum obstacle height that can be over-passed by the prototype: the height would be 4.3 cm without dynamic effects. Torque margin of the drive system allows the ballast mass to be rotated a complete revolution around the axis of rotation. This means, that when the Thistle stops against an obstacle, the ballast mass finally travels over the upper dead center and the following consequence is that the Thistle autonomously backs off half revolutions. Due to instability the Thistle simultaneously usually also turns a bit. This behavior makes the Thistle to get around the obstacles autonomously also without any active steering.

The Thistle was also tested on a snow bed during Finnish winter. Low mass of the Thistle allowed it to roll successfully on the snow surface, although the operator (the author himself) was standing knee-deep in snow. Soft structure of snow effectively damped out structural vibrations of the Thistle and driving and steering was clearly easier and overall behavior was better predictable. See the caterpillar-like track left behind the Thistle in the Fig. 87 below. Similar effect may be expected on soft sandy surfaces. Indeed, the motorized thistle could have favorable properties to be used as a roving vehicle on soft

sandy or snowy surfaces of foreign planets, where small-wheeled car-like rovers would not be successful.

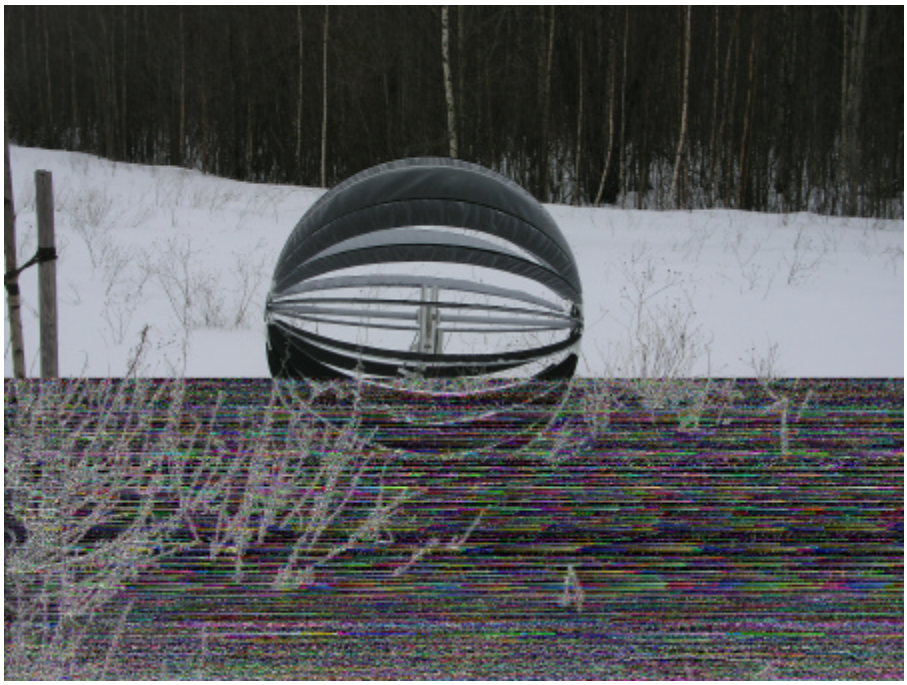

Fig. 87. The Thistle prototype rolls successfully on a Finnish snow-bed.

14.4 Controller development

Currently a computer controlled steering and navigation system is being developed to replace the manual RC-control system. The drive system will be based on an on-board controller on the Thistle and a wireless radio-link connection that sends high-level commands from the operator. Due to elastic properties and irregular motion odometry can not be utilized for navigation, but GPS or pseudo-GPS –based systems must be implemented. Returning to old-fashion navigation by the stars, the Moon or the Sun is not ruled out. Controlling of this device will require special approach. Usually the response for a given command (motor torque) is known, but in this case the Thistle behavior may temporarily be quite unexpected. Therefore a tight feed-back loop can not be used. Instead a certain type of flexible control system that aims to an average desired behavior must be developed.

14.5 An alternative drive mechanism

The drive system presented in the prototype takes quite inefficient use of the motor torque. The maximum motor torque directed to the rolling axis is defined by the length of the ballast arm and the ballast mass. On Earth it would be after the belt drive (9.81 m/s^2 * 5.5 kg * 0.4 m) = 21.58 Nm. However, the effective rolling torque, when over-passing a 4.3 cm high obstacle is defined by the ball radius, mass and obstacle height. On Earth it would be (after some geometric calculation) only 9.12 Nm. The difference originates from the fact that the effective driving torque arm length is only the minor part of the

lever which extends in front of the obstacle. However, the complete lever length stresses the system.

The ‘hamster ball’ –design presented earlier provides a solution for the matter. Since the open structure of the Thistle does not provide a proper running surface for the drive system, some additional development is needed. Below in Fig. 88 and in Fig. 89 is presented a new design where a strip of tooth-belt runs inside the Thistle. The belt is mounted from single points to the each of the arcs with a piece of steel cable or similar flexible wire. The mounting definitely will require a lot of development to mature into reliable and durable solution. Necessarily the mounting of the flexible belt into flexible rods provides a flexible system. The flexibility itself is not a problem, provided that structural strength is sufficient and all moving systems are provided with sufficient guidance and support.

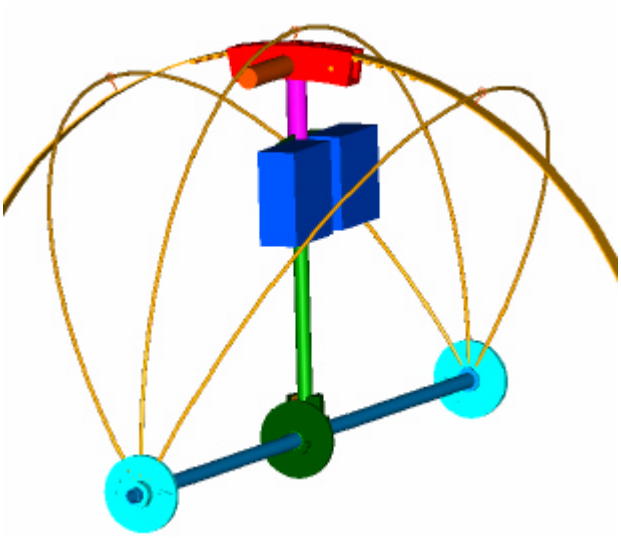

Fig. 88. Illustration of a tangential belt drive.

The design includes a rigid guiding block through which the tooth belt runs. The drive motor is mounted to the block and it pulls the belt directly with a cog-wheel, or with several cog-wheels. The guiding block gets additional support and guidance from the lever that is passively mounted to the Thistle axis of rotation with a bearing assembly. The lever also has a telescopic structure that allows the drive system to follow natural shape changes of the Thistle during locomotion.

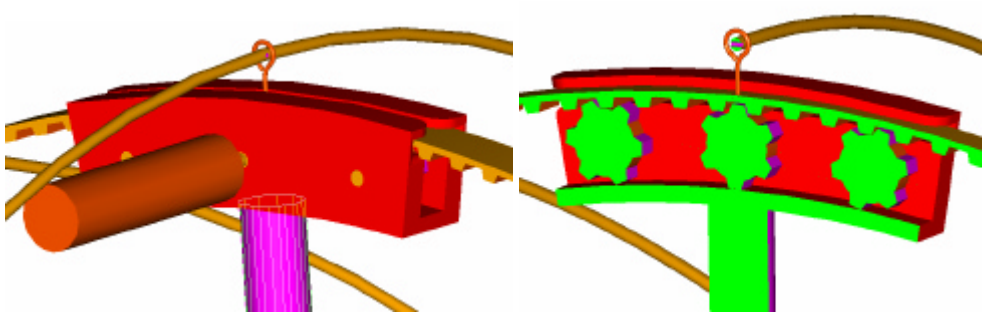

Fig. 89. Details of the tangential belt drive.

If we wish to compare performance of this design to the performance of the prototype, we can calculate the needed force to elevate the ballast mass into maximum height. Maximum ballast mass load on Earth is 9.81 m/s^2 * 5.5 kg = 53.96 N. If we assume that the ballast mass is located close to the cog-wheel, and the cog-wheel has a radius of 3 cm, we can calculate that the needed motor torque is 53.96 N * 0.03 m = 1.62 Nm. Hence we can achieve similar locomotion performance with 13 times smaller motor torque. Further, diameter of the ball does not have any negative effect on motor torque. The lever drive of the prototype needs increase in motor torque proportional to lever length. It may be noted here that for the ballast drive the strength of gravitational field does not affect on locomotion capability. When ignoring dynamic effects the performance is dependent on geometry and mass distribution only.

For steering the lever would not be pivoted any more and the belt and belt-drive would follow more or less rigid path. Necessary tilting for the steering would be achieved with an additional side-ways motion of ballast mass (batteries etc.) aside of the lever or along the central axis of rotation. Needed torque for steering tilt is only a fraction of that needed for locomotion.

15 Conclusion

This work has studied locomotion and energy production on Martian surface over a large range of technologies. The final conclusion and system proposal is in large extent a conceptual and preliminary one. Relevance of the design was tried to maintain considering the Martian environment, examining real scientific instrumentation, and with theoretical calculations –added with some testing- on mobility. 3D-modelling reveals volumetric relevance.

Locomotion capability calculations presented here are based mostly on measured data on the rock distribution and wind velocity. Since wind conditions and rock-distribution may depend on location of the landing site, and wind-conditions also on landing time, propulsion consideration should be repeated when the time and place of landing is known. It must be considered what should be obstacle overcoming capacity by wind propulsion under expected local wind conditions, and what should be performance of the ballast drive.

Detailed mechanical design, strength, mass, mass distribution, motor dimensioning and folding deserve in future close attention in order to produce solid concept that could be realized and tested as a mechanical conceptual model or as a proof-of-principle.

The conceptual prototype realized is 1.3 meters in diameter, as atmospheric density on Earth is more than sufficient with respect to one on Mars. The prototype has revealed the challenges associated with guidance of the elastic structure and torque requirements of the ballast drive. Different technical solutions has been proposed to improve driveability and motor torque response. Effectiveness of wind-propulsion with the ballast driven Thistle is yet to be tested.

16 References

[1] Peter Jakubik, Jussi Suomela, Mika Vainio, Tomi Ylikorpi, (2004) Biologically inspired solutions for robotic surface mobility. ARIADNA AO4532-03/6201 Final Report, Helsinki university of technology, Automation technology laboratory, Finland.

[2] ESA ExoMars09 , CDF Study Report: CDF-14(A), August 2002

[3] The Planetary Society, http://www.planetary.org/mars/

[4] NASA planetary sciences at the NSSDC, http://nssdc.gsfc.nasa.gov/planetary/lunar/apollo_lrv.html

[5] Mars Pathfinder Rover, http://nssdc.gsfc.nasa.gov/database/MasterCatalog?sc=MESURPR

[6] NASA/JPL Mars Rovers, http://marsrovers.jpl.nasa.gov/home/index.html

[7] Beagle home page, http://www.beagle2.com

[8] NASA planetary sciences at the NSSDC, http://nssdc.gsfc.nasa.gov/planetary/mars_future.html

[9] ESA Advanced concepts team home page, http://www.esa.int/gsp/ACT/

[10] The Bacterial Flagellum, Michael J. Behe, 1998, http://www.arn.org/docs/mm/flagellum_all.htm

[11] Stomatopod Biology, A. San Juan, March 7,1998, http://www.blueboard.com/mantis/bio/wheel.htm (Partly adapted from Full R, Earls K, Wong M, and Caldwell R. (1993). Locomotion like a wheel? Nature 365, 495.)

[12] A Novel Antipredator Mechanism in Salamanders: Rolling Escape in Hydromantes platycephalus, MARIO GARCÍA-PARÍS AND STEPHEN M. DEBAN, Museum of Vertebrate Zoology and Department of Integrative Biology, University of California, Berkeley, California 94720, USA, Journal of Herpetology, Vol. 29, No. 1, pp. 149-151, 1995 Copyright 1995 Society for the Study of Amphibians and Reptiles

[13] Hop David, P. O. Box 39, Ajo, Arizona 85321, USA http://www.clowder.net/hop/curlups/curlups.html

[14] DesertUSA.com, Digital West Media Inc., P.O. Box 270219, San Diego, CA 92198-0219, USA, http://www.desertusa.com/mag01/may/papr/tweed.html

[15] Tomi Ylikorpi and Jussi Suomela (2005) Ball-shaped Robots; Historical Overview and Recent Developments at TKK, Helsinki University of Technology, P.O. Box 5500, 02015 TKK, Finland, to be presented in The 5th International Conference on Field and Service Robotics, July 29-31 2005, Port Douglas Australia

[16] Brian Chemel, E. Mutschler, H. Schempf Cyclops: Miniature Robotic Reconnaissance System. Field Robotics Center, Robotics Institute, Carnegie Mellon University, Pittsburgh, PA 15213, USA.

[17] Rotundus AB, c/o UUAB, Uppsala Science Park, SE-751 83 Uppsala, Sweden.

[18] Francois Michaud and Serge Caron (2001) Roball, the Rolling Robot. LABORIUS - Research Laboratory on Mobile Robotics and Intelligent Systems, Universite de Sherbrooke, Sherbrooke (Quebec Canada) J1K2R1.

[19] A. Bicchi(*), A. Balluchi(*), D. Prattichizzo(*), A. Gorelli(**) (1997) Introducing the Sphericle: an Experimental Testbed for Research and Teaching in Nonholonomy, (*)Centro E. Piaggio, Universita di Pisa, Pisa (Italia), (**) Facolta di Ingegneria, Universita di Siena, Siena (Italia)

[20] Halme A., Schönberg T., Wang Y.: Motion Control of a Spherical Mobile Robot, 4. International Workshop on Advanced Motion Control, Tsu, Japan.1996.

[21] Hajos, G., Jones, J., Behar A., Dodd, M.: "An Overview of Wind-Driven Rovers for Planetary Exploration," AIAA-2005-0245, 43rd AIAA Aerospace Sciences Meeting and Exhibit, Reno, NV, January 10-13

[22] Hajos, G., Jones, J., Behar A., Dodd, M., "An Overview of Wind-Driven Rovers for Planetary Exploration," *43rd AIAA Aerospace Sciences Meeting and Exhibit*, Reno, NV, January 10-13, 2005, NPO-20283.

[23] Antol, J., " A New Vehicle for Planetary Surface Exploration: The Mars Tumbleweed," *1st Space Exploration Conference: Continuing the Voyage of Discovery* , Orlando, 31 January – 1 February 2005.

[24] Hille, C., Moody, C., Rose, S., and Kerr K., “Wind Powered Martian Robot,” Midterm Report submitted to, Dr. Maxwell, ME 4370, College of Engineering, Texas Tech University, 2001.

[25] Hanrahan, H., Minton, D., DeJarnette, F., Camelier, I., Fleming, M., “Mars Tumbleweed: A New Way to Explore Mars,” *Planetary Probe Atmospheric Entry and Descent Trajectory Analysis and Science Workshop*, Lisbon Portugal, 6-9 October 2003.

[26] Heimendahl, M., Estier, T., Lamon, P., Siegwart, R., (2004), “Windball,” Swiss Federal Institute of Technology Lausanne, Autonomous Systems Laboratory, 2004.

[27] Abas Kangi (2004), Wormsphere Rover Pattern for DiscoveringUnderground Water on Mars' Surface, Department of Geology, Islamic Azad University, Shahrod, Iran, in JBIS, Vol. 57, pp.298-300, 2004

[28] THE SEARCH FOR EARLY LIFE ON MARS: AN ESA EXOBIOLOGY SCIENCE TEAM STUDY. P. Clancy, A. Brack, B. Hofmann, G. Horneck, Gero Kurat, J. Maxwell, G. Gabriele Ori, C. Pillinger, F. Raulin, N. Thomas, F. Westall, and B. Fitton, Workshop on the Issue of Martian Meteorites

[29] Antol J., Calhoun P., Flick, Hajos G., Kolacinski R., Minton, Owens R., Parker, "Low Cost Mars Surface Exploration: The Mars Tumbleweed," NASA/TM-2003-212411, August 2003.

[30] Matthews, J., "Development of the Tumbleweed Rover," NASA Jet Propulsion Laboratory, Robotic Vehicles Group, Pasadena, California, May 2003.

[31] The DLR HRSC-Experiment web-page, http://berlinadmin.dlr.de/Missions/express/marsfacts/marsfactsheet.shtml

[32] Mars physical and orbital statistics, comparisons, http://www.student.oulu.fi/~jkorteni/space/mars/properties.html

[33] The NASA National Space Science Data Center (NSSDC) Mars Fact Sheet, http://nssdc.gsfc.nasa.gov/planetary/factsheet/marsfact.html

[34] CONCEPTUAL DESIGN OF A MARTIAN POWER GENERATING SYSTEM UTILIZING SOLAR AND WIND ENERGY, Amir Hemmat, Chi Nguyen, Bharat Singh, Keir Wylie, University of Houston, Presented at SECOND ANNUAL HEDS-UP FORUM, May 6–7, 1999, Lunar and Planetary Institute 3600 Bay Area Boulevard, Houston, TX 77058-1113

[35] ROCKS AT THE PATHFINDER LANDING SITE, MARS: IDENTIFICATION AND SIZE DISTRIBUTION. E. Hauber, R. Jaumann, C. Mosangini, N. Russ, F. Trauthan, K.-D. Matz, O. Fabel, DLR, Institute of Planetary Exploration, Rudower Chaussee 5, D-12489 Berlin-Adlershof, Germany (Ernst.Hauber@dlr.de).

[36] NASA Quest, http://quest.arc.nasa.gov/mars/events/wwprimer.html

[37] Mars Pathfinder Historical Weather Data, http://mars.sgi.com/ops/asimet.html

[38] Reaching for Mars, NASA MARSPORT DESIGN COMPETITION 2002, Mars Deployable Greenhouse, Gary Ballmann et. Al, University of Central Florida/Florida Space Institute, 12424 Research Parkway, Suite 400, Orlando, FL 32826, http://mmae.ucf.edu/~aiaa/greenhouse/DDR_final-report-greenhouse.pdf

[39] Richard M. Kolacinski, Daniel W. Palmer, Patrick M. Cloutier and Jason E. Schatz, 'Biologically Inspired Design for Low Cost Exploration of Space: Swarms of Martian Rovers Based upon the Russian Thistle', Advanced Controls Engineering Group, Orbital Research, Inc., 673 G Alpha Dr., Cleveland, OH 44143-2140 USA and Dept. of Mathematics and Computer Science , John Carroll University, 20700 North Park Blvd., University Heights, OH, 44118

[40] On-board Power Sources for Mobile Robots, V. Gromov, S. Matrossov, V. Petriga, Science and Technology Rover Company Ltd, Russian Mobile Vehicle Engineering Institute, 2 Zarechnaja Street, 198323, St. Petersburg, Russia, ASTRA 2002, Advanced Space Technologies for Robotics and Automation, 19-21 November, 2002, ESTEC, Noordwijk, The Netherlands, pp. 307-314

[41] Mars Exploration Rover Landings Press Kit, NATIONAL AERONAUTICS AND SPACE ADMINISTRATION , January 2004

[42] Actuator Design Using Shape Memory Alloys, 2. ed., Tom C Waram, 1063 Kng St. W., Suite 204 Hamilton, Ontario L8S 1L8, Canada, 1993

[43] The VT1 Shape Memory Alloy Heat Engine Design, Jillcha Fekadu Wakjira, Thesis submitted to the Faculty of, the Virginia Polytechnic Institute and State University, January 2001, Blacksburg, VA

[44] JPL Thermoelectrics Website, Thermoelectric Science and Engineering, http://www.its.caltech.edu/~jsnyder/thermoelectrics/history_page.htm

[45] Jagdish U. Patel, Jean-Pierre Fleurial, G. Jeffrey Snyder, and Thierry Caillat, Miniature Radioisotope Thermoelectric Power Cube, Caltech for NASA's Jet Propulsion Laboratory, Pasadena, California. www.techbriefs.com/tsp NPO-30328 under the Physical Sciences category

[46] Micro Electric Machines for Micro Turbomachinery, J. L. Steyn (C. Livermore, R. Khanna, J. H. Lang, S. D. Umans, and E. P. Warren in collaboration with A. H. Epstein and M. A. Schmidt, and A. Forte, T. Lyszczarz, and J. Yoon of MITLL), http://www-mtl.mit.edu/mtlhome/mems/powermems.shtml

[47] http://aerodyn.org/ Drag/tables.html, Copyright © A. Filippone (1999-2004).

[48] Granger, R. A., "*Fluid Mechanics*", Dover Edition, Dover Publications Inc. New York, 1995.

[49] Yuuta Sugiyama and Shinichi Hirai, "Crawling and Jumping by a Deformable Robot", Proc. Int. Symp. on Experimental Robotics, Singapore, June, 2004. http://www.ritsumei.ac.jp/se/~hirai/research/softrobot-e.html